Chapter 1 : Introduction

Alström syndrome (AS) was first reported in 1959.(Alstrom, Hallgren et al. 1959) It is a rare genetic disorder manifesting as childhood obesity, type 2 diabetes mellitus (T2DM) and neurosensory deficits, with a prevalence of less than one per million population.(Orphanet 2010) Over the 50 years since its initial description, approximately 450 AS patients have been diagnosed worldwide.

1. Genetics of AS

AS is an autosomal recessive genetic disorder affecting both sexes equally. Homozygosity mapping and linkage studies have revealed that AS was due to a mutation in the ALMS1 gene located on the short arm of chromosome 2 (2p13).(Collin, Marshall et al. 1997; Macari, Lautier et al. 1998; Collin, Marshall et al. 1999; Zumsteg, Muller et al. 2000) The ALMS1 gene comprises 23 exons and AS mutations predominantly occur in exons 8, 10 or 16 resulting in nonsense or missense frameshift-inducing insertions or deletions (Minton, Owen et al. 2006; Joy, Cao et al. 2007) (Figure 1-1) Almost 100 different ALMS1 mutations have been identified. It was reported that patients with exon 16 mutations had more severe clinical features and those with exon 8 mutations less renal disease (Marshall, Hinman et al. 2007), however other studies have not replicated these findings.(Bond, Flintoff et al. 2005; Minton, Owen et al. 2006)

ALMS1 RNA is widely expressed in many tissues and splice variants have been identified in human brain and testis suggesting that Alms1 protein may perform different functions in different organs.(Collin, Marshall et al. 2002)

Alms1 is a large 461 kDa protein and AS mutations typically result in a premature stop codon and the generation of a truncated Alms1 protein.(Collin, Marshall et al. 2002; Joy, Cao et al. 2007) ALMS1 exon 8 encodes a 44 amino acid large tandem repeat (34 imperfect repeats) and a leucine zipper domain. Other Alms1 domains include a short polyglutamine and polyalanine segment and a conserved motif near the C-terminus. (Figure 1-1) The leucine zipper domain could suggest a role for Alms1 in protein-DNA or protein-protein interactions (Hearn, Renforth et al. 2002), although Alms1 has an extra-nuclear localisation on immunohistochemistry, being localised to the centrosome. The ubiquitous expression of ALMS1 across tissues correlates with the wide range of organ dysfunction in AS. The C-terminal portion of the Alms1 protein that is commonly missing in AS patients therefore appears to play an important role in cellular function in many tissues.

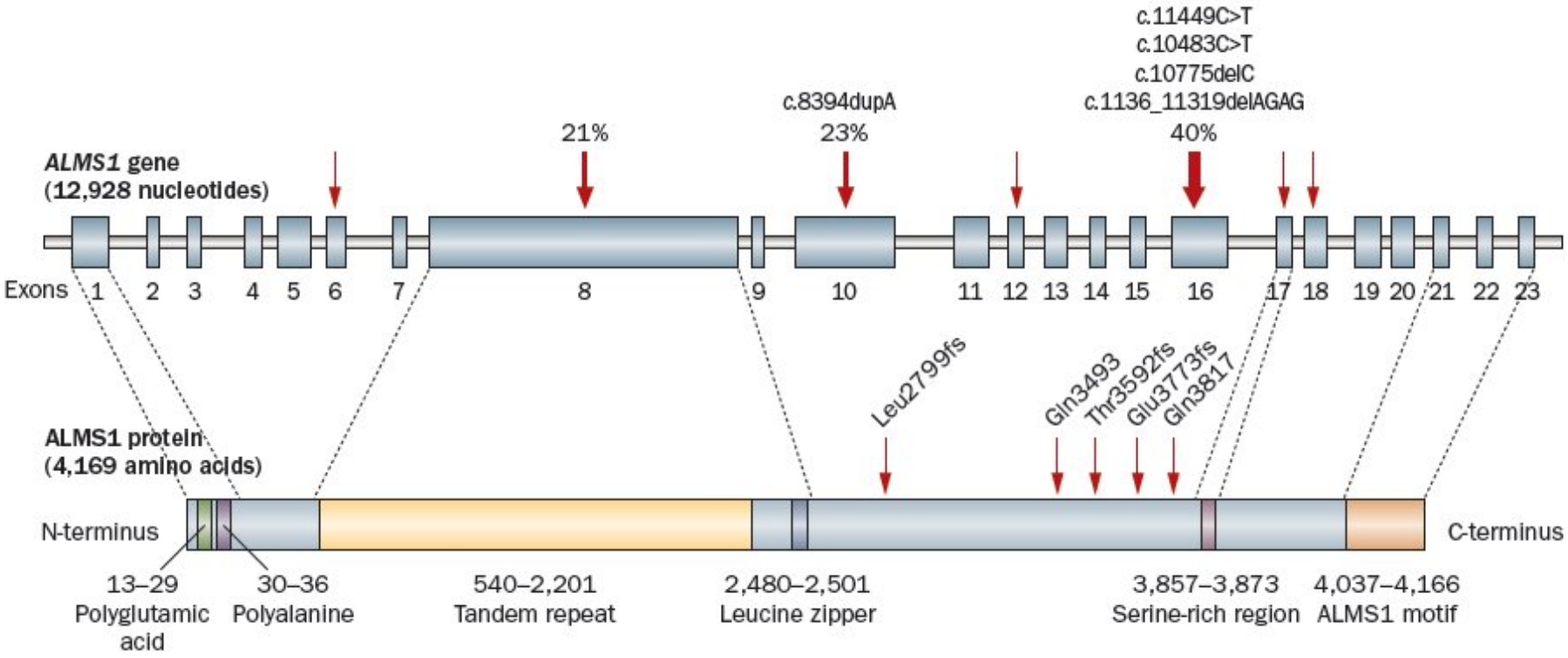
c.11449C>T
c.10483C>T
c.10775delC
c.1136_11319delAGAG
40%
c.8394dupA
23%
21%
ALMS1 gene
(12,928 nucleotides)
Exons 1 2 3 4 5 6 7 8 9 10 11 12 13 14 15 16 17 18 19 20 21 22 23
Leu2799fs
Gln3493
Thr3592fs
Glu3773fs
Gln3817
ALMS1 protein
(4,169 amino acids)
N-terminus
C-terminus
13–29
Polyglutamic acid
30–36
Polyalanine
540–2,201
Tandem repeat
2,480–2,501
Leucine zipper
3,857–3,873
Serine-rich region
4,037–4,166
ALMS1 motif

Figure 1-1: Human ALMS1 gene and Alms1 protein schematic

Not drawn to scale. Exons 16, 10 and 8 are mutational hotspots with mutations seldom being found in exons 6, 12, 17 and 18.(Joy, Cao et al. 2007; Marshall, Hinman et al. 2007) The protein domains identified *in silico* are mainly coded by exon 1, 8, 17 and 21-23. Exon 8 codes for a tandem repeat and leucine zipper domain. The most common mutations are represented at both the ALMS1 gene and Alms1 protein level. In mutant condition, Alms1 protein loses the Alms1 motif at the C terminus.

2. Clinical features of Alström syndrome

AS is characterised by the progressive development of severe multi-organ pathology starting in infancy and leading to high morbidity and reduction of life expectancy. (Michaud, Héon et al. 1996; Marshall, Bronson et al. 2005; Marshall, Beck et al. 2007)

2.1. Primary symptoms

At an early age, AS patients develop truncal obesity associated with insulin resistance, hyperinsulinemia, hyperleptinemia and hyperlipidemia.(Satman, Yilmaz et al. 2002) This progresses to clinical T2DM with the high prevalence of childhood diabetes (~70% by 20 years of age) distinguishing AS from other genetic causes of childhood obesity, such as Bardet-Biedl syndrome (BBS), where despite equivalent level of obesity T2DM affects less subjects and at a later age. Early life subcutaneous fat accumulation is a feature of AS, with implications that the Alms1 protein may play a specific role in adipocyte development.(Paisey, Hodge et al. 2008) Intriguingly, AS subjects exhibit an inverse correlation between waist circumference, body mass index (BMI) and total body fat and increasing age, a feature not typically seen in other obesity disorders.(Minton, Owen et al. 2006) Despite this age-related reduction in body fat, insulin resistance continues to increase with age, suggesting a potential role of the Alms1 protein in

downstream insulin signalling pathways.(Marshall, Bronson et al. 2005; Minton, Owen et al. 2006)

Consistent with the severe insulin resistance, *acanthosis nigricans* is a common clinical feature. Cases of acute pancreatitis have been reported secondary to hypertriglyceridaemia, a common clinical feature of AS.(Wu, Chen et al. 2003; Paisey, Carey et al. 2004) Liver function test abnormalities are a common feature, secondary to non-alcoholic fatty liver disease.(Connolly, Jan et al. 1991; Awazu, Tanaka et al. 1997)

Hypogonadotropic hypogonadism results in infertility and female subjects manifest features of polycystic ovarian disease and hyperandrogenism, a feature also seen in other causes of obesity-associated insulin resistance.(Dunaif 1997; Poretsky, Cataldo et al. 1999; Marshall, Beck et al. 2007) Other endocrine disorders include short stature associated with growth hormone deficiency and hypothyroidism.(Marshall, Bronson et al. 2005; Maffei, Boschetti et al. 2007; Mihai, Catrinoiu et al. 2009)

2.2. Other features

Other major clinical features of AS are progressive neurosensory deficits.(Welsh 2007) Nystagmus and photophobia manifest in the first year of life with progressive visual loss leading to blindness in adulthood.(Russell-Eggitt, Clayton et al. 1998; Malm, Ponjavic et al. 2008)

Sensorineural hearing loss is also common in the first decade of life.(Van den Abeele, Craen et al. 2001) Interestingly, AS patients despite their early age of onset of T2DM do not appear to develop typical diabetic peripheral sensory neuropathy, suggesting the Alms1 mutation might in some as yet unexplained manner, protect against hyperglycaemia-induced neuropathy.(Paisey, Paisey et al. 2009)

Cardiomyopathy is a common cause of death in AS patients.(Worthley and Zeitz 2001; Hoffman, Jacobson et al. 2005) Echocardiography and cardiac magnetic resonance imaging reveals both right and left ventricular dysfunction.(Makaryus, Zubrow et al. 2007; Loudon, Bellenger et al. 2009; Corbetti, Razzolini et al. 2012) Augmented aortic systolic pressure may also contribute to heart failure.(Smith, McDonnell et al. 2007)

Other variable clinical features in AS include renal and pulmonary dysfunction.(Goldstein and Fialkow 1973; Marshall, Bronson et al. 2005) Autopsies of AS subjects also showed marked fibrosis in liver, kidney, myocardium, ovary and seminiferous tubules.(Goldstein and Fialkow 1973; Awazu, Tanaka et al. 1997; Marshall, Bronson et al. 2005; Corbetti, Razzolini et al. 2012) The origin of the fibrosis and its contribution to the multi-organ patholgy of AS remain unknown.

2.3. Diagnosis

Diagnosis of AS is confounded by the heterogeneity in the clinical phenotype even within the same affected family.(Titomanlio, De Brasi et al. 2004; Hoffman, Jacobson et al. 2005; Özgül, Satman et al. 2007; Mahamid, Lorber et al. 2012) The most consistent clinical features of AS are childhood obesity, T2DM and retinopathy, with only one case of AS without obesity ever being reported.(Koç, Bayrak et al. 2006) So far, however, two studies have not shown genetic variation in the Alms1 gene in patients with T2DM.(Hart, Maassen et al. 2003; Patel, Minton et al. 2006) Diagnostic criteria have been established to assist in accurate clinical diagnosis of AS (Table 1-1).(Marshall, Beck et al. 2007)

Age	Minimum diagnosis	Major criteria	Minor criteria	Other variable supportive evidence
Birth–3 years	Two major criteria or one major criteria and two minor criteria	*ALMS1* mutation in one allele and/or family history of AS Visual defects (nystagmus, photophobia)	Obesity, DCM and/or CHF	Recurrent pulmonary infections Normal digits Delayed development
3–14 years	Two major criteria or one major criteria and three minor criteria	*ALMS1* mutation in one allele and/or family history of AS Visual defects (nystagmus, photophobia, diminished acuity, if old enough to undergo cone dystrophy testing by ERG)	Obesity and/or insulin resistance and/or T2DM History of DCM and/or CHF Hearing loss Hepatic dysfunction Renal failure Advanced bone age	Recurrent pulmonary infections Normal digits Delayed development Hyperlipidemia Scoliosis Flat, wide feet Hypothyroidism Hypertension Recurrent UTI Growth hormone deficiency
14 years–adulthood	Two major criteria and two minor criteria or one major criteria and four minor criteria	*ALMS1* mutation in one allele and/or family history of AS Visual defects (history of nystagmus, legal blindness, cone and rod dystrophy on ERG)	Obesity and/or insulin resistance and/or T2DM History of DCM and/or CHF Hearing loss Hepatic dysfunction Renal failure Short stature Hypogonadism (in male patients) Irregular menses and/or hyperandrogenism (in female patients)	Recurrent pulmonary infections Normal digits History of developmental delay Hyperlipidemia Scoliosis Flat, wide feet Hypothyroidism Hypertension Recurrent UTI and/or urinary dysfunction Growth hormone deficiency Alopecia

Diagnosis requires AS genetic testing plus clinical observations. The number of required criteria increases with the patient's age. Abbreviations: AS, Alström syndrome; CHF, congestive heart failure; DCM, dilated cardiomyopathy; ERG, electroretinography; T2DM, type 2 diabetes mellitus; UTI, urinary tract infection.

Table 1-1: Diagnostic criteria for Alström syndrome

Diagnosis requires AS genetic testing and clinical observations. The number of required criteria increases with patient age. (Marshall, Beck et al. 2007) Abbreviations: DCM/CHF, dilated cardiomyopathy with congestive heart failure; ERG, electroretinogram; T2DM, type 2 diabetes mellitus; UTI, urinary tract infection.

3. AS is a new ciliopathy

AS has recently been recognised as a ciliopathy disorder.(Badano, Mitsuma et al. 2006; Baker and Beales 2009) Ciliopathies are caused by gene mutations that lead to defective function of an ubiquitous intracellular organelle known as the primary cilium.

3.1. Ciliopathy Classification

Ciliopathies can be monogenic like AS or multigenic like Bardet-Biedl syndrome (BBS). Fourteen different BBS genes have been identified with a predominance of mutations affecting BBS1, BBS10 and BBS12.(Muller, Stoetzel et al. 2010) In some cases the same mutated gene, e.g. NPHP1, CEP290, or CXORF can be involved in different diseases (Table 1-2).

Disease	OMIM	Mutated gene(s)
Structural–metabolic–developmental		
Alström syndrome	203800	*ALMS1*
Bardet–Biedl syndrome	209900	*BBS1, BBS2, ARL6, BBS4, BBS5, MKKS, BBS7, TCC8, BBS9, BBS10, TRIM32, BBS12, MKS1, CEP290*
Structural–metabolic		
Mental retardation, truncal obesity, retinal dystrophy and micropenis	610156	*INPP5E*
Structural–developmental		
Meckel–Gruber syndrome	249000	*MKS1, TMEM67, CEP290, RPGRIP1L, CC2D2A*
Joubert syndrome	213300	*INPP5E, TMEM216, NPHP1, AHI1, CEP290, RPGRIP1L, TMEM67, ARL13B, CC2D2A, OFD1*
Jeune asphyxiating thoracic dystrophy syndrome	208500	*ATD, IFT80, DYNC2H1*
Short-rib polydactyly syndrome I–IV	263510, 263520, 236530, 269860	*DYNC2H1*
Cranioectodermal dysplasia (Sensenbrenner syndrome)	218330	*IFT122*
Orofaciodigital syndrome 1	311200	*OFD1*
Ellis–van Creveld syndrome	225500	*EVC, EVC2*
Kartagener syndrome	244400	*DNAI1, DNAI2, DNAH5, TXNDC3, DNAH11, C14orf104, RSPH4A, RSPH9, LRRC50*
Structural		
Primary ciliary dyskinesia	244400	*DNAI1*
Autosomal recessive polycystic kidney disease	263200	*PKHD1*
Polycystic kidney disease	173900	*PKD1–3*
Senior–Løken syndrome	266900	*NPHP1, NPHP3, NPHP4, IQCB1, CEP290*
Nephronophthisis	256100	*INVS, NPHP3, NPHP4, GLIS2, NEK8, RPGRIP1L*
Retinitis pigmentosa*	268000	*SPATA7, LRAT, LCA3, AIPL1, OSBPL1A, RHO, CRB1, TULP1, ABCA4, RPE65, EYS, CERKL, SEMA4A, PRCD, NR2E3, MERTK, USH2A, PDE6B, PROM1, PDE6A, RGR, CNGB1, IDH3B, SAG, CNGA1, TTC8, C2orf71, PRPH2, RP9, IMPDH1, PRPF31, PRPF8, CA4, PRPF3, ABCA4, NRL, FSCN2, TOPORS, SNRNP200, SEMA4A, NR2E3, KLHL7, RGR, GUCA1B, BEST1, CRX, RP2, RPGR, MT-TS2*
Leber congenital amaurosis	204000	*GUCY2D, RPE65, SPATA7, AIPL1, LCA5, RPGRIP1, CRX, CRB1, CEP290, IMPDH1, RD3, RDH12, LRAT*

*Retinitis pigmentosa is included in this Table as it has genetic and phenotypic overlap with ciliopathies such as Alström syndrome and Bardet–Biedl syndrome, although other forms of retinitis pigmentosa might have causes unrelated to defective primary cilium function. Abbreviation: OMIM, online mendelian inheritance in man.

Table 1-2: Ciliopathies with their respective OMIM number and gene(s) involved

Overview of ciliopathies with their respective OMIM number, gene(s) involved (Hildebrandt and Otto 2005; Badano, Mitsuma et al. 2006; Baker and Beales 2009). *Retinis pigmentosa is included in this Table as it has genetic and phenotypic overlap with ciliopathies such as Alström syndrome and Bardet-Biedl syndrome, although other forms of retinitis pigmentosa might have causes unrelated to defective primary cilium function. Abbreviations: OMIM: online Mendelian inheritance in man.

Ciliopathies may only affect a single organ, for example Leber congenital amaurosis or polycystic kidney disease, or may affect multiple organs, for example AS, BBS or Joubert syndromes (JS).(Adams, Smith et al. 2008; Cardenas-Rodriguez and Badano 2009) They are pleiotropic genetic disorders displaying overlapping phenotypes.

A proposed ciliopathy classification scheme was defined in reference to the predominant phenotypic feature, namely structural, metabolic and/or developmental defects (Table 1-3, 1-4 and 1-5). Structural defects are common to all the ciliopathies listed and may or may not be associated with metabolic or developmental defects. AS and BBS show the widest spectrum of phenotypic features with a dominant developmental defect phenotype in BBS and a more dominant metabolic dysfunction phenotype in AS. These differences suggest that unlike BBS proteins Alms1 is not directly involved in the Wnt and sonic hedgehog (Shh) developmental signaling pathway but may be more involved in hormonal signaling pathways. MORM syndrome is another ciliopathy featuring truncal obesity and is due to mutation in the INPP5E gene encoding inositol polyphosphate-5-phosphatase E.(Hampshire, Ayub et al. 2006) The INPP5E defect is involved in primary cilium stability and signaling and is one of the genes responsible for JS.(Bielas, Silhavy et al. 2009; Jacoby, Cox et al. 2009)

Symptom	Symptom incidence (%)		
	Alström syndrome*	Bardet–Biedl syndrome	MORM
Structural			
Vision pathology	75–100	75–100	75–100
Sensory deficit	75–100	<25	NA
Endocrine and/or reproductive defect	50–75	75–100	75–100
Pulmonary defect	25–50	NA	NA
Renal defect	25–50	50–75	NA
Hepatic defect	<25	<25	NA
Developmental delay	25–50	50–75	75–100
Cardiac disease	25–50	<25	NA
Metabolic			
Obesity	~100	50–75	75–100
Type 2 diabetes mellitus	50–75	<25	NA
Developmental			
Skeletal defect	25–50	NA	NA
Polydactyly	NA	50–75	NA
Situs inversus	NA	<25	NA
Brain malformation	NA	<25	NA

*Some ciliopathies in this group are also associated with developmental defects. Abbreviations: MORM, mental retardation, truncal obesity, retinal dystrophy and micropenis; NA, not applicable.

Table 1-3: Ciliopathies classified as having both structural and metabolic defects

Alström syndrome and Bardet-Biedl syndrome are also associated with developmental defects. Abbreviations: MORM: mental retardation, truncal obesity, retinal dystrophy and micropenis; OMIM: online Mendelian inheritance in man; NA: not applicable.

Symptom	Symptom incidence (%)							
	Meckel–Gruber syndrome	Joubert syndrome	Jeune asphyxiating thoracic dystrophy syndrome	Short-rib polydactyly syndrome I–IV	Cranioectodermal dysplasia (Sensenbrenner syndrome)	Orofaciodigital syndrome 1	Ellis–van Creveld syndrome	Kartagener syndrome
Structural								
Vision pathology	75–100	75–100	NA	NA	25–50	NA	NA	NA
Sensory deficit	NA	NA	NA	NA	NA	NA	NA	75–100
Endocrine and/or reproductive defect	NA	NA	NA	NA	NA	NA	NA	75–100
Pulmonary defect	NA	NA	75–100	NA	50–75	NA	NA	75–100
Renal defect	75–100	75–100	25–50	25–50	50–75	25–50	NA	NA
Hepatic defect	75–100	75–100	25–50	NA	50–75	NA	NA	NA
Developmental delay	75–100	75–100	NA	NA	NA	25–50	<25	<25
Cardiac disease	25–50	NA	NA	25–50	50–75	NA	50–75	NA
Developmental								
Skeletal defect	NA	NA	75–100	75–100	75–100	75–100	75–100	NA
Polydactyly	50–75	<25	<25	75–100	NA	25–50	75–100	NA
Situs inversus	NA	NA	NA	NA	NA	NA	NA	75–100
Brain malformation	75–100	75–100	NA	NA	NA	NA	NA	NA

Abbreviation: NA, not applicable.

Table 1-4: Ciliopathies classified as having both structural and developmental defects

Abbreviations: NA: not applicable.

Symptom	Symptom incidence (%)						
	Primary ciliary dyskinesia	Autosomal recessive polycystic kidney disease	Polycystic kidney disease	Senior–Løken syndrome	Nephronophthisis	Retinitis pigmentosa*	Leber congenital amaurosis
Vision pathology	NA	NA	NA	75–100	NA	75–100	75–100
Sensory deficit	75–100	NA	NA	NA	NA	NA	NA
Endocrine and/or reproductive defect	75–100	NA	NA	NA	NA	NA	NA
Pulmonary defect	75–100	25–50	NA	NA	NA	NA	NA
Renal defect	NA	75–100	75–100	75–100	75–100	NA	NA
Hepatic defect	NA	25–50	25–50	<25	<25	NA	NA
Developmental delay	<25	NA	NA	NA	NA	NA	NA
Cardiac disease	NA	NA	<25	NA	NA	NA	NA

*Retinitis pigmentosa is included in this Table as it demonstrates genetic and phenotypic overlap with ciliopathies such as Alström syndrome and Bardet–Biedl syndrome, although some forms of retinitis pigmentosa might have causes unrelated to defective primary cilium function. Abbreviation: NA, not applicable.

Table 1-5: Ciliopathies classified as having structural defects

*Retinitis pigmentosa (RP) is included in the ciliopathy classification as it has genetic and phenotypic overlap with ciliopathies such AS and BBS even although other forms of RP may have causes not related to defective primary cilium function. Abbreviations: NA: not applicable.

3.2. Structure of the primary cilium

The primary cilium is an evolutionary-conserved organelle that is an extension or protrusion from the cell membrane.(Badano, Teslovich et al. 2005) Nearly all mammalian cells have a single, non-motile, primary cilium. The primary cilium is comprised of a basal body, transition fiber and outer cilium. The core of the primary cilium is called the axoneme and is a microtubular backbone extending from the basal body.(Davenport and Yoder 2005) The axoneme consists of nine double microtubules in a 9+0 arrangement that distinguishes the primary cilium from motile cilia, that typically have an additional central microtubule pair giving them a 9+2 arrangement.(Dawe, Farr et al. 2006; Toriello and Parisi 2009) Non-motile 9+2 and motile 9+0 arrangements can also be found in the specific case of kinocilium in the inner ear and embryonic nodal cilium, respectively.(Fliegauf, Benzing et al. 2007)

Protein transport within the primary cilium is mediated by intra-flagellar transport (IFT). IFT consists of bidirectional transport of cargo proteins between the base and the distal tip of the cilium. Anterograde transport is mediated by kinesin II cargo proteins bound to IFT molecules and retrograde transport by Dynein.(Rosenbaum and Witman 2002; Lucker, Behal et al. 2005) Interestingly, many proteins mutated in BBS have been shown to collectively form part of the primary cilium IFT complex and have together being named the BBSome.(Yen, Tayeh et al. 2006; Leroux 2007)

The role of BBS proteins in protein transport within the primary cilium may provide a critical clue to a similar or related role of the Alms1 protein.

3.3. Primary cilium function

In the central nervous system the primary cilium acts as a sensory organelle playing a role in olfaction and photoreception and canonical and non-canonical Wnt and Shh pathways.(Fliegauf, Benzing et al. 2007; Simpson, Kerr et al. 2009; Zaghloul and Katsanis 2009) As a critical part of its sensory function the primary cilium must transport signalling molecules up and down its length via the IFT mechanism, such that a stream of freshly synthesized sensing receptors are transported from the Golgi to the tip of the primary cilium where they are inserted in the membrane and can bind to signalling molecules in the extracellular space or exposed on the membranes of adjacent cells. Conversely, signalling molecules and no longer needed receptors internalised at the tip of the primary cilium must be transported in a retrograde fashion for transmission of signals to the nucleus or for disposal, respectively. It is disruption in specific elements of this primary cilium machinery that results in the various ciliopathy phenotypes.

In renal tubular cells the primary cilium acts predominantly as a mechanical sensor, allowing the cells to sense fluid flow within the nephron lumen and thereby guiding tubular development and function, explaining how defects

in the primary cilium of the nephron lead to polycystic kidney disease.(Praetorius and Spring 2003; Deane and Ricardo 2007)

The primary cilium not only acts as a mechanical or chemical sensor but also plays a role in cellular development, morphogenesis, and homeostasis.(Davis, Brueckner et al. 2006; Michaud and Yoder 2006; Singla and Reiter 2006; Gerdes, Davis et al. 2009) The primary cilium may also have a potential role as a secretory organelle, with the presence of exosomes observed on the tip of *Chlamydomonas* flagella.(Baldari and Rosenbaum 2009). Not surprisingly, given its multiplicity of functions the primary cilium is an extremely complex structure with recent proteomic studies identifying approximately two thousand different proteins - the ciliome - involved in primary cilium function.(Liu, Tan et al. 2007; Ishikawa, Thompson et al. 2012)

3.4. AS: a new "model" ciliopathy

Clues indicating that AS might be a ciliopathy initially came from immuno-histochemistry studies showing that Alms1 protein localised to the centrosome, the structure from which the primary cilium arises.(Hearn, Spalluto et al. 2005) While clinical features of AS overlap with other ciliopathy syndromes, particularly BBS, AS patients develop more severe sensorineural deafness and early-onset T2DM and do not share the polydactyly and cognitive impairment seen in BBS.(Beales, Elcioglu et al.

1999; Badano, Mitsuma et al. 2006; Adams, Awadein et al. 2007) These differences in clinical features could help localise the exact intracellular pathways where Alms1 exerts its role. The wide spectrum of organs clinically affected in AS together with the ubiquitous tissue expression of the ALMS1 gene suggests that the Alms1 protein plays a role in many different tissues. By immuno-histochemistry, Alms1 protein localizes to the centrosome and basal bodies of the primary cilium, which could suggest a role of Alms1 in intracellular transport. (Hearn, Renforth et al. 2002; Andersen, Wilkinson et al. 2003; Hearn, Spalluto et al. 2005; Jagger, Collin et al. 2011)

4. Animal models of AS

Study of AS have been assisted by the recent availability of Alström mutant mouse models. One such Alström model was artificially generated using microinjections with Alms1 gene-trapped ES cell line in a C57BL6 background.(Collin, Cyr et al. 2005) A spontaneous AS model named the “Fat Aussie (FA) mouse" has also been reported.(Arsov, Silva et al. 2006) The FA mutation was identified by the sudden appearance of obese offspring in a non-obese diabetic (NOD) mouse colony and was found to consist of a small 11 bp deletion (*foz*) in exon 8 of the ALMS1 gene causing a frameshift and a premature stop codon (Figure 1-2). This was similar in exon location and style of mutation to ALMS1 mutations mapped in human AS cases, suggesting that exon 8 of ALMS1 forms a 'mutational hotspot'.

Due to the premature stop codon, the Alms1 protein in FA mice is truncated and missing approximately two-third of its C-terminal length.

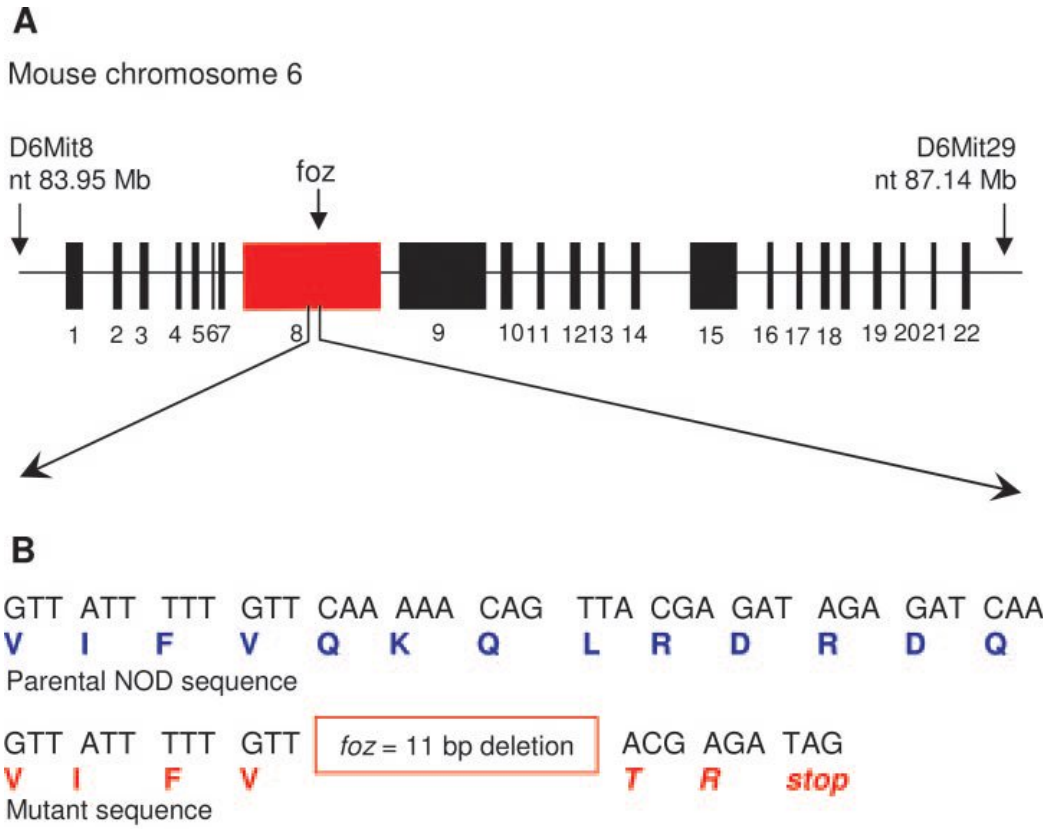

Figure 1-2: Mouse ALMS1 gene structure and *foz* deletion schematic

A: Mouse ALMS1 gene exons schematic. B: Sequence of normal and mutant cDNA showing the 11 bp *foz* deletion (nt 3918–3928) in exon 8. Normal protein (blue) and truncated protein (red) sequences are given below the normal and mutant nucleotide sequence. Abbreviations: bp: base pair; Nt, Nucleotide; Mb, megabase. (Arsov, Silva et al. 2006)

In homozygous condition (Alms1$^{foz/foz}$), FA mice demonstrate most clinical features of human AS including obesity (Figure 1-3a, 1-3b), hyperglycaemia, hyperinsulinaemia, hyperlipidaemia, steatohepatitis, infertility and sensorineuronal hearing loss.(Arsov, Larter et al. 2006; Arsov, Silva et al. 2006) Obesity in FA mice is associated with hyperphagia, as dietary restriction to the average daily food intake of a normal weight mouse, results in progressive weight loss in FA mice with stabilisation at approximately the same weight as age and sex matched wild-type littermate controls (Figure 1-3c). Whilst this suggests that obesity in FA mice is largely due to hyperphagia, FA mice also exhibit reduced locomotor activity when compared to wildtype control mice, reminiscent of the findings in obese BBS mouse models.(Davis, Swiderski et al. 2007 ; Rahmouni, Fath et al. 2008)

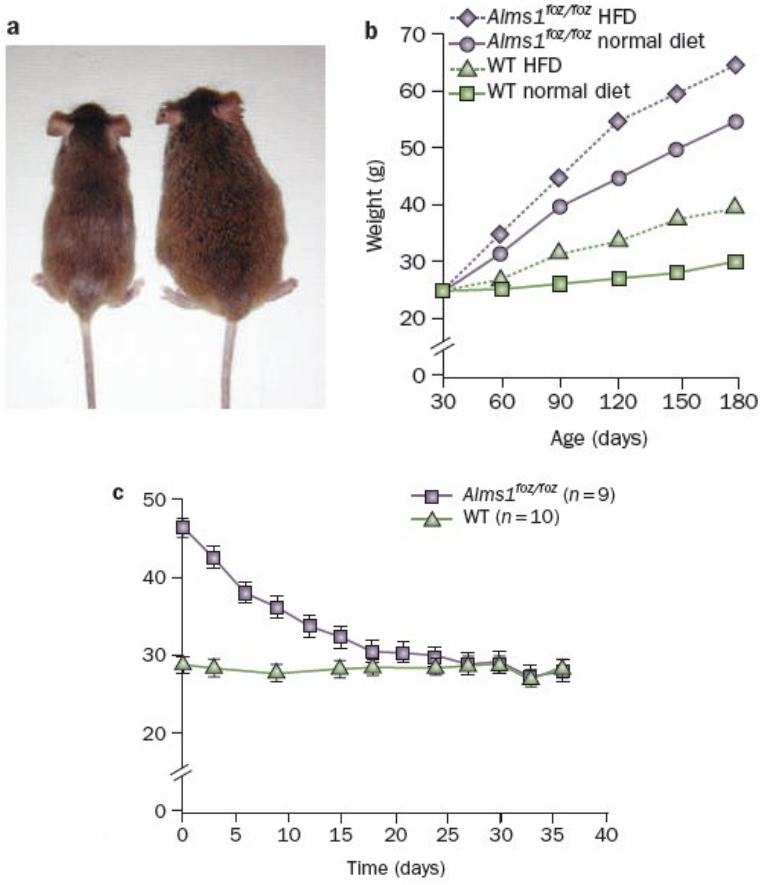

Figure 1-3: The "Fat Aussie" AS mouse model

(a) An Alms1$^{foz/foz}$ FA mouse (on right) displays severe obesity in comparison to its wildtype (WT) littermate (on left). (b) FA mice (purple lines) demonstrate greater weight gain when compared to wildtype (WT) mice (green lines) that commences from puberty and increases with age. A high fat diet (HFD) (dotted lines) exacerbates the obesity phenotype in FA mice. (c) When fed with a controlled intake of 40kJ/day (average daily energy intake for WT mice), obese FA mice (n=9; purple line) progressively lose weight and finally reach the average weight of WT littermates (n=10; green line) indicating hyperphagia is a major driver for obesity in the FA mouse. Abbreviation: FA: Fat Aussie mouse; HFD: High fat diet; WT: wildtype.

The Alms1 gene-trapped mouse also exhibits similar metabolic disturbances to human AS patients with obesity, hyperglycaemia, hyperinsulinaemia, steatohepatitis, infertility and sensorineuronal hearing loss.(Collin, Cyr et al. 2005) This shows the high level of consistency between both the spontaneous and genetically-manipulated AS mouse models and the human AS phenotype. For example, a high fat diet induced a saturation of the adipose tissue in FA mice leading to lipid partitioning in the liver and steatosis that progressed to steatohepatitis, mimicking human non-alcoholic fatty liver disease seen in AS subjects.(Arsov, Larter et al. 2006; Larter, Yeh et al. 2009) One small difference, however, is that whereas human AS subjects predominantly had elevation of plasma triglycerides rather than cholesterol, FA mice predominantly had elevation of plasma cholesterol rather than triglycerides.

Alms1 gene-trapped mice at 24 weeks of age had an abnormal accumulation of intracellular vesicles in the inner segments of their retinal photoreceptors, with rhodopsin being mislocalized to the outer nuclear layer, consistent with a role of Alms1 protein in intracellular transport.(Collin, Cyr et al. 2005) Expression of a dominant-negative, GDP-locked version of the Rab8 gene associated with BBS in *Xenopus laevis* photoreceptors, similarly caused rhodopsin to accumulate at the base of the connecting cilium.(Moritz, Tam et al. 2001) This highlights the close similarity between AS and BBS, consistent with a commonality of disrupted pathways. Electron microscopy of motile nasal epithelium, retinal connecting cilia and kidney primary cilia

appeared normal in the Alms1 gene-trapped mice, suggesting that the Alms1 protein is not involved in cilium development or, alternatively, that the mutant truncated Alms1 protein in these mice was sufficient for this function.(Collin, Cyr et al. 2005)

Unlike other genetic models of obesity such as leptin knockout mice where obesity commences during early infancy, in the FA model of AS body fat accumulation was only apparent from 6-8 weeks of age onwards (Figure 2b). With increasing age, both male and female FA mice developed hyperinsulinaemia, hyperleptinaemia and hyperglycaemia consistent with progressive insulin and leptin resistance. Insulin acts to decrease appetite via insulin receptors in the brain (Schwartz, Woods et al. 2000) and thus hyperinsulinaemia, a typical feature of AS, may contribute to the hyperphagia observed in FA mice. Insulin is stored in a granule pool in β-cells.(Bratanova-Tochkova, Cheng et al. 2002) Hypothalamic leptin resistance has been postulated to play a central role in the obesity of BBS mouse models and may similarly play a major role in AS models.(Rahmouni, Fath et al. 2008; Seo, Guo et al. 2009) Pancreatic islets are enormously hypertrophied in diabetic FA and gene-trapped AS mouse models, being up to ten times larger than in wildtype mice.(Collin, Cyr et al. 2005; Arsov, Silva et al. 2006) This is consistent with compensatory islet hypertrophy and hyperinsulinemia driven by severe insulin resistance. Many hypertrophied FA islets featured central cystic/necrotic spaces that may

reflect a form of loss of islet growth regulation through disruption of the primary cilium function in islet cells (Arsov, Silva et al. 2006).

FA mice exhibited hyperphagia, a major contributing factor to their development of obesity.(Arsov, Silva et al. 2006) The hypothalamus plays a key role in food intake and energy expenditure through hormonal and neuronal signals (Ellacott and Cone 2004; Coll, Farooqi et al. 2007). Specific hypothalamic regions regulate food intake with the ventromedial hypothalamic nucleus (VMN) acting as the 'satiety centre' and the lateral hypothalamic area as the 'hunger centre'. The arcuate nucleus (ARC) is also an important area with a key role in the energy balance pathway of hypothalamic coupled neurons: neuropeptide Y (NPY)/agouti-related protein (AGRP) and propiomelanocortin (POMC)/cocaine and amphetamine related transcript (CART) neurons. These two sets of hypothalamic neurons have antagonist actions; NPY/AGRP neurons mediate orexigenic (hyperphagic) signals whereas POMC/CART neurons mediate anorexigenic (hypophagic) signals.(Schwartz, Woods et al. 2000) Interestingly, genetic knockout mice for proteins involved in hypothalamic intra-flagellar transport IFT also display hyperphagia and severe obesity just like FA AS mice.(Davenport, Watts et al. 2007; Satir 2007) All neurons have a primary cilium (Fuchs and Schwark 2004; Whitfield 2004; Berbari, Bishop et al. 2007), IFT plays a role in hypothalamic neuron function and the Alms1 protein is expressed in the hypothalamus. It is possible, therefore, that Alms1 mutations disrupt hypothalamic satiety and hunger signalling via

disruption of IFT transport in hypothalamic coupled neurons.(Gupta PS, Prodromou NV et al. 2009; Mok, Héon et al. 2009)

Consistent with a broader neuronal role both FA and gene-trapped AS mutant mice display sensory hearing loss with abnormal auditory brain response (ABR). One role of the primary cilium in neurons is to guide axonal migration. One potential explanation for the sensorineural defects in AS, therefore could be that mutant Alms1 disrupts normal axonal development and migration. Such a neuronal IFT defect could similarly underlie the hypogonadotrophic hypogonadism observed in AS models.(Collin, Cyr et al. 2005; Arsov, Silva et al. 2006)

A recent study focused on kidney defects in another AS mouse model generated by ethyl nitroso urea-forward genetic screen. This study identified an age-dependent loss of tubular cell primary cilia, with dilated tubules being found in kidneys of six month old AS mice. It was reassuring that this third AS model also shared common phenotypic features with the previous two AS mouse models, supporting the consistency of the AS phenotype across different murine models. (Li, Vega et al. 2007)

5. Postulations on Alms1 protein function

Research into AS and BBS is casting new light on cellular pathways involved in a wide range of conditions including obesity, T2DM and heart disease. The growing importance of ciliopathy research is highlighted by the fact that multiple ciliopathy databases have been created including the CentrosomeDB Database (Nogales-Cadenas, Abascal et al. 2009), the Ciliome Database (Inglis, Boroevich et al. 2006) and the Ciliaproteome. (Gherman, Davis et al. 2006) Most recently, a database called Cildb has been created dedicated to proteins involved in centrioles, centrosomes, basal bodies, cilia and flagella in eukaryotes.(Arnaiz, Malinowska et al. 2009)

The ALMS1 gene is expressed ubiquitously but better understanding of Alms1 protein function may assist understanding of common diseases such as obesity, T2DM and heart disease. AS mouse models provide a powerful research tool and, for example, the FA mouse has proven to be useful for the study of the pathogenesis of non-alcoholic steatohepatitis (NASH).(Arsov, Larter et al. 2006; Larter, Yeh et al. 2009; Teoh, Williams et al. 2010; Van Rooyen, Larter et al. 2011; Arteel 2012) Still, relatively little is known about the Alms1 protein function but data supports its involvement in primary cilium function, particularly intracellular trafficking and protein transport by microarray analysis (Genter, Van Veldhoven et al. 2003) and proteomics studies.(Andersen, Wilkinson et al. 2003; Liu, Tan et al. 2007)

After maturation, proteins need to be transported from the Golgi apparatus to other parts of the cell including the primary cilium and Alms1 may participate in this transport. The primary cilium uses IFT to transport molecules to and from the cell membrane. Proteins involved in IFT belong to the cilium proteome or "ciliome"(Gherman, Davis et al. 2006; Inglis, Boroevich et al. 2006) BBS is caused by mutations in proteins that interact with Rab8 and mediate the movement of proteins to the membrane by the IFT cargo complex.(Leroux 2007; Nachury, Loktev et al. 2007) Alms1 is a large protein and may similarly play a role in the IFT cargo complex trafficking proteins within the cilium (Figure 1-4).

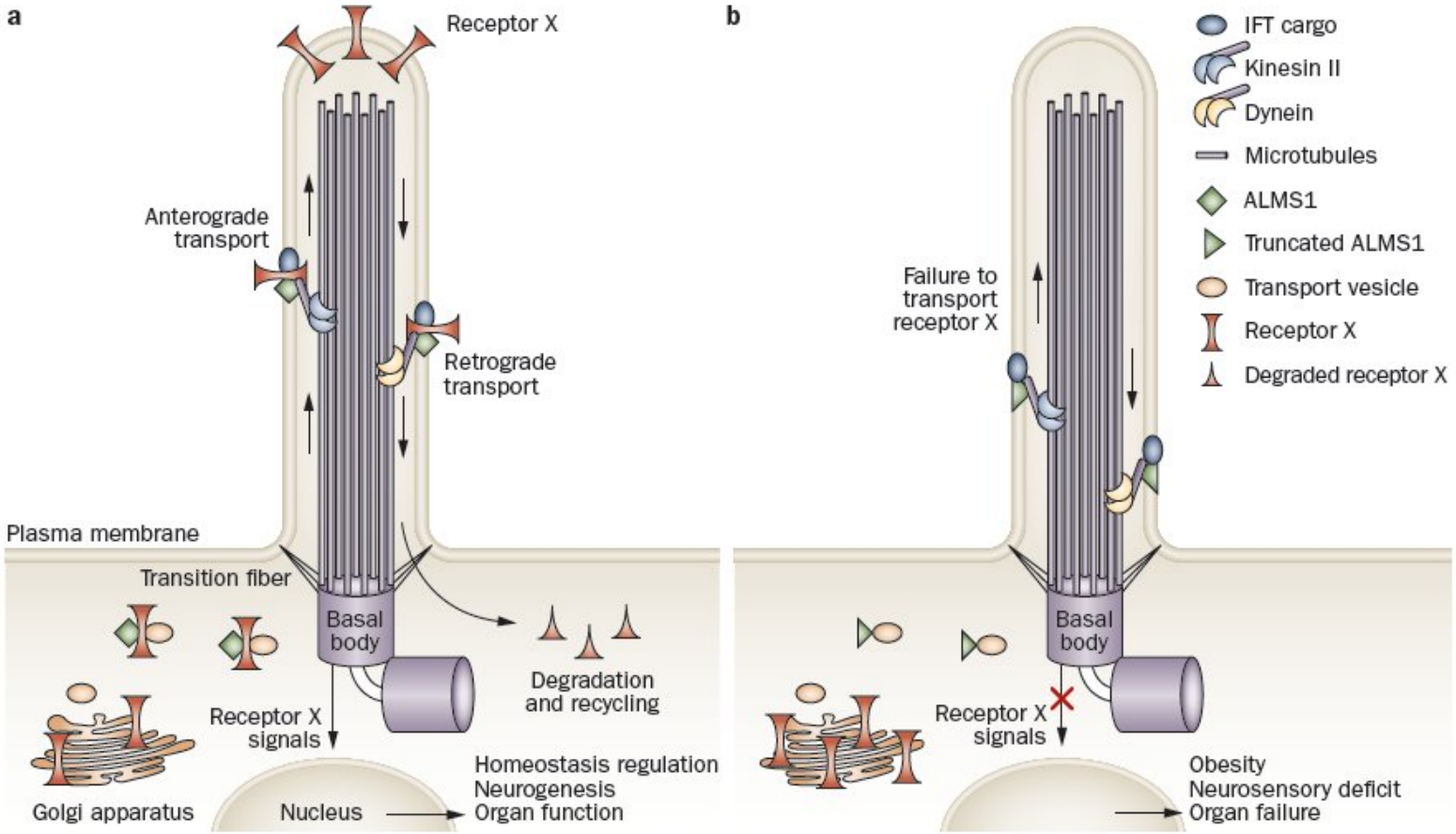
a
Receptor X
Anterograde transport
Retrograde transport
Plasma membrane
Transition fiber
Basal body
Degradation and recycling
Receptor X signals
Golgi apparatus
Nucleus
Homeostasis regulation
Neurogenesis
Organ function
b
IFT cargo
Kinesin II
Dynein
Microtubules
ALMS1
Truncated ALMS1
Transport vesicle
Receptor X
Degraded receptor X
Failure to transport receptor X
Basal body
Receptor X signals
Obesity
Neurosensory deficit
Organ failure

Figure 1-4: Postulated function of Alms1 protein

a: The native Alms1 protein might be involved in intracellular trafficking to the primary cilium membrane of one or more as yet uncharacterized receptors (eg: 5HT6, SSTR3 or MCHR1) depicted in the figure as 'Receptor X'. Alms1 could be involved in vesicle transport from the Golgi apparatus to the cilium and/or in IFT transport. In this model, signals received from Receptor X contribute to the regulation of cellular homeostasis, neurogenesis or organ function. b: The mutant truncated Alms1 fails to transport Receptor X via Golgi vesicle transport and/or IFT thus inducing defective cell signalling. The lack of Receptor X signalling in AS leads to obesity, neurosensory deficit and organs failure. Abbreviations: 5HT6: 5-hydroxytryptamine receptor 6; IFT: intraflagellar transport; MCHR1: melanin concentrating hormone receptor 1; SSTR3: somatostatin receptor 3.

IFT transport is not restricted to ciliated cells and has been found to occur in immune cells with a role in immune synapse formation.(Finetti, Paccani et al. 2009) A mislocalisation or deficient transport of specific receptors within the cilium will have a deleterious effect on cell signalling. Receptors such as the somatostatin receptor 3 (SSTR3), melanin concentrating hormone receptor 1 (MCHR1) and 5-hydroxytryptamine receptor 6 (5HT6) are known to be transported within neuronal primary cilia.(Händel, Schulz et al. 1999; Brailov, Bancila et al. 2000; Pazour and Witman 2003; Berbari, Lewis et al. 2008; Stanic, Malmgren et al. 2009) Of note, the MCHR1 receptor is involved in the regulation of energy homeostasis (Chen, Hu et al. 2002) explaining how disrupted transport of this receptor might lead to obesity, and similarly a disruption of SSTR3 and 5HT6 signalling in hypothalamic neurons could adversely affect energy expenditure and feeding behaviour leading to obesity.

Other receptors shown to traffic in the cilium include integrins in Madin–Darby canine kidney (MDCK) cells (Praetorius, Praetorius et al. 2004), vasopressin receptors (VR2) in renal epithelial cells (Raychowdhury, Ramos et al. 2009) and dopamine receptors in fibroblasts and neurons.(Marley and von Zastrow 2010) Interestingly, the insulin like growth factor 1 (IGF-1) receptor shows higher sensitivity to insulin when it localises to the primary cilium indicating that even where a receptor is expressed elsewhere on the cell membrane, its failure to localize on the primary cilium may impact overall cell signalling.(Zhu, Shi et al. 2009)

Of potential interest to research into the cause of obesity in AS, recent studies have indicated a role of the primary cilium in adipose tissue. Using a murine preadipocyte cell line, 3T3-L1, Alms1 mRNA was found to be lost during adipocyte differentiation, suggesting a role in early adipogenesis. Differentiating 3T3-L1 cells display a transient primary cilium and dysfunction in this primary cilium during adipogenesis could, therefore, contribute to the pathogenesis of obesity.(Marion, Stoetzel et al. 2009) However, changes in adipocyte insulin sensitivity did not affect Alms1 expression in 3T3-L1 preadipocytes.(Romano, Milan et al. 2008) Defective 3T3-L1 adipocyte differentiation due to Alms1 gene knockdown was associated with moderate impairment in glucose uptake indicating that adipocyte insulin signaling and sensitivity is adversely affected when Alms1 expression is reduced.(Huang-Doran and Semple 2010) However, the relatively modest effect observed when Alms1 is knocked down in adipocytes suggests that the major site of the severe insulin resistance observed in AS is elsewhere, such as in the muscle or liver.

Experiments using kidney epithelial cells showed abnormal primary cilium formation when ALMS1 gene expression was suppressed with siRNA. The stunted–cilium phenotype was rescued with a 5' fragment of ALMS1 cDNA, suggesting Alms1 plays a role in development of the primary cilium in some cells.(Li, Vega et al. 2007) A stunted–cilium phenotype was also observed when ALMS1 gene expression was knocked down in hTERT-RPE1 retinal pigment epithelial cells.(Graser, Stierhof et al. 2007) However, in contrast to

the aforementioned studies, fibroblasts with disrupted ALMS1 expression were found to have normal primary cilia.(Hearn, Spalluto et al. 2005) The explanation for such differences may lie in the fact that these knockdown studies were designed to suppress expression of the whole Alms1 protein, whereas, in AS subjects and in the mouse models described below a truncated Alms1 protein is expressed that may maintain some primary cilium functions. Thus, it is still possible that most clinical features of AS result from the mutated Alms1 protein causing impaired function of the primary cilium rather than defective structural development.

Alms1 protein may also be involved in vesicle exocytosis. Studies have shown abnormal accumulation of rhodopsin vesicles in the retina of AS mouse models, suggesting mutation of Alms1 may disrupt transport of vesicles or disrupt the exocytosis mechanism itself by, for example, interfering with vesicle docking.(Collin, Cyr et al. 2005) Defective secretion of insulin vesicles with a consequent accumulation in islet β cells could also be a contributing factor to the massive islet hypertrophy observed in AS.(Collin, Cyr et al. 2005; Arsov, Silva et al. 2006)

Recently, the ALMS1 gene was reported to be regulated by factor Sp1 and transcription factors belonging to the regulatory factor X (RFX) family.(Purvis, Hearn et al. 2010) RFX transcription factors are involved in development and

maintenance of nodal cilia.(Bonnafe, Touka et al. 2004) In the mouse embryo, beating nodal cilia generate a leftward nodal flow that defines left/right asymmetry.(Essner, Vogan et al. 2002) Impaired ciliary development can lead to disruption of nodal flow causing *situs inversus* or embryonic death.(Nonaka, Tanaka et al. 1998; Essner, Vogan et al. 2002; Nonaka, Shiratori et al. 2002) *Situs inversus* is frequently observed in BBS and Kartagener syndrome (Table 2) but is not a feature of AS suggesting that Alms1 is not directly involved in nodal cilia function.

6. Therapy of AS

There is no specific therapy for AS with treatment remaining supportive. With only several hundred AS patients scattered worldwide, systematic large-scale clinical trials to identify the most effective medical treatments for the many clinical conditions that can occur in AS or patients with other ciliopathies is simply not possible. In this respect the availability of mouse models of AS represent a major breakthrough enabling specific testing of candidate therapies to identify those most beneficial for AS patients. This is important given the complexity of the cellular pathways involved. For example, AS patients with T2DM may not behave identically to typical T2DM patients, as the severity of the insulin resistance appears to be a much worse in AS than typical T2DM.

Thus, for example, the massive islet hypertrophy seen in AS models is not typical of islet histology in other models of T2DM.

The main causes of death in AS are from heart, kidney or liver failure.(Benso, Hadjadj et al. 2002; Marshall, Bronson et al. 2005) Major morbidity comes from vision and hearing loss and T2DM. Early diagnosis is important to allow counselling of parents and institution of appropriate supportive medical treatment.

The major clinical treatment focus is on control of obesity and T2DM treatment. The insulin sensitisers, metformin and thiazolidenediones, are appropriate first and second line treatments, given the severe underlying insulin resistance in T2DM complicating AS.(Sinha, Bhangoo et al. 2007) Positive glycaemic effects in diabetic AS subjects of the glucagon like peptide (GLP)-1 analogue, exenatide, have recently been reported.(Paisey 2009) Caloric restriction helps control obesity, glucose intolerance and hyperinsulinemia (Holder, Hecker et al. 1995; Paisey, Hodge et al. 2008; Lee, Marshall et al. 2009) although dietary compliance may be a major problem as is seen with children with other genetically acquired obesity syndromes. Lipid lowering therapy with statins or fibrates can help control AS-associated hyperlipidaemia.(Paisey 2009)

Given the evidence of impaired growth hormone (GH)-IGF1 axis function in AS, therapy with recombinant (rhGH) has been reported to be beneficial for some metabolic parameters in isolated cases.(Tai, Lin et al. 2003; Mihai, Catrinoiu et al. 2008; Mihai, Catrinoiu et al. 2009) Hypothyroidism requires therapy with L-thyroxine. Testosterone supplementation is an option for hypogonadal male patients and metformin and estroprogestin compounds have been successfully used to manage irregular menses in female AS patients.(Marshall, Beck et al. 2007) Successful heart-lung and kidney transplantation have been reported for AS patients with terminal cardiomyopathy or renal failure. (Marshall, Bronson et al. 2005; Goerler, Warnecke et al. 2007; Hitz, Bertram et al. 2008)

In the absence of specific therapy to correct the underlying genetic defect, AS remains a progressive disease and regular medical follow up is important to track progression and watch for the emergence of new symptoms and disease manifestations. Given that cardiomyopathy, kidney and liver disease are the main causes of death, regular cardiac, renal and liver review should be routinely performed in all AS patients.

7. Conclusions

Apart from polycystic kidney disease (PKD), the ciliopathies are relatively uncommon medical disorders, individually affecting as few as one per million population. As awareness of the ciliopathies grows amongst clinicians and scientists, so too does the number of human disorders identified as being mediated by primary cilium dysfunction. The recent development of murine models of AS and BBS provide powerful new tools for researchers to identify the cellular role of proteins including Alms1 that when mutated lead to cilium dysfunction. Thus, research into AS could provide unique insights into the role of Alms1 protein in endocrine signalling pathways as well as shedding light on pathogenic mechanisms of more common disorders with shared clinical features including obesity, T2DM, retinal degeneration, hearing loss, cardiomyopathy and renal failure.

8. Research aims and plan

This project has been focusing on the phenotypic characterisation of the Alms1$^{foz/foz}$ mouse model of AS. The Alms1$^{foz/foz}$ mouse represents a unique tool to provide new insights into the pathogenicity of AS associated disorders and shed lights into the function of Alms1 protein.

Metabolic disorders such as insulin resistance and obesity are the cardinal symptoms in children with AS but little is known about the onset of these features. The first aim of this project was to better characterise the extent of metabolic disorders by comparing 6 month old Alms1$^{foz/foz}$ with wildtype controls and determine what primary defect occurs in young (< 60days old) non obese Alms1$^{foz/foz}$ mice. A possible role of Alms1 protein in the insulin pathway signalling was also investigated.

T2DM and T1DM share common ground and recent reports suggest that obesity and insulin resistance may accelerate the onset of T1DM in children. In the following study, the *foz* mutation was backcrossed into a NOD background in order to investigate the impact of metabolic disorders on the onset and progression of auto-immune T1DM using female NOD/Alms1$^{foz/foz}$ mice.

The function of Alms1 protein in CNS function is unknown. In the next study, the involvement of Alms1 protein in neuronal function was investigated by characterising the cognitive function of Alms1$^{foz/foz}$ mice compared to wildtype controls and assessing if the Alms1 protein was transported via axonal trafficking.

To finish, the possible role of Alms1 protein in cellular trafficking was further investigated by characterising the catecholamine secretory activity of Alms1$^{foz/foz}$ chromaffin cells by amperometry and determining if the *foz* mutation impacted on the mechanism of exocytosis.

Chapter 2 : Characterisation of early onset insulin resistance in Alms1$^{foz/foz}$ mice

1. Abstract

The "Fat Aussie" (FA) mouse is a model for Alström syndrome (AS) developing the same disorders seen in human patients. From 60 days of age onwards Alms1$^{foz/foz}$ mice exhibit a strong metabolic phenotype leading to severe obesity and type 2 diabetes mellitus (T2DM). As T2DM requires combined defects of insulin resistance and a relative insulin deficiency, the objective was to investigate whether peripheral insulin resistance or an insulin secretory defect comes first in young, non-obese, pre-diabetic Alms1$^{foz/foz}$ mice. Insulin tolerance tests (ITT), intraperitoneal glucose tolerance tests (IPGTT), fasting and post-challenge serum insulin levels and HOMA-IR score determination were performed in age and sex-matched young lean Alms1$^{foz/foz}$ mice and wildtype littermates. Insulin sensitive tissues were also harvested for Western blot in order to assess the integrity of the insulin signalling pathway in 6 month old non-fasted Alms1$^{foz/foz}$ mice. When compared to wildtype littermates, young Alms1$^{foz/foz}$ mice had a significantly reduced glucose lowering response to insulin during the ITT while after the IPGTT no differences were observed in the glucose profile and endogenous insulin levels. Male Alms1$^{foz/foz}$ mice had significantly higher fasting hyperinsulinemia and HOMA-IR scores compared to wildtype littermates with a similar trend in female Alms1$^{foz/foz}$ mice but which did not reach statistical significance. Insulin pathway signalling was intact down to the level of pAS160 in Alms1$^{foz/foz}$ mice.

These data indicate that insulin resistance precedes the development of obesity in young Alms1$^{foz/foz}$ mice and prior to the development of any observable relative insulin secretory deficiency. Thus early peripheral insulin resistance appears to be an inherent primary consequence of the Alms1$^{foz/foz}$ mutation and may thereby drive the subsequent metabolic complications in the FA mouse model. It also suggests that the native Alms1 protein may play a hitherto unrecognised role in the insulin signalling pathway at the level of Glut4 translocation.

Key words: obesity, insulin resistance, hyperinsulinenia, adipocyte hypertrophy, insulin pathway.

2. Introduction

Strong metabolic defects distinguish Alström syndrome (AS) from other ciliopathies with the exception of Bardet-Biedl (BBS) and MORM syndromes showing milder metabolic phenotype.(Girard and Petrovsky 2011) Cardiomyopathy and organ failure are the main causes of death in AS but obesity and T2DM cause high morbidity and reduce the quality of life of AS patients.(Marshall, Maffei et al. 2011) AS is characterized by childhood truncal obesity, hyperinsulinemia and severe insulin resistance progressing towards

type 2 diabetes mellitus (T2DM).(Marshall, Bronson et al. 2005) The onset and development of obesity and T2DM remain unclear and due to the restricted number of patients, the possibilities of undertaking clinical studies are limited. Thus, AS represents a monogenic model of metabolic syndrome.

The study of AS mouse models provides an alternative to investigate the onset and progression metabolic phenotype associated with AS. A previous study has shown that spontaneous mutant Alms1$^{foz/foz}$ mice develop hyperphagia and show increasing body weight from 60 days old onwards. Along with body weight gain, adult Alms1$^{foz/foz}$ mice display an impaired response to glucose challenge.(Arsov, Silva et al. 2006) Interestingly, in both Alms1$^{foz/foz}$ and gene-trapped Alms1$^{-/-}$ mice, obesity was associated with hyperinsulinemia suggesting peripheral and/or hepatic insulin resistance.(Collin, Cyr et al. 2005; Arsov, Silva et al. 2006) The relationship between increasing body weight and insulin resistance needs further investigation and in particular to determine what is the primary defect that drives Alms1$^{foz/foz}$ mice to develop insulin resistance and T2DM.

Young (< 60days old) and 6 month old Alms1$^{foz/foz}$ and wildtype littermates were used to evaluate the extent of their metabolic disorders and investigate what primary impairment leads Alms1$^{foz/foz}$ mice to insulin resistance and T2DM. The integrity of the insulin pathway was also assessed by Western blot

in insulin sensitive tissues from 6 month old non-fasted Alms1$^{foz/foz}$ and wildtype controls.

3. Material and methods

Animal maintenance

This study was performed in accordance with the recommendations in the "Australian code of practice for the care and use of animals for scientific purposes" of the National Health and Medical Research Council. This project was approved by the Animal Ethics Committee of Flinders University under the approval number #671/08.

Alms1$^{foz/foz}$ mice and Alms1$^{+/+}$ (WT) littermates were maintained on a C57BL/6J background in the animal facility at Flinders Medical Centre in a 12 hourly light/dark cycle. Mice had free access *ad libitum* to water and either normal chow containing 5.4% fat, energy content 12 MJ/kg (Gordon's rat and mouse maintenance pellets, Gordon's specialty stockfeeds, Australia) or high fat diet (HFD) containing 23% Fat, High Simple carbohydrate, 0.19% cholesterol, energy content 20 MJ/kg (SF03-020, Specialty feeds, Australia). Primers

flanking the *foz* mutation were used for PCR genotyping: forward ACA ACT TTT CAT GGC TCC AGT; reverse TTG GCT CAG AGA CAG TTG AAA.

Insulin resistance monitoring by ITT and IPGTT

Mice were tested for insulin resistance by the insulin tolerance test (ITT) and intraperitoneal glucose tolerance test (IPGTT). The ITT screening is used to assess insulin sensitivity using an exogenous insulin challenge. Following injection, the response to insulin is seen as a reduction of plasma glucose levels as glucose is transported by GLUT4 into insulin-sensitive tissues (liver, fat and muscle) as well as a suppression of hepatic glucose production. For the ITT, mice were fasted 4 hours with no access to food but free access to water. Mice were weighed and insulin (Humulin R, Eli Lilly, USA) was injected ip at 0.75 U/kg body weight in 0.9% saline for injection (Pfizer, USA). The tail was snipped for blood collection and the plasma glucose was determined for each mouse using a glucometer (Optium Xceed, Abbott, USA) and blood glucose test strips (Optium point of care, Abbott, USA) at 0, 15, 30 and 60 min after insulin injection.

The IPGTT assay is used to assess the capacity of mice to produce insulin and uptake glucose. Following glucose injection, plasma glucose rises and then decreases in response to endogenous insulin release. For the IPGTT, mice were fasted 18 hours and injected at 2mg/g body weight with D-glucose (Analar,

VWR, USA) in 0.9% saline for injection. Plasma glucose was determined for each mouse using a glucometer with sampling via tail vein at 0, 15, 30, 60 and 120 min after glucose injection.

Plasma insulin measurement

Blood was collected on conscious animals via cheek bleeding. After collection, blood samples were kept on ice and spun at 17000g, 10min at 4˚C. Insulin levels were assayed using a commercial ultrasensitive mouse insulin ELISA kit (Crystal Chem Inc., USA).

HOMA-IR scoring

The homeostasis model assessment of insulin resistance (HOMA-IR) index was calculated using individual mouse fasting insulin and fasting glucose levels. The following formula was used: HOMA-IR = [fasting glucose (mg/dL) × fasting insulin (μU/mL)]/405.

Adipored staining of adipose tissue and microscopy analysis

Fat tissue was isolated and briefly washed in PBS (3.2 mM Na2HPO4, 0.5 mM KH2PO4, 1.3 mM KCl, 135 mM NaCl, pH 7.4). Samples were then placed in 4% paraformaldehyde (in 0.1M sodium phosphate buffer, pH 7.2) for 15 min

and then washed in PBS. Samples were incubated in AdipoRed dye (1/25; Lonza, Switzerland) and 30µM DAPI (Sigma-Aldrich, USA) in PBS for 15 minutes then washed 3 times with PBS. Samples were mounted on slides and pictures were taken using BX50 fluorescence microscope (Olympus, Japan).

Polyclonal sheep anti-Alms1$_{Nter}$ antibody generation

An adult sheep was injected intramuscularly at week 1, 4 and 7 with Alms1 N_{ter} peptide C-MEPEDLPWPDELE conjugated with KLH (keyhole limpet hemocyanin) carrier. Antibodies generated against this peptide sequence can recognise both human and murine Alms1 protein. For the prime injection, 0.5mg of KLH-Alms1$_{Nter}$ was co-administered subcutaneously (SC) with complete Freund's adjuvant. For two following boost injection, 0.5mg of KLH-Alms1$_{Nter}$ was injected subcutaneously with incomplete Freund's adjuvant. 20ml of sheep blood was sampled before the prime injection (pre-immune) and one week after boost injections for Alms1 N_{ter} peptide direct ELISA screening. At week 8, the sheep was bled-out and serum collected. Polyclonal sheep anti-Alms1$_{Nter}$ antibodies were affinity purified with Alms1$_{Nter}$ peptide coupled to CNBr-activated Sepharose 4B beads (GE Healthcare, UK).

Western blotting

Male Alms1$^{foz/foz}$ and WT littermates were anaesthetised. The following insulin sensitive tissues: liver, heart, muscle and adipose tissue were harvested and directly placed in RIPA buffer (Tris 50mM, NaCl 150 mM, 0.1% SDS, 1% Triton-X100) supplemented with Complete mini protease inhibitor cocktail and PhosSTOP phosphatase inhibitor cocktail (Roche, Switzerland). Samples were sonicated and centrifuged 30 min at 17 000g, 4°C 30min. Protein concentration assayed with BCA assay (Thermo Fisher Scientific, USA). Sample were boiled at 100°C for 10min and 25µg of protein was loaded in a 5% stacking, 10% separation acrylamide gel following by transfer into 0.2µm PVDF membrane using "Mixed protein" program on Transblot Turbo (Bio-rad, USA). Membrane was blocked 30 min in 5% Milk in TBS-T (50mM Tris, 150mM NaCl, 0.05% Tween-20), quickly rinsed in TBS-T and then incubated overnight at 4˚C with the following detection antibodies (1/1000, CST, USA): rabbit anti-C/EBPα, rabbit anti AS160; rabbit anti phosho-AS160, rabbit anti-phospho-Akt, rabbit rabbit anti-Akt, D7C5 rabbit anti-IRAP and rabbit anti-glut4 (1/1000; Merck Millipore, USA) and mouse anti-GAPDH as loading control (1/5000; Abcam, UK). Membrane was incubated 1h at RT with anti-rabbit-HRP (1/3000, CST, USA), biotin anti-mouse IgG1 (1/10000, Abcam, UK) with streptavidin-HRP (1/2000, BD, USA), anti-goat-HRP (1/10000, Sigma-Aldrich, USA). Membrane was washed with TBS-T and incubated with either SuperSignal

West Pico Chemiluminescent substrate or SuperSignal West Femto Chemiluminescent substrate (Thermo Fisher Scientific, USA). Western blot pictures were taken using ImageQuant LAS 4000 imager (GE Healthcare, UK).

Statistical analysis

Statistical analyses were performed using GraphPad Prism 5 software (GraphPad Software, Inc., USA). Results are presented as mean ± SEM (standard error of the mean). Unpaired student t test or the non-parametric Mann-Whitney U test was used for statistical comparison of BMI and AUC data. A p value <0.05 was considered statistically significant.

4. Results

Alms1$^{foz/foz}$ mice display obesity, insulin resistance and type 2 diabetes.

Six month old Alms1$^{foz/foz}$ mice were obese with an average body weight of 45.5g ± 1.7g compared to 26.4g ± 1.3g for wildtype littermates ($p<0.001$, Figure 2-1A). Mice were injected with a standard insulin injection of 0.75U/kg body weight and their glycemia was followed for an hour post injection. Plasma glucose levels in Alms1$^{foz/foz}$ mice after 4h fasting were higher than wildtype

mice. The glucose response to insulin in Alms1$^{foz/foz}$ mice during ITT was impaired. Alms1$^{foz/foz}$ mice glycemia hardly changed during the ITT with only a slight decrease observed 30 minutes post insulin injection. Therefore, Alms1$^{foz/foz}$ mice glucose levels were higher than the level of wildtype littermates at all time points ($p<0.001$, Figure 2-1B; $p=0.007$ Figure 2-1C). These data confirm that adult Alms1$^{foz/foz}$ mice have reduced insulin sensitivity in association with obesity.

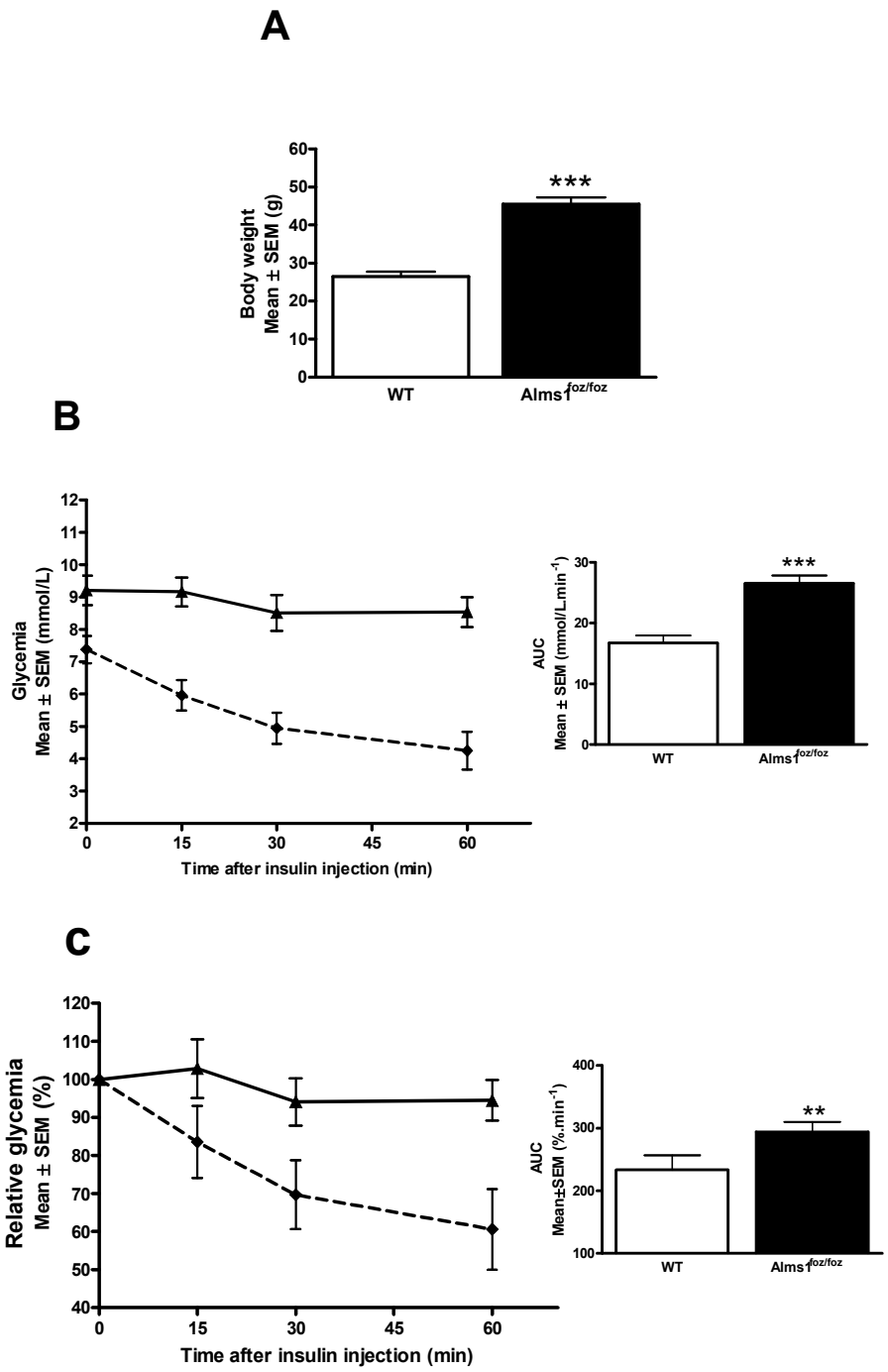
A
Body weight
Mean ± SEM (g)
***
WT
Alms1foz/foz
B
Glycemia
Mean ± SEM (mmol/L)
Time after insulin injection (min)
AUC
Mean ± SEM (mmol/L.min-1)
***
WT
Alms1foz/foz
C
Relative glycemia
Mean ± SEM (%)
Time after insulin injection (min)
AUC
Mean±SEM (%.min-1)
**
WT
Alms1foz/foz

Figure 2-1: Body weight record and ITT screening in 6 month old Alms1$^{foz/foz}$ mice

6 month old Alms1$^{foz/foz}$ mice (plain line, black bar, n=15) and wildtype littermates (dotted line, white bar, n=11) were challenged with an injection of insulin at 0.75U/kg body weight. A: Body weight; B: Blood glucose monitoring during ITT; C: Relative blood glucose monitoring during ITT. Abbreviations: AUC: area under curve; ITT: insulin tolerance test; SEM: standard error of the mean, WT: wildtype. ** $p<0.01$; *** $p<0.001$.

Alms1$^{foz/foz}$ mice were then placed on a high fat diet (HFD) and were regularly screened by ITT. When Alms1$^{foz/foz}$ mice are fed with HFD, the obesity phenotype is exacerbated.[6]

As previously seen with mice on a normal chow diet, Alms1$^{foz/foz}$ mice on a HFD didn't respond to ITT with an insulin injection of 0.75U/kg body weight. Indeed, Alms1$^{foz/foz}$ mice on a HFD needed more than 20 times the standard insulin dose to achieve a reduction in their plasma glucose ($p<0.001$, Figure 2-2A and 2-2B). This suggests that dietary modulation by HFD markedly aggravates the insulin resistance in Alms1$^{foz/foz}$ mice.

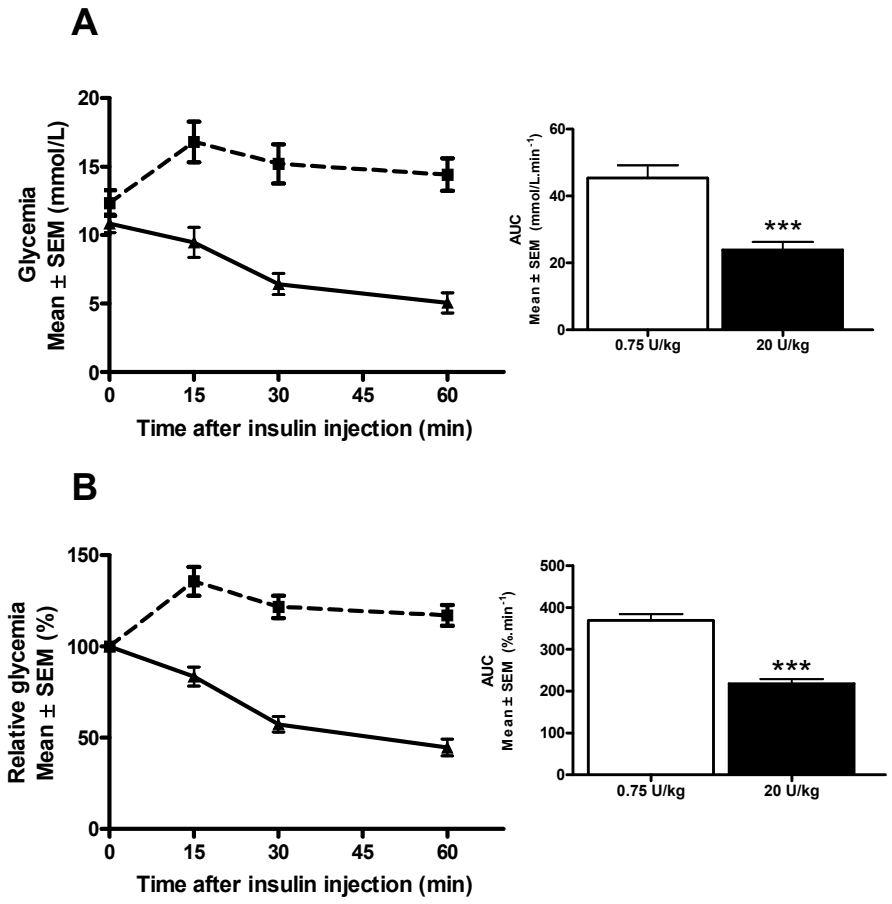

Figure 2-2: ITT screening in 6 month old Alms1$^{foz/foz}$ mice fed with high fat diet

6 month old Alms1$^{foz/foz}$ mice (n=19) fed with HFD were challenged with an injection of insulin at 0.75U/kg (dotted line, open bar) or 20 U/kg body weight (plain line, black bar). A: Blood glucose monitoring during ITT; B: Relative blood glucose monitoring during ITT. Abbreviations: AUC: area under curve; HFD: high fat diet; ITT: insulin tolerance test; SEM: standard error of the mean. *** $p<0.001$.

Another sign of insulin resistance was seen when 6 month old Alms1$^{foz/foz}$ mice were tested for IPGTT. Alms1$^{foz/foz}$ mice showed a significantly higher fasting glycemia compared to wildtype mice (p=0.002, Figure 2-3A). This suggests that FA mice fail to maintain glycemia even when in the fasted state. During the IPGTT, mice were injected with D-glucose and their glycemia was followed for 2 hours post injection. Alms1$^{foz/foz}$ mice showed a significant delay in glucose uptake and their plasma glucose never reached the level of wildtype mice (p=0.004, Figure 2-3B). These data confirm insulin resistance as a major contributor to T2DM in Alms1$^{foz/foz}$ mice.

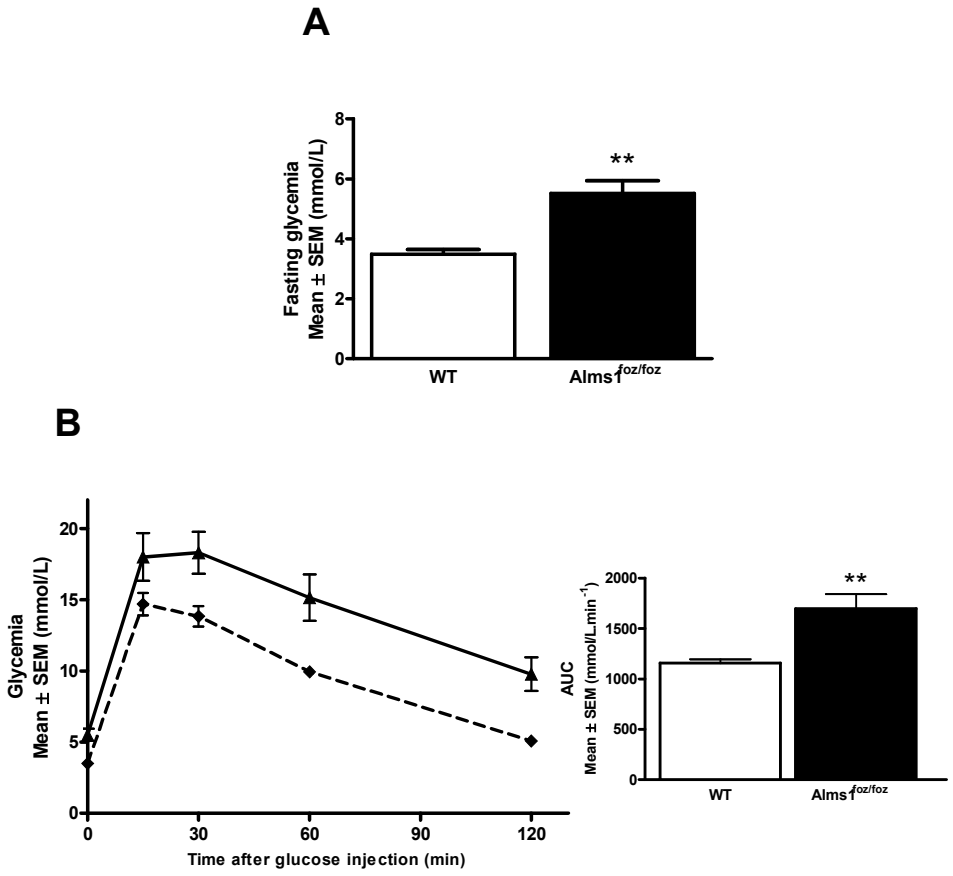

Figure 2-3: Fasting glycemia and IPGTT screening in 6 month old Alms1$^{foz/foz}$ mice

6 months old Alms1$^{foz/foz}$ mice (plain line, black bar, n=7) and wildtype littermates (dotted line, white bar, n=11) mice were challenged with an injection of D-glucose at 2mg/g body weight. A: Fasting blood glucose; B: Blood glucose monitoring during IPGTT. Abbreviations: AUC: area under curve; IPGTT: intraperitoneal glucose tolerance test; SEM: standard error of the mean. ** $p<0.01$

Alms1$^{foz/foz}$ mice display early insulin sensitivity defect

In order to investigate further what primary defect is causing the metabolic defect seen in Alms1$^{foz/foz}$ mice, young weight-matched mice were used for metabolic phenotype screening. Use of young lean Alms1$^{foz/foz}$ mice gave the advantage of removing the confounding effect of the obesity on insulin signalling.

When male Alms1$^{foz/foz}$ mice are less than 60 days old, their body weight (24.2 ± 0.7g) is similar to wildtype littermates (23g ± 0.6g) (NS; Figure 2-4A). Young Alms1$^{foz/foz}$ males were injected with insulin and their glycemia was followed for an hour post injection. As seen before in older Alms1$^{foz/foz}$ mice, young Alms1$^{foz/foz}$ males' glycemia after 4 hours fasting was higher compared to wildtype mice. Male Alms1$^{foz/foz}$ mice also showed a significantly decreased insulin sensitivity compared to wildtype littermates with their glycemia staying above wildtype controls ($p<0.001$, Figure 2-4B). During the ITT Alms1$^{foz/foz}$ mice responded less to exogenous insulin than wildtype littermates ($p<0.001$; Figure 2-4C). These data indicate an early insulin sensitivity defect in male Alms1$^{foz/foz}$ mice that precedes the development of obesity.

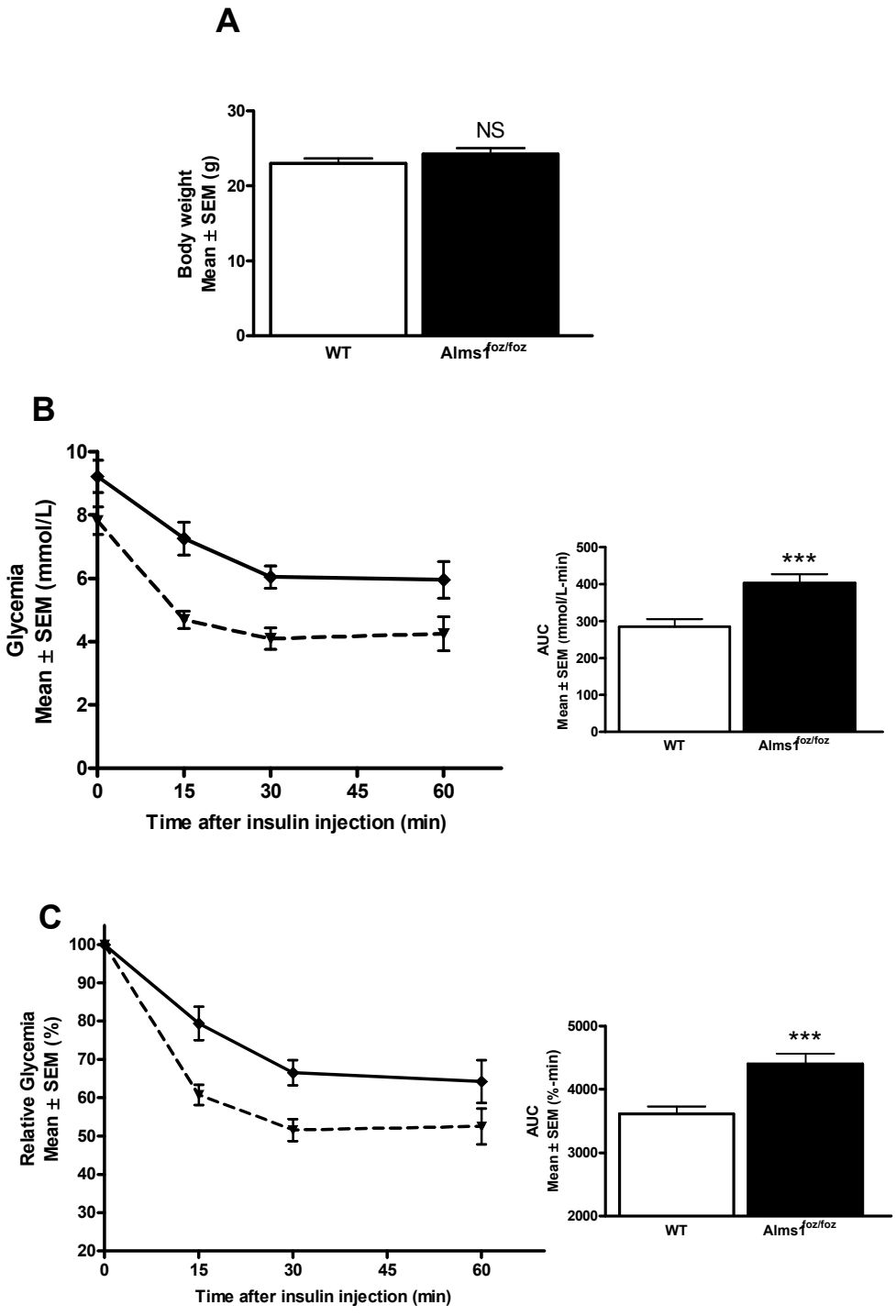
A
Body weight
Mean ± SEM (g)
30
20
10
0
NS
WT
Alms1foz/foz
B
Glycemia
Mean ± SEM (mmol/L)
10
8
6
4
2
0
0
15
30
45
60
Time after insulin injection (min)
AUC
Mean ± SEM (mmol/L-min)
500
400
300
200
100
0
***
WT
Alms1foz/foz
C
Relative Glycemia
Mean ± SEM (%)
100
90
80
70
60
50
40
30
20
0
15
30
45
60
Time after insulin injection (min)
AUC
Mean ± SEM (%-min)
5000
4000
3000
2000
***
WT
Alms1foz/foz

Figure 2-4: Body weight and ITT screening in young Alms1$^{foz/foz}$ males

<60 days old male Alms1$^{foz/foz}$ mice (plain line, black bar, n=11) and wildtype littermates (dotted line, white bar, n=15) were challenged with an injection of insulin at 0.75U/kg body weight. A: Body weight; B: Blood glucose monitoring during ITT; C: Relative blood glucose monitoring during ITT. Abbreviations: AUC: area under curve; ITT: insulin tolerance test; NS: not significant; SEM: standard error of the mean; WT: wildtype. *** $p<0.001$

Young weight-matched female Alms1$^{foz/foz}$ and wildtype mice were also tested by ITT with wildtype mice weighting 21.2g ± 0.8g and mutant Alms1$^{foz/foz}$ weighing 22.2g ± 1.0g (NS; Figure 2-5A). Like Alms1$^{foz/foz}$ male, female Alms1$^{foz/foz}$ mice baseline glycemia was higher compared to wildtype females and after insulin injection, Alms1$^{foz/foz}$ mice glycemia never reached the glycemia of wildtype controls (p=0.013; Figure 2-5B). However, female Alms1$^{foz/foz}$ relative glycemia response after insulin injection was not significantly different to wildtype littermates. (NS; Figure 2-5C) This suggests that young female Alms1$^{foz/foz}$ mice show the same defect in baseline glycemia equivalent to male Alms1$^{foz/foz}$ mice but at this particular age female insulin sensitivity upon exogenous insulin injection is not impaired.

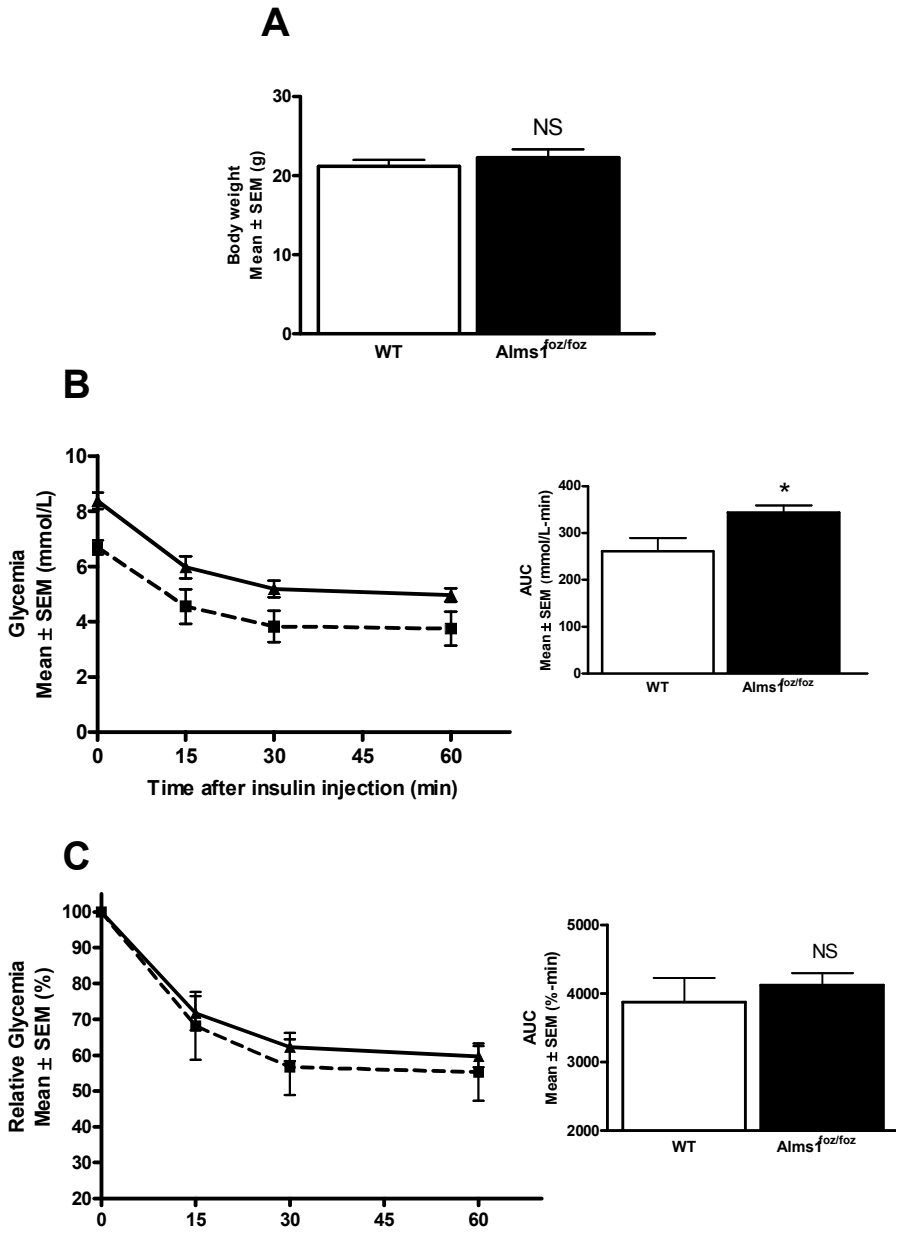
A
Body weight
Mean ± SEM (g)
30
20
10
0
NS
WT
Alms1foz/foz
B
Glycemia
Mean ± SEM (mmol/L)
10
8
6
4
2
0
0
15
30
45
60
Time after insulin injection (min)
AUC
Mean ± SEM (mmol/L-min)
400
300
200
100
0
*
WT
Alms1foz/foz
C
Relative Glycemia
Mean ± SEM (%)
100
90
80
70
60
50
40
30
20
0
15
30
45
60
AUC
Mean ± SEM (%-min)
5000
4000
3000
2000
NS
WT
Alms1foz/foz

Figure 2-5: Body weight and ITT screening in young Alms1$^{foz/foz}$ females

<60 days old female Alms1$^{foz/foz}$ mice (plain line, black bar, n=10) and wildtype littermates (dotted line, white bar, n=8) were challenged with an injection of insulin at 0.75U/kg body weight. A: Body weight; B: Blood glucose monitoring during ITT; C: Relative blood glucose monitoring during ITT. Abbreviations: AUC: area under curve; ITT: insulin tolerance test; NS: not significant; SEM: standard error of the mean; WT: wildtype. * $p<0.05$

Weight-matched Alms1$^{foz/foz}$ and wildtype male and female were then tested for glucose disposal by endogenous insulin production during IPGTT. Young Alms1$^{foz/foz}$ mice had similar 18 hours fasting plasma glucose levels to wildtype controls (NS; Figure 2-6A). After glucose injection, Alms1$^{foz/foz}$ mice plasma glucose response was similar to wildtype littermates (NS; Figure 2-6B). These data show that Alms1$^{foz/foz}$ mice are able to produce insulin and can efficiently regulate their glycemia during IPGTT. It suggests that the production of insulin by the β-cells in the pancreas is not affected at this age.

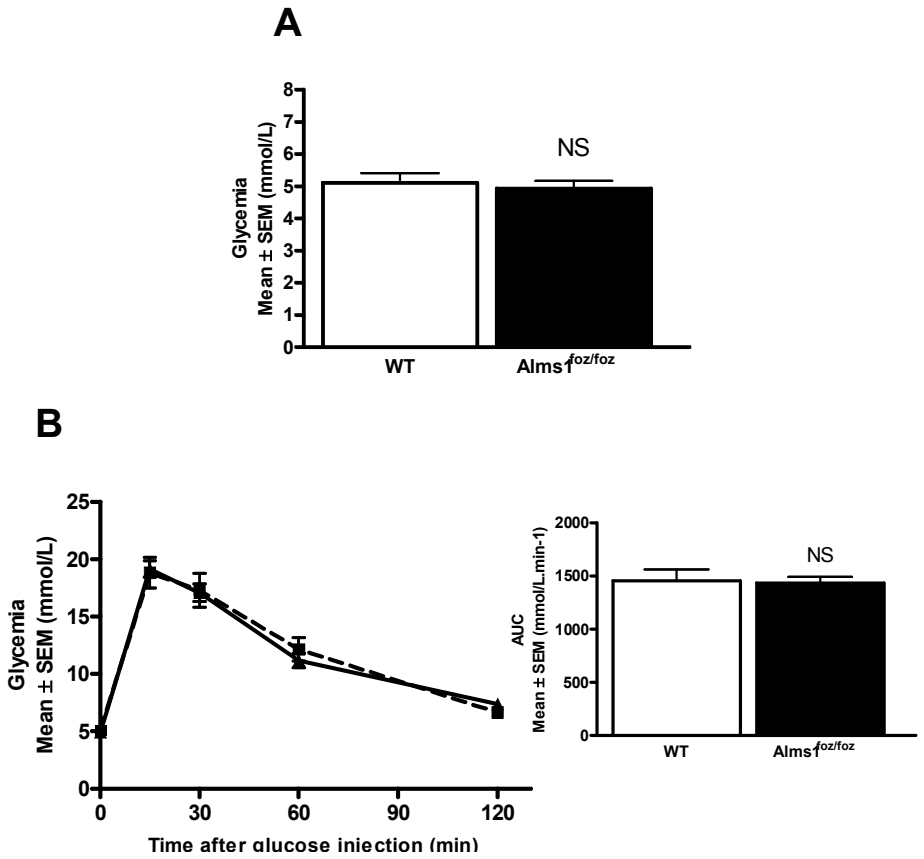

Figure 2-6: Body weight and IPGTT screening in young Alms1$^{foz/foz}$ mice

<60 days old Alms1$^{foz/foz}$ mice (plain line, black bar, n=19) and wildtype littermates (dotted line, white bar, n=18) were challenged with an injection of D-glucose at 2mg/g body weight. A: Fasting blood glucose; B: Blood glucose monitoring during IPGTT. Abbreviations: AUC: area under curve; IPGTT: intraperitoneal glucose tolerance test; NS: not significant; SEM: standard error of the mean; WT: wildtype.

Alms1$^{foz/foz}$ mice display early-onset hyperinsulinemia and insulin resistance.

In order to further investigate if young Alms1$^{foz/foz}$ mice show signs of insulin resistance, mice were fasted 18 hours in order to determine their fasting insulinemia and calculate a HOMA-IR score.

As previously seen, male Alms1$^{foz/foz}$ mice have a similar fasting glycemia compared to wildtype (NS; Figure 2-7A) but have significantly higher fasting insulin levels (p=0.009; Figure 2-7B). Male Alms1$^{foz/foz}$ mice had a significantly higher HOMA-IR score than wildtype mice, consistent with insulin resistance (p=0.017; Figure 2-7C).

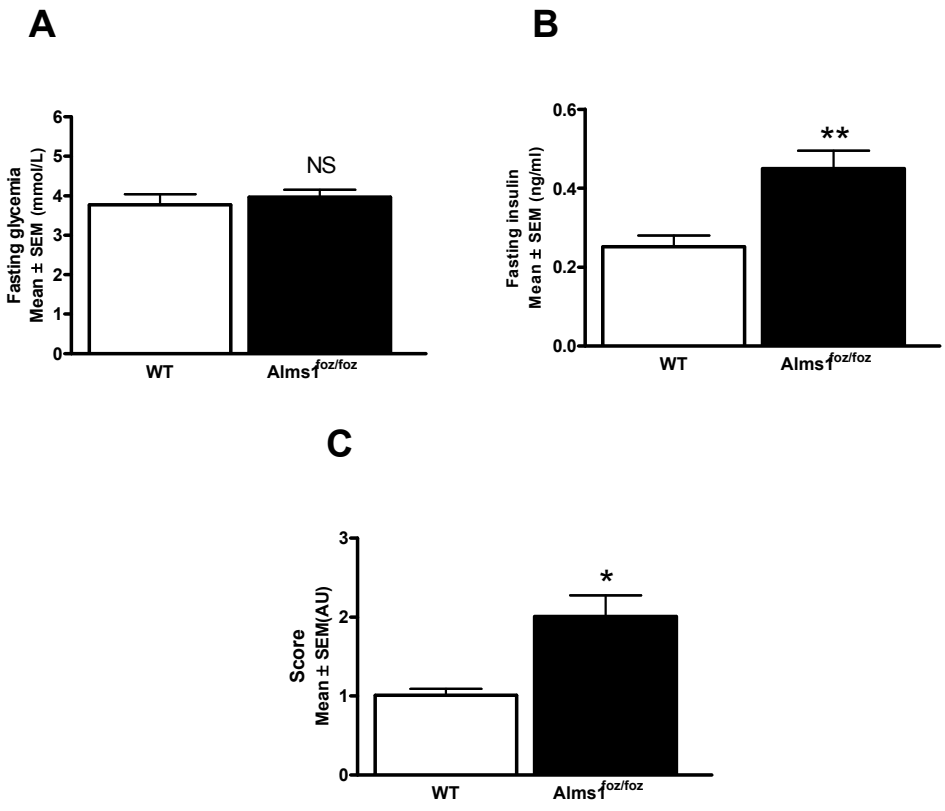

Figure 2-7: Fasting parameters and HOMA-IR scoring in young Alms1$^{foz/foz}$ males

<60 days old male Alms1$^{foz/foz}$ mice (black bar, n=11) and wildtype littermates (white bar, n=6) fasting parameters and HOMA-IR scores were determined. A: Fasting blood glucose; B: Fasting insulinemia concentration; C: HOMA-IR scoring. Abbreviations: AU: arbitrary unit; HOMA: Homeostatic model assessment; IR: insulin resistance; NS: not significant; SEM: standard error of the mean; WT: wildtype. * $p<0.05$; ** $p<0.01$

Interestingly, young female Alms1$^{foz/foz}$ mice did not show signs of insulin resistance with an average fasting glucose, fasting insulin and HOMA-IR score similar to wildtype female littermates (NS; Figure 2-8A, 2-8B, 2-8C).

This suggests that young female Alms1$^{foz/foz}$ mice have less pronounced metabolic defects than young male Alms1$^{foz/foz}$ mice.

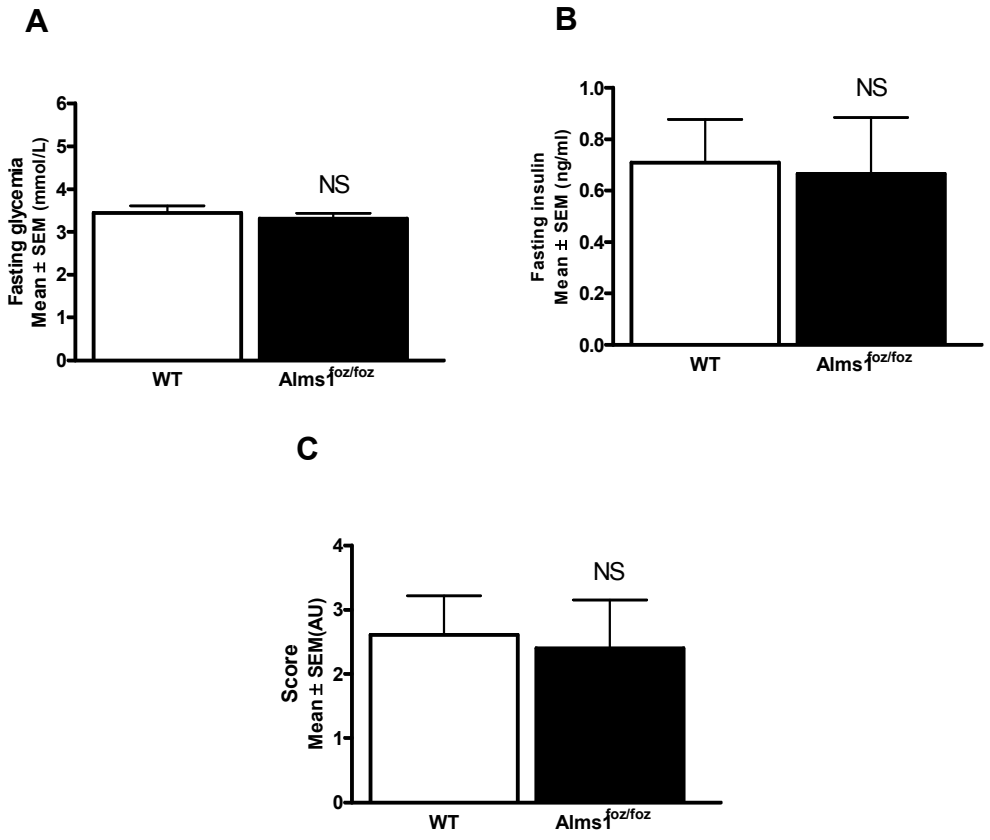

Figure 2-8: Fasting parameters and HOMA-IR scoring in young Alms1$^{foz/foz}$ females

<60 days old female Alms1$^{foz/foz}$ mice (black bar, n=9) and wildtype littermates (white bar, n=13) fasting parameters and HOMA-IR scores were determined. A: Fasting blood glucose; B: Fasting insulinemia concentration; C: HOMA-IR scoring. Abbreviations: AU: arbitrary unit; HOMA: Homeostatic model assessment; IR: insulin resistance; NS: not significant; SEM: standard error of the mean; WT: wildtype.

Young Alms1$^{foz/foz}$ mice display reduced insulin sensitivity but this defect could still be associated with a relative β-cell secretory defect. In order to further investigate a possible defect in insulin secretion by pancreatic β-cells, plasma insulin levels were measured in response to glucose challenge. Alms1$^{foz/foz}$ mice showed higher insulin production compared to wildtype mice, confirming that β-cells in young Alms1$^{foz/foz}$ mice remain fully functional (NS, Figure 2-9). However, FA mice have markedly enlarged islets and this result does not exclude a reduced insulin secretory capacity of each individual Alms1$^{foz/foz}$ β-cell.

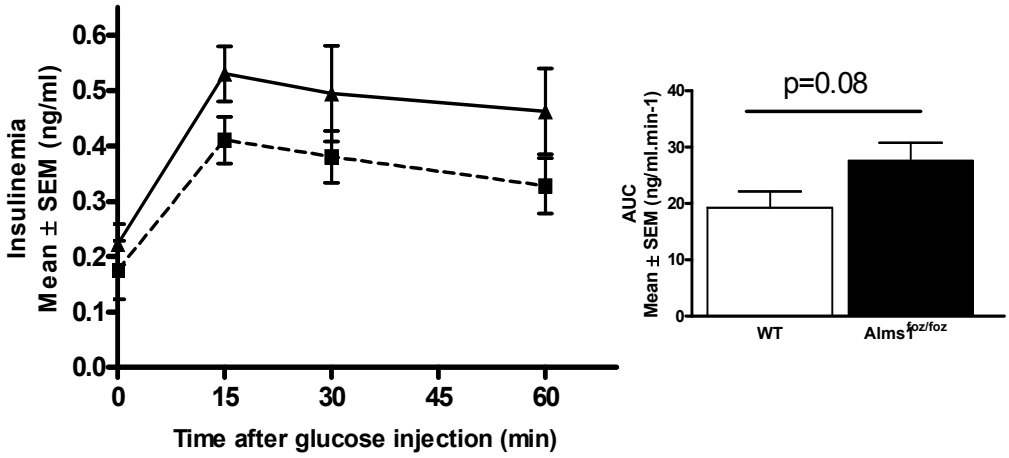

Figure 2-9: Endogenous insulin response following glucose challenge in young Alms1$^{foz/foz}$ mice

<60 days old Alms1$^{foz/foz}$ mice (plain line, black bar, n=9) and wildtype littermates (dotted line, white bar, n=6) insulinemia time-course monitoring following D-glucose challenge at 2mg/g body weight. Abbreviations: AUC: area under curve; SEM: standard error of the mean; WT: wildtype.

Obese Alms1$^{foz/foz}$ mice have adipocyte hypertrophy.

Alms1$^{foz/foz}$ mice display increasing body weight from 60 days old onwards. This is mainly due to hyperphagia, leading to increased fat tissue mass. Obesity could reflect either a higher number of adipocytes or greater adipocyte size. Interestingly, using Adipored staining of fat, young lean Alms1$^{foz/foz}$ male mice already showed enlarged adipocytes compared to age and weight-matched wildtype littermates (Figure 2-10A, 2-10B). Adipocyte size increased with age in both mutant and wildtype mice but Alms1$^{foz/foz}$ adipocytes became increasingly large and hypertrophic (Figure 2-10C, 2-10D). These data indicate that the increasing adipose mass in Alms1$^{foz/foz}$ mice is not due to adipocyte hyperplasia but to adipocyte hypertrophy due to increased triglyceride storage.

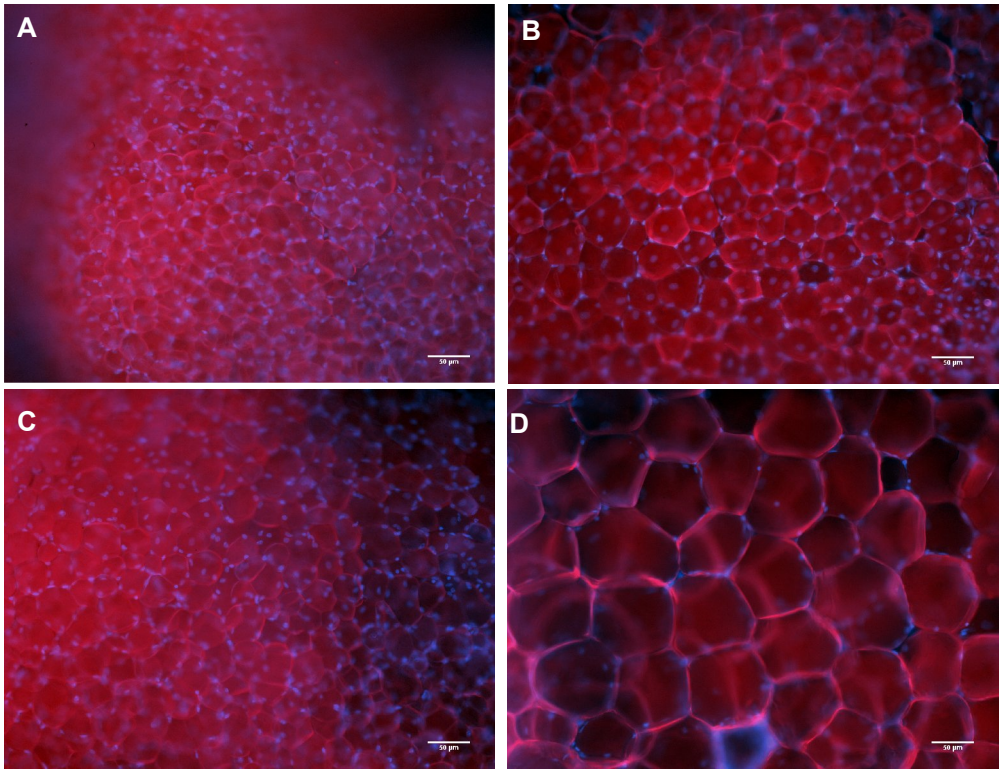

Figure 2-10: Alms1$^{foz/foz}$ mouse adipocyte morphology

Representative Adipored (red) and Dapi (blue) staining of male Alms1$^{foz/foz}$ and wildtype littermates' visceral adipose tissue, objective 10X. A: 60 days old WT body weight <25g; B: 120 days old wildtype body weight 30-35g; C: 60 days old Alms1$^{foz/foz}$ body weight <25g; D: 120 days old Alms1$^{foz/foz}$ body weight 40-45g. Abbreviations: WT: wildtype.

The insulin pathway is intact down to the level of pAS160 in Alms1$^{foz/foz}$ mice

Western blot was performed on insulin sensitive tissues harvested from 6 month old non-fasted Alms1$^{foz/foz}$ and wildtype littermates in order to investigate if the insulin pathway was disrupted in the Alms1$^{foz/foz}$ condition. Results showed that the expression of IRAP, GLUT4, Akt and C/EBP-α was similar or higher in Alms1$^{foz/foz}$ condition with the exception of heart IRAP expression. Interestingly, without insulin stimulation, pAS160 and pAkt expression was higher in Alms1$^{foz/foz}$ tissues, especially in white adipose tissue (WAT). (Figure 2-11) These data suggests an upregulation of the insulin pathway in non-fasted state. It also indicates that the insulin pathway is intact in Alms1$^{foz/foz}$ mice down to the phosphorylation of AS160. Thus, the defect leading to insulin resistance in Alms1$^{foz/foz}$ mice must be downstream AS160 phosphorylation

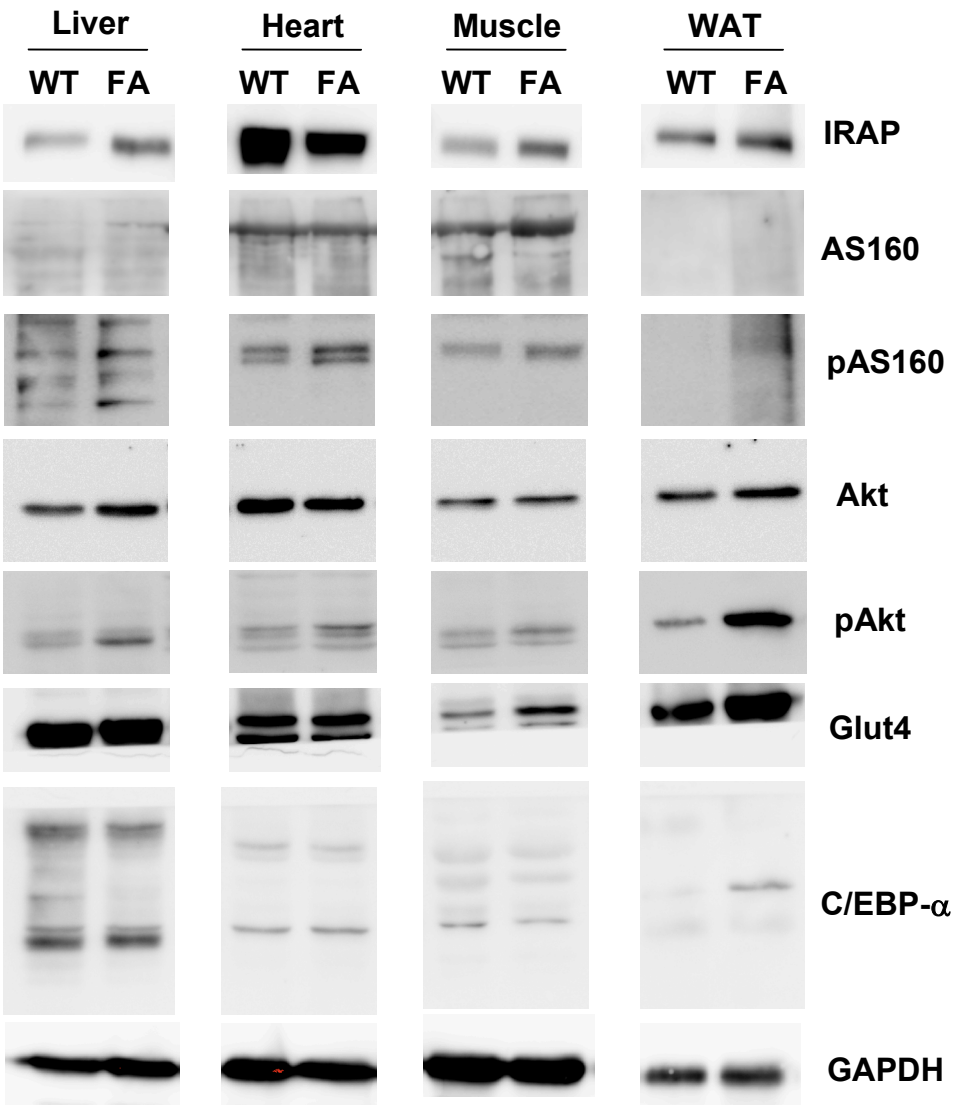
Liver
Heart
Muscle
WAT
WT FA
WT FA
WT FA
WT FA
IRAP
AS160
pAS160
Akt
pAkt
Glut4
C/EBP-α
GAPDH

Figure 2-11: Insulin pathway proteins screening by Western blot on 6 month old non-fasted Alms1$^{foz/foz}$ insulin sensitive tissues

6 month old non-fasted Alms1$^{foz/foz}$ and wildtype liver, heart, muscle and WAT insulin signalling pathway proteins were screened by Western blot. 25μg of total protein were loaded per lane in SDS-PAGE. Abbreviations: AS160 (or TBC1D4): Akt Substrate of 160 kDa; C/EBP-α: CCAAT/enhancer-binding protein alpha; FA: "Fat Aussie"; GAPDH: Glyceraldehyde 3-phosphate dehydrogenase; Glut4: Glucose transporter 4; IRAP: Insulin-regulated aminopeptidase; IRS1: Insulin receptor substrate 1; WAT: white adipose tissue; WT: wildtype.

5. Discussion

Clinical case reports on AS patients often describe contradictory outcomes. One study showed that OGTT response of 15 AS patients was similar to age-matched controls and in AS insulin responses increase between 7-18 years old. (Bettini, Maffei et al. 2012) After 18 years the study showed insulin production declines along with decreasing β-cell function.(Bettini, Maffei et al. 2012) Another study on 7 AS children showed that fasting glycemia was normal but random blood glucose values were elevated.(Mokashi and Cummings 2011) However, the most consistent disorder in AS is insulin resistance which is more severe in AS than in typical T2DM.(Minton, Owen et al. 2006)

In the present study, FA mouse model of AS was used to assess the extent of impairment of glucose metabolism and investigate what primary defect drives Alms1$^{foz/foz}$ mice towards insulin resistance and T2DM.

ITT and GTT in 6 months old Alms1$^{foz/foz}$ mice highlighted a phenotype of severe obesity, insulin resistance and T2DM. The failure of Alms1$^{foz/foz}$ mice to respond normally to insulin in the ITT is consistent with peripheral and/or hepatic insulin resistance whereas the delayed glucose utilisation during IPGTT is consistent with superimposed β-cell insulin secretory impairment.

Obesity is also another parameter that could be directly causing insulin resistance in FA mice since data shows that increased obesity due to a high fat diet aggravates the deficient response to insulin in Alms1$^{foz/foz}$ mice.

Using young and weight-matched FA mice helped identify the primary defect leading to insulin resistance and T2DM. Both young Alms1$^{foz/foz}$ male and female mice displayed an early defect in 4 hour fasting glucose when compared to wildtype mice. This suggests an early insulin resistance that worsens with increasing age and obesity. The onset of insulin resistance and hyperinsulinemia was more severe in male compared to female Alms1$^{foz/foz}$ mice, suggesting gender-related differences in onset of the metabolic disorders in FA mice.

According to the IPGTT and fasting insulinemia screening, Alms1$^{foz/foz}$ mice show a peripheral defect in the ability to respond to insulin at a time when the mice were not obese and there was no deficiency in insulin production and release. This suggests that reduced insulin sensitivity in FA mice is not primarily due to obesity. Thus, early insulin resistance may be an inherent consequence of the Alms1$^{foz/foz}$ mutation and may drive the subsequent metabolic complications in the FA mouse model.

In this study, another observation was early onset adipocyte hypertrophy in Alms1$^{foz/foz}$ male mice suggesting excessive lipid storage. These data could

suggest that the adipose tissue is still insulin sensitive at this stage. Therefore, the main source of insulin resistance might come from either the liver, muscle or both. Interestingly, it has been reported in AS patients that obesity (BMI and waist circumference) decreases with age, whereas insulin resistance increases with age.(Minton, Owen et al. 2006) This suggests that with age and progression of the metabolic complications, the adipose tissue becomes less responsive to insulin. Other mechanisms involved in adipocyte hypertrophy could include increased macrophage infiltration and/or excessive lipolysis (Sun, Kusminski et al. 2011).

Finally, this study has shown that the insulin pathway is intact in Alms1$^{foz/foz}$ mice insulin responsive tissues from the phosphorylation of Akt down to the phosphorylation of AS160. AS160 is involved in the final step of the insulin signalling pathway. Upon insulin stimulation, pAS160 allows the translocation of GLUT4 from the cytoplasm to the cell membrane, which then leads to the intracellular uptake of glucose.(Sakamoto and Holman 2008; Stockli, Davey et al. 2008) Western blot results suggest that the defect leading to insulin resistance in Alms1$^{foz/foz}$ mice must be downstream of AS160 phosphorylation and might concern either the translocation of GLUT4 or its recycling.

Chapter 3： NOD/Alms1$^{foz/foz}$ mice are protected against both spontaneous and cyclophosphamide-induced Type 1 Diabetes Mellitus

1. Abstract

The "Accelerator hypothesis" suggests that childhood obesity and associated insulin resistance may by accelerating β cell death be an underlying cause for recent global increases in incidence of autoimmune type 1 diabetes mellitus (T1DM). To test this hypothesis, obese NOD mice were generated by introduction of a hyperphagia-promoting mutation, by backcrossing them with "Fat Aussie" mice (Alms1$^{foz/foz}$) that carry a spontaneous mutation in exon 8 of the ALMS1 gene. NOD/Alms1$^{foz/foz}$ mice, as expected, became increasingly obese starting from 90 days of age. Female NOD/Alms1$^{foz/foz}$ and NOD wildtype control mice were monitored for diabetes and insulin resistance by ITT, GTT and HOMA-IR scoring. Surprisingly, although obese NOD/Alms1$^{foz/foz}$ mice became increasingly insulin resistant and hyperglycaemic, they were protected against autoimmune β-cell destruction as determined by preservation of insulin secretory capacity and reduced insulitis on pancreas histology. Obese NOD/Alms1$^{foz/foz}$ mice were then placed in restricted diet (RD) to assess whether the protective effect of obesity and/or insulin resistance on T1DM could be reversed. When the weight and glucose tolerance of NOD/Alms1$^{foz/foz}$ mice on RD was reduced to normal they continued to be hyperinsulinemic and remained protected against spontaneous and cyclophosphamide-induced T1DM. These data do not support the "Accelerator hypothesis", but instead

suggest that insulin resistance and/or hyperinsulinemia, whether obesity-associated or genetically-induced, are protective against autoimmune diabetes.

Keys words: Spontaneous type 1 diabetes mellitus, type 2 diabetes mellitus, hyperinsulinemia, cyclophosphamide.

2. Introduction

Type 1 diabetes mellitus (T1DM) is the result of insulin deficiency arising from immune-mediated destruction of insulin-producing β cells. (Bach 1994) Conversely, type 2 diabetes mellitus (T2DM) is caused by genetic or obesity-mediated insulin resistance associated with impaired insulin secretion.(James and Piper 1994; Association 2006) The recent explosion in childhood obesity raises the important question of how this might impact on the incidence of T1DM.

The "accelerator hypothesis" proposes that the increasing T1DM incidence is actually being driven by the rise in childhood obesity, with obesity-associated insulin resistance and associated hyperinsulinemia acting to accelerate autoimmune β cells destruction.(Wilkin 2001; Wilkin 2009; Wilkin 2011) This is supported by data showing that T1DM diabetes occurs at a younger age in

children with higher body weight.(Kibirige, Metcalf et al. 2003; Betts, Mulligan et al. 2005; Kordonouri and Hartmann 2005; Donath and Ehses 2006; Reinehr, Shober et al. 2006) However, an alternative explanation is that overweight children may develop T1DM earlier simply because in the face of insulin resistance their insulin reserves more rapidly reach the point where they are not sufficient to meet the higher than normal insulin requirements and thereby maintains normoglycemia. In this alternative model, insulin resistance does not exacerbate the autoimmune destructive process but just brings forward the time of clinical presentation with hyperglycaemia.

The non obese diabetic (NOD) mouse is a widely used model of T1DM due to spontaneous immune-mediated β-cell destruction.(Harada and Makino 1984; Anderson and Bluestone 2005) To test the accelerator hypothesis, a hyperphagic, obese, insulin-resistant, NOD strain was produced by backcrossing the *foz* mutation into the NOD background (NOD/Alms1$^{foz/foz}$). Results show that rather than accelerating autoimmune β-cell destruction, obesity and insulin resistance protected against autoimmune disease thereby arguing against the "accelerator hypothesis".

3. Material and Methods

NOD/FA colony generation

The *foz* mutation, a spontaneous 11pb deletion located in the exon 8 of the Alms1 gene, has been previously characterised in the "Fat Aussie" (FA) mouse model of Alström syndrome.(Arsov, Silva et al. 2006) The NOD/FA colony was generated by ten successive backcrosses of the *foz* mutation in a NOD (non obese diabetic) background. Primers flanking the *foz* mutation were used for the PCR analysis: forward ACA ACT TTT CAT GGC TCC AGT; reverse TTG GCT CAG AGA CAG TTG AAA.

Animal maintenance

This study was performed in accordance with the recommendations in the "Australian code of practice for the care and use of animals for scientific purposes" of the National Health and Medical Research Council. This study was approved by the Animal Ethics Committee of Flinders University under the project number #671/08.

Female mutant NOD/Alms1$^{foz/foz}$ and wildtype NOD control littermates were maintained in the animal facility at Flinders Medical Centre under pathogen

free conditions in a 12 hourly light/dark cycle. Mice had free access to autoclaved water and food (Gordon's rat and mouse maintenance pellets, Gordon's specialty stockfeeds, NSW, Australia). 250 days old NOD/Alms1$^{foz/foz}$ mice were placed in restricted diet (RD) to induce significant body weight loss and reach body weight equivalent to NOD littermates. NOD/Alms1$^{foz/foz}$ mice were fed with 3g/mouse/day and were monitored closely for health and change in body weight.

Insulin resistance monitoring by ITT and IPGTT

NOD/FA mice were tested for insulin resistance by the insulin tolerance test (ITT) and intraperitoneal glucose tolerance test (IPGTT). The ITT screening is used to assess insulin sensitivity using an exogenous insulin challenge. Following injection, the response to insulin is seen as a reduction of plasma glucose levels as glucose is transported into insulin-sensitive tissues (liver, fat and muscle).

For the ITT, mice were fasted 4 hours with no access to food but free access to water. Mice were weighed and insulin (Humulin R, Eli Lilly, USA) was injected ip at 0.75 U/kg body weight in 0.9% saline for injection (Pfizer, USA). The tail was snipped for blood collection and the plasma glucose was determined for each mouse using a glucometer (Optium Xceed, Abbott, USA)

and blood glucose test strips (Optium point of care, Abbott, USA) at 0, 15, 30 and 60 min after insulin injection.

The IPGTT assay is used to assess the capacity of mice to produce insulin and uptake glucose. Following glucose injection, plasma glucose rises and then decreases in response to endogenous insulin release. For the IPGTT, mice were fasted 18 hours and injected at 2mg/g body weight with D-glucose (Analar, VWR, USA) in 0.9% saline for injection. Plasma glucose was determined for each mouse using a glucometer with sampling via tail vein at 0, 15, 30, 60 and 120 min after glucose injection.

T1DM incidence monitoring

NOD/FA mice were monitored regularly and signs of sickness associated with T1DM such as excessive drinking/urinating and scruffy fur). Glucose screening in the urine (Glycosuria) was performed when a mouse shows signs of sickness, using a Keto-Diastix glycosuria test strips (Bayer, Germany). When glycosuria reading was greater than 5.5 mmol/L, diabetes diagnosis was confirmed by measuring random glycemia. Tail was snipped for blood collection and glycemia was determined using a glucometer (Optium Xceed, Abbott, USA). Mice showing glycemia above 18 mmol/L were confirmed type 1 diabetic.

Fasting insulinemia

Mice were fasted 18h and blood was collected on conscious animals via cheek bleeding. The fasting glycemia was recorded using a glucometer (Optium Xceed, Abbott, USA) and blood glucose test strips (Optium point of care, Abbott, USA). After collection, blood samples were kept on ice and then spun at 17000g, 10min at 4˚C. Insulin levels were assayed using a commercial ultrasensitive mouse insulin ELISA kit (Crystal Chem Inc., USA).

HOMA-IR scoring

The homeostasis model assessment of insulin resistance (HOMA-IR) index was calculated using individual mouse fasting insulin and fasting glucose levels. The following formula was used: HOMA-IR = [fasting glucose (mg/dL) × fasting insulin (μU/mL)]/405.

Pancreas histology

Pancreases were collected and incubated in 4% paraformaldehyde (in 0.1M sodium phosphate buffer, pH 7.2) following by paraffin embedding. Sections were stained by Hematoxylin and Eosin (H&E). β-islet infiltration was scored blinded using BX50 brightfield imaging microscope with Q imaging digital

camera (Olympus, Japan). Scoring used: 0–4: 0, no infiltrate; 1, peri-islet infiltrate; 2, circumferential accumulation of inflammatory cells; 3, intra-islet infiltration; 4, severe structural derangement and complete loss of β cells.

T1D induction by Cyclophosphamide (CY) injection

CY (Endoxan, Baxter, USA) was diluted in 0.9% saline for injection (Pfizer, USA) to a concentration of 25 mg/ml is injected IP at a dose of 200 mg/kg. Mice were monitored during 14 days for signs of type 1 diabetes related symptoms. The diagnosis of type 1 diabetes was performed by testing mice glycosuria, random glycemia and ITT as described earlier.

Statistical analysis

Statistical analyses were performed using GraphPad Prism 5 software (GraphPad Software, Inc., USA). Mean are given as mean ± SEM. Unpaired student t test was used for statistical comparison of BMI and AUC data. One way ANOVA was used for multiple comparisons. Survival curve between NOD/Alms1$^{foz/foz}$ and NOD group were compared by Logrank test. A p value <0.05 is considered statistically significant.

4. Results

NOD/Alms1$^{foz/foz}$ mice develop obesity, insulin resistance leading to T2DM.

Metabolic defects in the NOD/FA cohort were characterised over time by monitoring age-matched female NOD/Alms1$^{foz/foz}$ mice and NOD wildtype controls. At 90 days old, NOD/Alms1$^{foz/foz}$ mice were significantly heavier compared to their NOD littermates ($p<0.001$; Figure 3-1A). The ITT screening showed that NOD/Alms1$^{foz/foz}$ mice display signs of reduced insulin sensitivity with a significantly impaired response to exogenous insulin injection ($p<0.001$; Figure 3-1B). Interestingly, NOD/Alms1$^{foz/foz}$ mice displayed similar fasting glycemia compared to NOD control (NS; Figure 3-1C). NOD/Alms1$^{foz/foz}$ mice also showed a significantly delayed blood glucose uptake during IPGTT consistent with glucose intolerance ($p<0.001$; Figure 3-1D).

At 180 days old, the obesity phenotype seen in NOD/Alms1$^{foz/foz}$ mice became more severe with mice displaying pronounced obesity compared to NOD mice ($p<0.001$; Figure 3-1E). Along with obesity, the impaired insulin sensitivity during ITT worsened. After 15 minutes during the ITT, NOD/Alms1$^{foz/foz}$ mice were not responsive to exogenous insulin injection and their relative glycemia hardly got below 90% while NOD mice easily reached on average 60-70% ($p<0.001$; Figure 3-1F). As NOD/Alms1$^{foz/foz}$ mice became older, they showed

significantly higher fasting glycemia compare to NOD littermates ($p<0.001$; Figure 3-1G) and impaired glucose uptake during IPGTT was still observed ($p=0.0029$; Figure 3-1H). Interestingly, 180 days old NOD mice showed a slight delay in the glucose uptake at 30 minutes that could be due to a pre-type 1 diabetic status. These data show that NOD/Alms1$^{foz/foz}$ mice display severe obesity associated with peripheral insulin resistance. Thus, NOD/Alms1$^{foz/foz}$ mice showed metabolic disturbances leading to the development of T2DM and represent a new mouse model susceptible to test the effect of T2DM on the pathogenesis of T1DM.

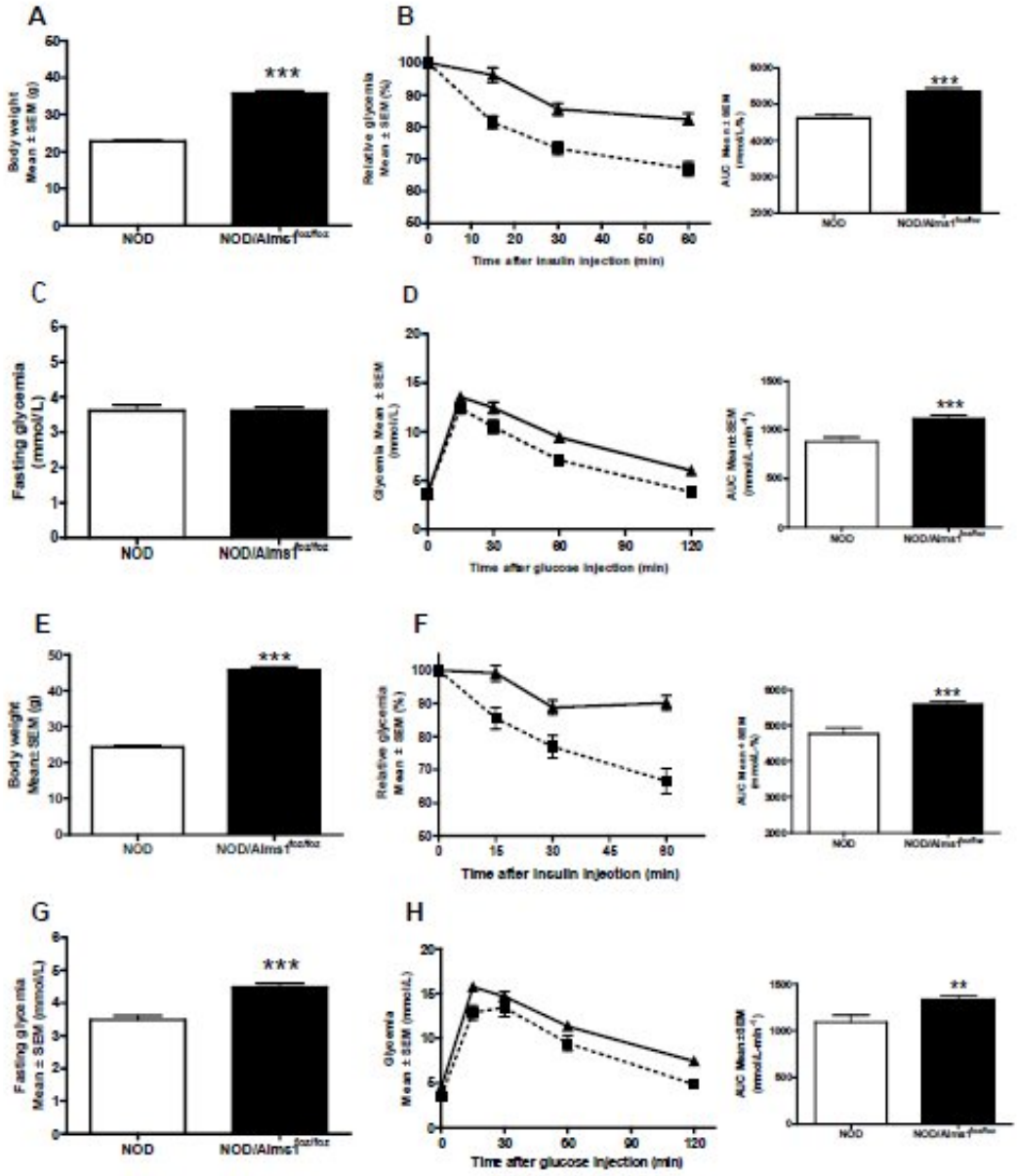
A
B
C
D
E
F
G
H
Body weight Mean ± SEM (g)
Relative glycemia Mean ± SEM (%)
Time after insulin injection (min)
Fasting glycemia (mmol/L)
Glycemia Mean ± SEM (mmol/L)
Time after glucose injection (min)
Time after insulin injection (min)
Glycemia Mean ± SEM (mmol/L)
Time after glucose injection (min)
NOD
NOD/Alms1foz/foz
***
**

Figure 3-1: Obesity and insulin resistance monitoring in NOD/FA mice

90 days old (A-D) and 180 days old female (E-H) NOD/Alms1$^{foz/foz}$ mice (plain line, black bar, n=40) and NOD littermates (dotted line, white bar, n=28-41) were monitored for the onset and progression of obesity and insulin resistance. (A, E) body weight; (B, F) relative blood glucose monitoring during ITT; (C, G) fasting blood glucose; (D, H) blood glucose monitoring during IPGTT. Abbreviations: AUC: area under curve; IPGTT: intraperitoneal glucose tolerance test; ITT: insulin tolerance test; NOD: non obese diabetic; SEM: standard error of the mean. ** $p<0.01$; *** $p<0.001$

Obese and insulin resistant NOD/Alms1$^{foz/foz}$ mice are protected against T1DM.

NOD/FA mice were monitored for a year in order to evaluate T1DM incidence and determine if a different trend toward the onset and severity of the disease was seen in obese and insulin resistant NOD/Alms1$^{foz/foz}$ mice compared to wildtype NOD mice.

The spontaneous onset of T1DM in the female NOD/FA colony followed a typical pattern starting at 90 days of age. T1DM incidence in female NOD controls reached almost 80% which is the average incidence expected in a female NOD cohort. Surprisingly, NOD/Alms1$^{foz/foz}$ mice showed a significantly reduced T1DM onset with only 5% incidence ($p<0.001$; Figure 3-2).

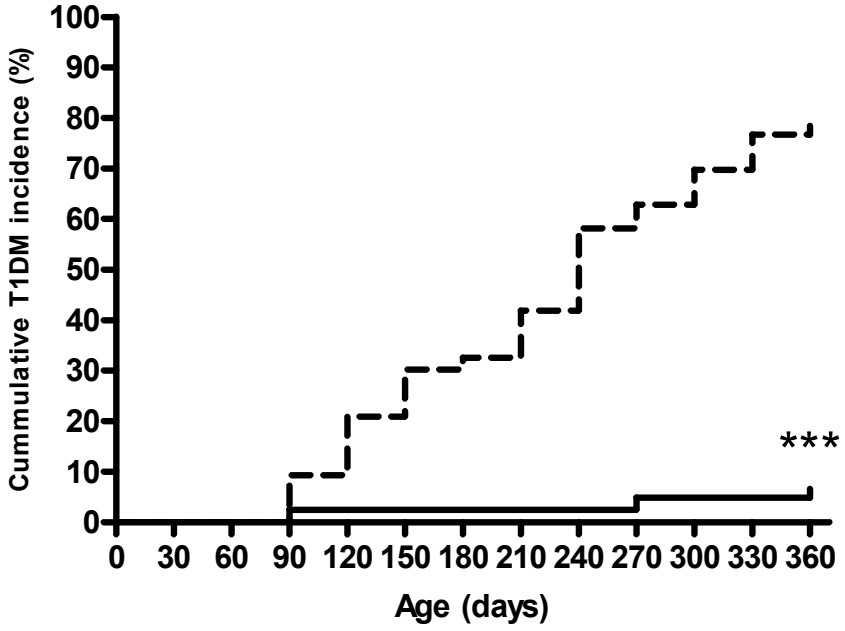

Figure 3-2: Cumulative T1DM incidence in the female NOD/FA cohort

TIDM onset was monitored in female NOD/Alms1$^{foz/foz}$ mice (plain line, n=43) and NOD littermates (dashed line, n=41). Abbreviations: FA : « Fat Aussie » NOD: non obese diabetic; T1DM: type 1 diabetes mellitus. *** $p<0.001$

Insulin secretory capacity and islet integrity are preserved in NOD/Alms1$^{foz/foz}$ mice.

TIDM leads to the destruction of insulin-producing β cells by the immune cells. Although NOD/Alms1$^{foz/foz}$ mice did not show signs of T1DM symptoms, histopathology analysis of the pancreas was performed in order to assess the infiltration level of immune cell in the islets. H&E staining of pancreas sections showed that NOD/Alms1$^{foz/foz}$ mice had a significantly lower insulitis score compared to NOD littermates ($p<0.001$; Figure 3-3A). Intact hyperplastic islets with only minimal peripheral insulitis were observed in NOD/Alms1$^{foz/foz}$ mice (Figure 3-3B, 3-3C) whereas NOD mice showed prominent insulitis and β-islet destruction (Figure 3-3D; 3-3E). Islet hyperplasia has been previously reported in Alström syndrome mouse models and could suggest a high proliferation rate of β cells.(Collin, Cyr et al. 2005; Arsov, Silva et al. 2006).

These data highlight that the protection against T1DM in NOD/Alms1$^{foz/foz}$ mice is due to suppression of insulitis. Whether the β cell hyperplasia itself contributes to this phenomenon is not known.

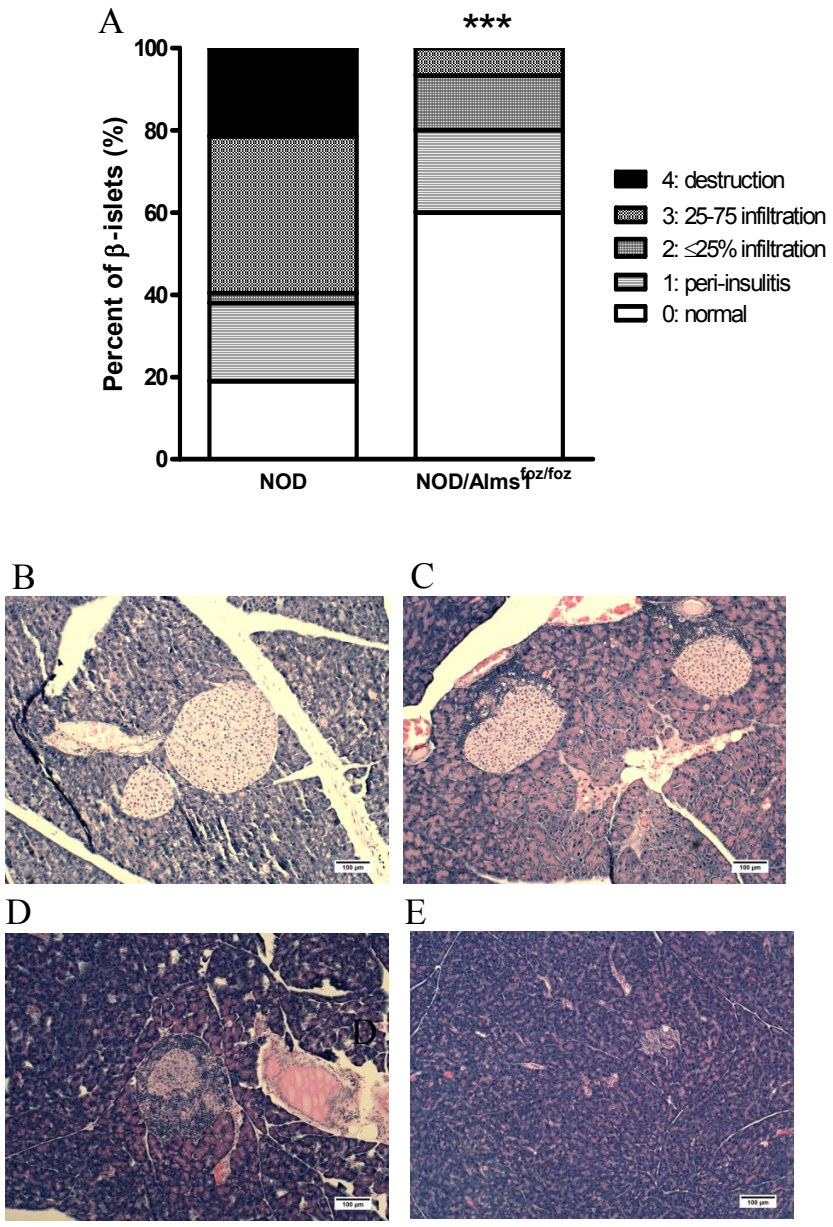

Figure 3-3: Histopathology of pancreatic β-islets by H&E staining

A: Pancreatic insulitis score (NOD, n=42; NOD/Alms1$^{foz/foz}$, n=14); B-E: Pancreas histopathology H&E staining, B-C: NOD/Alms1$^{foz/foz}$, D,-E: NOD. Abbreviations: FA: "Fat Aussie"; NOD: non obese diabetic. *** $p<0.001$

NOD/FA mice insulin secretion capacity was also assessed in order to evaluate the integrity of β cell function. Interestingly, NOD/Alms1$^{foz/foz}$ mice displayed significantly higher fasting blood insulin compared to NOD littermates which correlated with the insulin resistance phenotype observed when mice were younger and the hyperplastic islets ($p<0.001$; Figure 3-4A). Type 1 diabetic NOD mice also show significantly lower fasting blood insulin compared to non diabetic NOD due to islets destruction ($p=0.04$; Figure 3-4A).

The HOMA-IR scoring confirmed these findings with NOD/Alms1$^{foz/foz}$ mice showing an average HOMA-IR score significantly higher ($p<0.001$; Figure 3-4B). Altogether, these data showed that NOD/Alms1$^{foz/foz}$ mice insulin secretory capacity remained preserved.

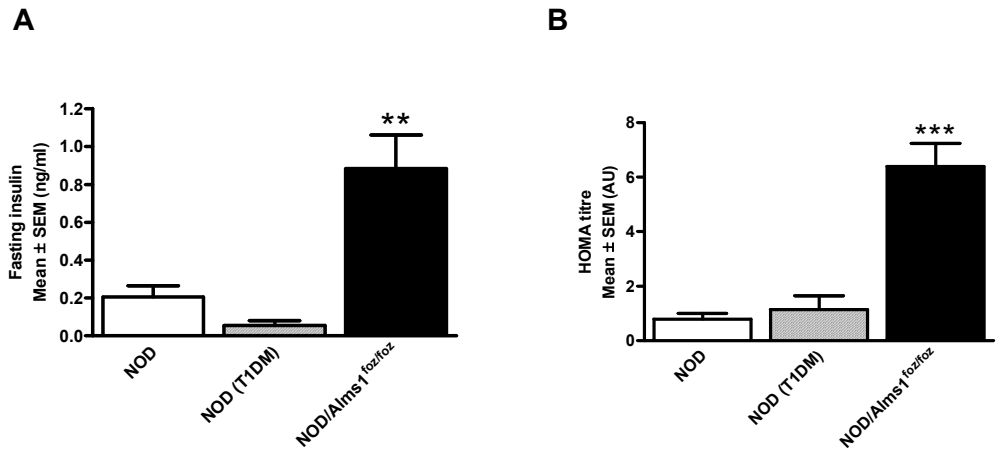

Figure 3-4: Fasting blood insulin and HOMA-IR scoring in 250 days old NOD/FA mice

Healthy NOD mice (white bar, n=18), Type 1 diabetic NOD mice (striped bar, n=12) and NOD/Alms1$^{foz./foz}$ mice (black bar, n=38) were screened for fasting insulinemia and HOMA-IR scores. A: Fasting insulinemia; B: HOMA-IR score. Abbreviations: AU: arbitrary unit; FA: "Fat Aussie"; HOMA: Homeostatic model assessment; IR: insulin resistance; NOD: non obese diabetic; SEM: standard error of the mean; T1DM: Type 1 diabetes mellitus. ** $p<0.01$; *** $p<0.001$

Weight loss improves metabolic function in NOD/Alms1$^{foz/foz}$ mice but does not remove T1DM protection.

In order to further investigate if obesity and insulin resistance were the main causes of protection against T1DM, obese 250 day old NOD/Alms1$^{foz/foz}$ mice were placed on a restricted diet (RD) until their body weight stabilised and reached the weight of NOD controls.

Obese NOD/Alms1$^{foz/foz}$ mice on RD progressively lost weight and, after two months, their average body weight was stabilised between 20-25g. ($p<0.001$; Figure 3-5A). Interestingly, although NOD/Alms1$^{foz/foz}$ became leaner, no difference was observed in their fasting blood glucose (NS, Figure 3-5B). However, NOD/Alms1$^{foz/foz}$ mice insulin sensitivity significantly improved with weight loss. After one month on a RD a positive trend was observed with NOD/Alms1$^{foz/foz}$ mice responding to exogenous insulin after 15 min during ITT. This trend was confirmed during the second and third month in RD with NOD/Alms1$^{foz/foz}$ mice displaying significantly improved overall insulin sensitivity ($p<0.05$; Figure 3-5C). Glucose tolerance also improved over time in the NOD /Alms1$^{foz/foz}$ mice. Starting from 1 month on a RD, the mice were able to significantly increase their blood glucose utilisation during IPGTT. ($p<0.001$; Figure 3-5D).

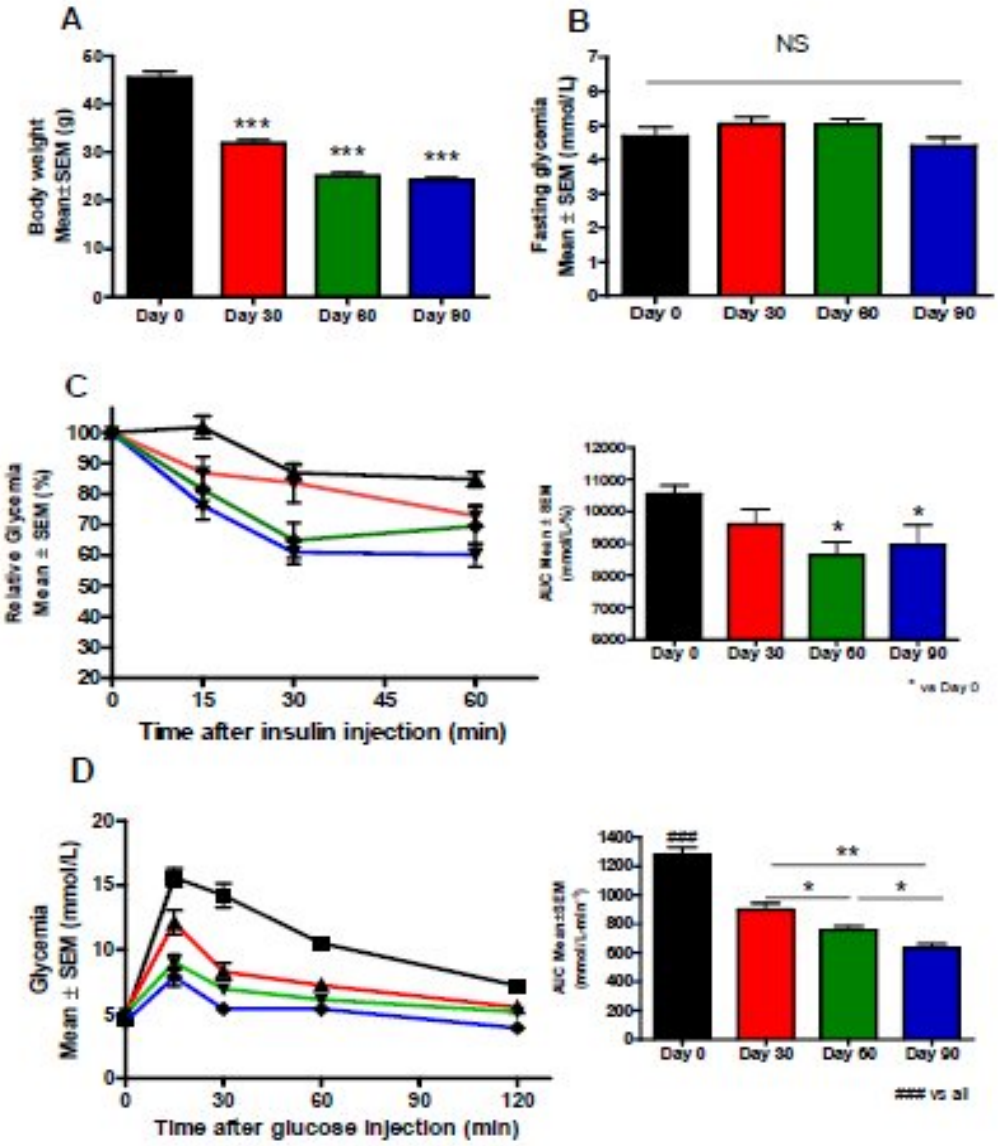
A
Body weight Mean±SEM (g)
***
***
***
Day 0
Day 30
Day 60
Day 90
B
NS
Fasting glycemia Mean ± SEM (mmol/L)
Day 0
Day 30
Day 60
Day 90
C
Relative Glycemia Mean ± SEM (%)
Time after insulin injection (min)
AUC Mean ± SEM (mmol/L*%)
*
*
Day 0
Day 30
Day 60
Day 90
* vs Day 0
D
Glycemia Mean ± SEM (mmol/L)
Time after glucose injection (min)
AUC Mean±SEM (mmol/L*min⁻¹)
###
**
*
*
Day 0
Day 30
Day 60
Day 90
vs all

Figure 3-5: Effect of RD on insulin resistance in NOD/Alms1$^{foz/foz}$ mice

The metabolic parameters of 180 days old NOD/Alms1$^{foz/foz}$ (black line and bar, n=15), NOD/Alms1$^{foz/foz}$ after 30 days in RD (red line and bar, n=15), NOD/Alms1$^{foz/foz}$ after 60 days in RD (green line and bar, n=15) and NOD/Alms1$^{foz/foz}$ after 90 days in RD (blue line and bar, n=15) were monitored. A: NOD/Alms1$^{foz/foz}$ mice body weight monitoring during RD; B: NOD/Alms1$^{foz/foz}$ mice fasting insulin blood; C: NOD/Alms1$^{foz/foz}$ mice relative blood glucose monitoring during ITT; D: NOD/Alms1$^{foz/foz}$ mice blood glucose monitoring during IPGTT. Abbreviations: AUC: area under curve; IPGTT: intraperitoneal glucose tolerance test; ITT: insulin tolerance test; NOD: non obese diabetic; NS: not significant; RD: restricted diet; SEM: standard error of the mean. * $p<0.05$; ** $p<0.01$; *** $p<0.001$, ### $p<0.001$ versus all.

The effect of RD on insulin secretion was assessed in NOD/Alms1$^{foz/foz}$ mice by measurement of fasting blood insulin. Mice still displayed high fasting blood insulin after two and three month on RD (NS; Figure 3-6A). Similarly after two and three month on RD NOD/Alms1$^{foz/foz}$ mice still displayed a high HOMA-IR score (NS; Figure 3-6B).

These data indicate that NOD/Alms1$^{foz/foz}$ mice remain insulin resistant even when they re-attain a normal weight and their β-cells remain capable of producing and releasing a high quantity of insulin, consistent with ongoing protection against T1DM.

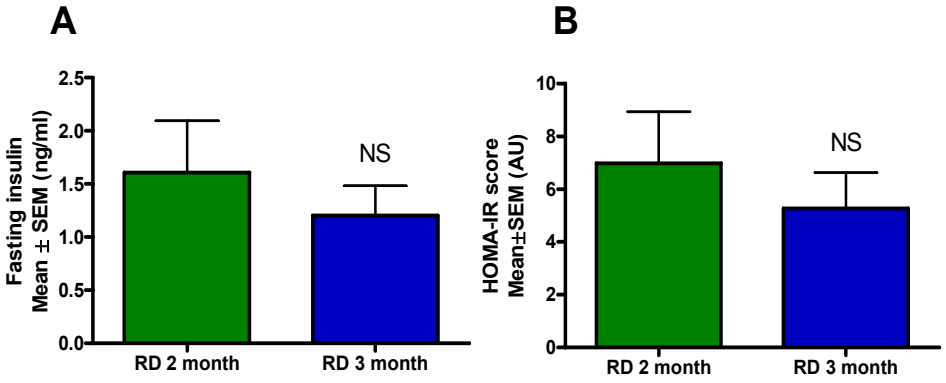

Figure 3-6: Effect of RD on fasting blood insulin and HOMA-IR scoring in NOD/Alms1$^{foz/foz}$ mice

Fasting insulinemia and HOMA-IR scored were determined in NOD/Alms1$^{foz/foz}$ after 60 days in RD (green line and bar, n=15) and NOD/Alms1$^{foz/foz}$ after 90 days in RD (blue line and bar, n=15). A: Fasting blood insulin; B: HOMA-IR scoring. Abbreviations: AU: arbitrary unit; HOMA: Homeostatic model assessment; IR: insulin resistance; NOD: non obese diabetic; NS: not significant; SEM: standard error of the mean

NOD/Alms1$^{foz/foz}$ mice are protected against both spontaneous and CY-induced T1DM even after weight reduction.

The main purpose of placing NOD/Alms1$^{foz/foz}$ mice on a RD was to assess whether the protective effect of NOD/Alms1$^{foz/foz}$ mice on T1DM could be reversed by removal of obesity. During the three months on RD none of the NOD/Alms1$^{foz/foz}$ mice developed features of T1DM. (Table 3-1)

As a follow up, NOD/Alms1$^{foz/foz}$ mice of >250 days old and age-matched NOD controls were injected with cyclophosphamide (CY). CY has been shown to accelerate the development of T1DM with an average onset period of 14 days post injection.(Harada and Makino 1984; Brode, Raine et al. 2006) None of the NOD/Alms1$^{foz/foz}$ mice placed on a RD displayed T1DM symptoms after CY injection, with only one NOD/Alms1$^{foz/foz}$ mouse on normal chow developing type 1 diabetes whereas as expected 50% of the wildtype NOD mice injected with CY developed T1DM ($p<0.05$; Table 3-1).

Together, these data confirm the ability of NOD/Alms1$^{foz/foz}$ mice to suppress the onset of T1DM by being resistant to CY induction. Considering that NOD/Alms1$^{foz/foz}$ mice on a RD were not obese, this indicates that the acquired protection against T1DM is not reversible after significant weight loss. It also suggests that obesity is not directly involved in the protection against T1DM,

whereas a role for hyperinsulinemia and/or insulin resistance cannot be ruled out.

Mice	Diet	CY injection	Total number	T1 diabetic number	T1DM incidence (%)	p value
NOD	ND	+	8	4	50	-
NOD/Alms1$^{foz/foz}$	RD	-	12	0	0	* (0.014)
NOD/Alms1$^{foz/foz}$	RD	+	12	0	0	* (0.014)
NOD/Alms1$^{foz/foz}$	ND	+	16	1	6.25	* (0.028)

Table 3-1: Effect of diet and CY on T1DM incidence in >250 days old NOD/FA mice

>250 days old NOD mice placed in ND and NOD/Alms1$^{foz/foz}$ mice placed either in RD or ND were injected with or without CY and monitored for the onset T1DM. Abbreviations: CY: cyclophosphamide; FA: “Fat Aussie”; ND: normal diet; NOD: non obese diabetic; RD: restricted diet; T1DM: type 1 diabetes mellitus. *$p<0.05$

5. Discussion

Along with the obesity pandemic, T1DM and T2DM incidence in children have dramatically increased. (Han, Lawlor et al. 2010; Forlenza and Rewers 2011; Swinburn, Sacks et al. 2011) T1DM and T2DM diabetes are closely related and, for some cases, it is difficult to clearly dissociate both diseases.(Donath and Ehses 2006; Pozzilli and Buzzetti 2006; Naik, Brooks-Worrell et al. 2009) The "accelerator hypothesis" proposes that T1DM is an accelerated form for T2DM involving insulin resistance as a driver of β-cell destruction.(Wilkin 2009) Clinical studies investigating the effect of obesity and insulin resistance on the onset of T1DM in youth have given mixed outcomes. Some studies have supported the concept of the "accelerator hypothesis" (Kibirige, Metcalf et al. 2003; Betts, Mulligan et al. 2005; Kordonouri and Hartmann 2005) while other reports question the evidence for this hypothesis.(Porter and Barrett 2004; O'Connell, Donath et al. 2007; Rewers 2011)

In this study, female NOD/Alms1$^{foz/foz}$ mice were used to investigate the effect of obesity and insulin resistance on the onset of T1DM. NOD/Alms1$^{foz/foz}$ showed a strong phenotype towards obesity and insulin resistance due to the effects of the Alms1 gene mutation. Thus, the NOD/Alms1$^{foz/foz}$ mouse represents a new mouse model to test the interplay between T1DM and T2DM.

The main finding of this study was that NOD/Alms1$^{foz/foz}$ mice were protected against T1DM. Immune-mediated β-cell destruction was suppressed in NOD/Alms1$^{foz/foz}$ mice with mice showing intact hyperplastic islets ,limited immune cell infiltration and unaltered insulin secretory capacity. Studies on the NOD-Lepr^{db-5J} mouse model have suggested a direct role of leptin resistance and associated metabolic disturbances in suppressing the onset of T1DM.(Lee, Reifsnyder et al. 2005; Lee, Chen et al. 2006) In the same way, this study suggests that metabolic disturbances in NOD/Alms1$^{foz/foz}$ mice might protect against T1DM.

Placing obese NOD/Alms1$^{foz/foz}$ mice on a RD induced significant body weight loss. Along with weight loss, insulin sensitivity and glucose tolerance significantly improved. However, the mice still displayed hyperinsulinemia and high HOMA-IR scores. The hyperinsulinemia can be explained by the hyperplastic islets compensating for underlying peripheral insulin resistance.

After three months on a RD, NOD/Alms1$^{foz/foz}$ mice did not show signs of spontaneous onset of T1DM. This suggests that obesity itself was not directly involved in T1DM prevention. Since islets showed limited insulitis, the resistance against β-cell destruction could be also due to an inhibition or tolerance of the immune system. For example, hyperinsulinaemia might induce a reduction of autoantibodies to insulin. (Gottlieb and Eisenbarth 2002; Visser,

Klatter et al. 2003) Moreover, both lean and obese NOD/Alms1$^{foz/foz}$ mice were resistant to cyclophosphamide-induced T1DM suggesting immune tolerance .(Brode, Raine et al. 2006) Since the ALMS1 gene is ubiquitously expressed, the loss of function of the Alms1 protein in the immune system could also have a direct impact on the onset and progression of T1DM in Alms1$^{foz/foz}$ mice.

In summary, obese, hyperinsulinemic and insulin resistant NOD/Alms1$^{foz/foz}$ mice were protected against autoimmune destruction of β cells thereby potentially arguing against the "accelerator hypothesis". However, a direct effect of a defective function of the mutant Alms1 protein in the pancreas and/or the immune system cannot be excluded as the reason why obese NOD/Alms1$^{foz/foz}$ are protected against autoimmune diabetes.

Chapter 4 : Characterisation of cognitive impairment in Alms1$^{foz/foz}$ mice and axonal transport of Alms1 protein

1. Summary

AS is characterised by neuronal pathology including retinal degeneration and sensorineural hearing loss, although unlike many other ciliopathies AS is not characterised by intellectual impairment. The aim of this study was to investigate whether Alms1 plays a role in neuronal function. Young (<60 days old) and 6 month old Alms1$^{foz/foz}$ mice and wildtype littermates were tested for cognitive impairment by the Morris water maze behavioural task. The neuronal transport of Alms1 protein and other neuro-transporters was investigated using a sciatic nerve ligation model. The results show that young Alms1$^{foz/foz}$ mice have a mild cognitive defect, which worsens with age. Alms1$^{foz/foz}$ mice had a reduced brain weight at all ages when compared to wildtype littermates consistent with a neuronal developmental defect underlying the cognitive impairment. The reduced cognitive function in older Alms1$^{foz/foz}$ mice was not reflected by neuronal degeneration as seen in Alzheimer disease or Huntington's syndrome, as brains of older Alms1$^{foz/foz}$ mice exhibited no evidence of beta amyloid plaques or neurofibrillary tangles. Sciatic nerve ligation studies showed that Alms1 protein is transported in a retrograde and anterograde fashion in the nerve axon. These data suggest that the cognitive impairment phenotype observed in Alms1$^{foz/foz}$ mice might be due to defective neuronal development, with the possibility that Alms1 protein is involved in neuronal signalling.

Key words: cognitive impairment, Morris task, brain mass, Alms1 protein, axonal transport

2. Introduction

Neurons display a primary cilium that acts as a sensory organelle in signal transduction (Fuchs and Schwark 2004; Whitfield 2004; Kumamoto, Gu et al. 2012) When the function of the neuronal primary cilium is impaired, it can have deleterious consequences on neurogenesis, axonal guidance and may lead to the disruption of neuronal signalling pathways essential for brain development and cognitive function.(Whitfield 2004; Lee and Gleeson 2010; Juric-Sekhar, Adkins et al. 2012). Many severe disorders arise from neuronal primary cilium defects including Joubert syndrome (JS), MORM syndrome or Bardet-Biedl (BBS) syndrome with patients showing brain malformation, mental retardation and anosmia. (Hampshire, Ayub et al. 2006; McEwen, Koenekoop et al. 2007; Louvi and Grove 2011)

Alström syndrome (AS) and BBS display an overlapping clinical phenotype but developmental delay is a feature more specific to BBS patients and is used to distinguish these disorders. Although patients with AS demonstrate near normal intelligence, several studies have reported mild impairment of cognitive

function. In a phenotypic study based on 182 cases, developmental milestones were delayed in 46% of AS patients. Autistic-spectrum behaviours were also observed in 20% of AS patients and several patients had frequent absence seizures.(Marshall, Bronson et al. 2005) Two other case reports support that AS patients can display mild to moderate delay in reaching major developmental milestones including gross motor and fine motor skills and intellectual development. (Michaud, Héon et al. 1996; Hamamy, Barham et al. 2006). Moreover, another study also reported cerebral anomalies in AS (Yilmaz, Çaksen et al. 2006). Altogether, these studies suggest that defective neuronal function might be an important feature of AS even if the symptoms are not as severe as in BBS patients.

Intraflagellar transport (IFT) is essential for primary cilium genesis, maintenance and signalling and consists of bi-directional transport of proteins, lipids and receptors. (Emmer, Maric et al. ; Rosenbaum and Witman 2002; Lucker, Behal et al. 2005; Leroux 2007) It has been shown that BBS proteins interact with Rab8 and mediate the movement of proteins to the membrane by the IFT cargo complex.(Leroux 2007; Nachury, Loktev et al. 2007) More specifically, it has been reported in several studies that BBS proteins are required for the localisation of G protein-coupled receptors to primary cilia on central neurons.(Berbari, Lewis et al. 2008; Domire, Green et al. 2011) Given its ubiquitous expression and its possible involvement in primary cilium function, Alms1 protein could be involved in protein trafficking within neurons

via the IFT explaining its impact on brain development and cognitive functions.

In this study, the cognitive function of age-matched Alms1$^{foz/foz}$ mice and wildtype littermates was assessed using the Morris water maze behavioural test and axonal transport of Alms1 protein and other neurotransporters was investigated using immunohistochemistry of the sciatic nerve.

3. Material and Methods

Animal maintenance

This study was performed in accordance with the recommendations in the "Australian code of practice for the care and use of animals for scientific purposes" of the National Health and Medical Research Council. This project was approved by the Animal Ethics Committee of Flinders University under the approval number #671/08.

Alms1$^{foz/foz}$ mice and Alms1$^{+/+}$ (WT) littermates were maintained in a C57BL/6J background in the animal facility at Flinders Medical Centre in a 12 hourly light/dark cycle. Mice had free access *ad libitum* to water and normal chow (Gordon's rat and mouse maintenance pellets, Gordon's specialty stockfeeds,

Australia). Primers flanking the *foz* mutation were used for PCR genotyping: forward ACA ACT TTT CAT GGC TCC AGT; reverse TTG GCT CAG AGA CAG TTG AAA.

Morris Water Maze behavioural task

Cognitive function and more precisely spatial memory of Alms1$^{foz/foz}$ and Alms1$^{+/+}$ mice was tested using a classic version of the Morris Water Maze behavioural task (Morris 1984). The protocol used was previously described and performed in the animal facility at Flinders Medical Centre.(Wang, Pollard et al. 2009; Wang, Wang et al. 2011) The test was conducted in a pool (200 cm diameter) which was filled with water (24 ± 2°C), made opaque with white non-toxic dye and surrounded by a set of spatial cues. The tank was imaginarily subdivided into four quadrants, and four start positions were located at the intersections of the quadrants.

Each daily training session consisted of four platform trials (East, North, West, South position) in which a round 8 cm diameter hidden escape platform was submerged 1 cm under the water surface in a fixed position in a quadrant. The mouse navigated in the pool to locate the hidden platform (target area) and was then able to escape. If the mouse failed to locate the platform within 120 seconds, it was directed to the platform and remained on it for 10 seconds. Once the mouse escaped onto the platform, it remained on the platform for 10

seconds. After five days of training, all mice were given a single probe trial in order to assess their memory strength. The platform was withdrawn two hours after the last platform trial and the duration for probe trial was set at 60 seconds.

Performances in all tasks were recorded and analyzed by a computer-based video tracking system and image analysing software (ANY-maze, Stoelting). For the training trials the latency or time to reach the platform from the start location and the average swim speed were compared between Alms1$^{foz/foz}$ and Alms1$^{+/+}$ mice. For the probe trial, the latency, the time spent in the target quadrant and platform area crossings were compared between Alms1$^{foz/foz}$ and WT littermates.

Brain mass and Congo red staining

Alms1$^{foz/foz}$ and Alms1$^{+/+}$ mice were anaesthetised with Ketamine at 75mg/kg (Ketamil, Troy laboratories, Australia) and Medetomidine at 1mg/kg (Domitor, Pfizer Animal Health, Australia)and cardiac perfused with 20ml of PBS (3.2 mM Na2HPO4, 0.5 mM KH2PO4, 1.3 mM KCl, 135 mM NaCl, pH 7.4). The whole brain was harvested and mass recorded. The brain was placed in 4% paraformaldehyde (in 0.1M sodium phosphate buffer, pH 7.2) for 2 days at 4˚C and then dehydrated overnight using 30% sucrose solution at 4˚C. Half of a hemisphere was embedded in OCT (Tissue Tek, Sakura Finetek, USA) and

35μm sections were cut using a cryostat (Leica, Germany). Brain sections were placed in 0.1 % sodium azide in PBS and mounted on slides for Congo red staining. Sections were washed in Milli-Q water for 2 minutes and then incubated 20 minutes in 0.01 % sodium hydroxide in saturated sodium chloride solution (Sigma-Aldrich, USA). Slides were then placed 20 minutes into working Congo red solution (Sigma-Aldrich, USA). Slides were successively placed in absolute ethanol, xylene and coverslip was mounted using DEPEX (BDH, UK). Images were captured using BX50 Brightfield microscope with Q Capture software (Olympus, Japan).

Sciatic nerve ligation

Alms1$^{foz/foz}$ and Alms1$^{+/+}$ mice were anaesthetized with Ketamine at 75mg/kg (Ketamil, Troy laboratories, Australia) and Medetomidine at 1mg/kg (Domitor, Pfizer Animal Health, Australia). The sciatic nerve ligation was performed using a protocol previously described. (Hui Wang 2006) A small incision was made below the femur. The sciatic nerve was identified and ligated using silk thread 5/0. The wound was closed using 9mm surgery wound clips (Becton Dickinson) and anti-inflammatory Neotopic-H topical cream was applied. A "sham" ligation control was performed on the other sciatic nerve by repeating the exact same procedure and passing the surgical thread underneath the nerve without actually ligating. Anaesthesia was reversed using Atipamezole at

1mg/kg (Antisedan, Pfizer Animal Health, Australia) and mice were monitored closely until they returned to homeostasis. After 24 hours, mice were anaesthetised and cardiac perfused with 20ml of PBS (3.2 mM Na2HPO4, 0.5 mM KH2PO4, 1.3 mM KCl, 135 mM NaCl, pH 7.4) followed by 40 ml of 4% paraformaldehyde (in 0.1M sodium phosphate buffer, pH 7.2). Sciatic nerves were harvested and store in 4% paraformaldehyde at 4°C.

Sciatic nerve immunohistochemistry

4% paraformaldehyde fixed sciatic nerves were dehydrated in 30% sucrose in PBS buffer overnight at 4°C and embedded in OCT (Tissue Tek, Sakura Finetek, USA). 5µm sections were cut using a cryostat (Leica, Germany) and were directly mounted on PEI coated slides (Sigma-Aldrich, USA). Sections were washed 15 minutes with PBST (3.2 mM Na2HPO4, 0.5 mM KH2PO4, 1.3 mM KCl, 135 mM NaCl, 0.05% Tween 20, pH 7.4) and then incubated in 1% H_2O_2 in 50% ethanol for 30 min. Slides were incubated two times 15 minutes in 50% ethanol and washed 15 minutes with PBST. Sections were incubated 2 hours in blocking buffer (5% Donkey serum, 0.5 % Triton X-100, 0.1% Tween-20, 0.1% gelatine, 2% BSA, PBS, 0.01% NaN_3, pH=7.4). Sections were incubated overnight at 4˚C with primary antibodies diluted 1/500 in blocking buffer: rabbit anti-Synaptogamin, rabbit anti-SNAP-25, rabbit anti-$Alms1_{Nter}$ and rabbit anti-p75NTR antibodies were kindly provided by Prof Xin-Fu Zhou

(Department of Human Physiology, Flinders University, Australia). The following day, sections were washed with PBST and were incubated 2h at RT with secondary antibodies and DAPI (Sigma-Aldrich, USA): anti-rabbit Alexa-488 or anti-goat Alexa-647 at 1/1000; in the dark 2h at RT. Sections were washed with PBST and mounted on slides (Mounting medium polyvinyl alcohol antifading, Fluka, Sigma-Aldrich, USA). Images were captured using Fluorescence microscope BX50 with AnalySIS image capture software (Olympus, Japan)

Statistics

Statistical analyses were performed using GraphPad Prism 5 software (GraphPad Software, Inc., USA). Results are presented as mean ± SEM (standard error of the mean). Unpaired student t test was used for statistical comparison of brain weight and Morris test behaviourial test on age and weight matched mice. For older mice studies, the Mann-Whitney U test was used to compare Alms1$^{foz/foz}$ and WT. A p value <0.05 was considered statistically significant.

4. Results

Young Alms1$^{foz/foz}$ mice display mild cognitive impairment.

Cognitive function in young non-obese Alms1$^{foz/foz}$ mice and WT controls was tested using the Morris watermaze behavioural task. Mice were trained for five days to visualise and memorise the fastest path to reach a hidden escape platform (or island) in a fixed position in a pool. At 40-60 days of age, Alms1$^{foz/foz}$ mice display the same average body weight (NS, Figure 4-1A) and an equivalent swim speed compared to wildtype littermates. (NS, Figure 4-1B)

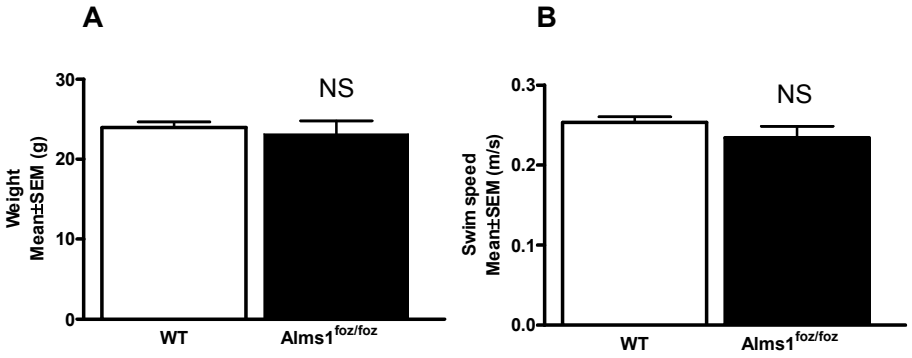

Figure 4-1: Young Alms1$^{foz/foz}$ mice average body weight and swim speed

40-60 days old Alms1$^{foz/foz}$ mice (black bar, n=8) and control wildtype mice (open bar, n=7). A: Body weight; B: Average swim speed during the Morris watermaze task. Abbreviation: NS: not significant; SEM: standard error of the mean; WT: wildtype.

Visual loss leading to blindness is an early feature occurring in AS patients. The training session allowed assessment of whether Alms1$^{foz/foz}$ mice have a visual impairment that could interfere with the outcome of the Morris Watermaze behavioural task. Results showed that during the training latency decreased over time in both Alms1$^{foz/foz}$ mice and wildtype controls. This indicates that the Alms1$^{foz/foz}$ mice were able to progressively learn and memorize the position of the hidden platform in the target area and can optimise their swimming path implying that in the young Alms1$^{foz/foz}$ mice being tested visual acuity was not significantly impaired.

However, Alms1$^{foz/foz}$ mice showed a significant learning delay compared to wildtype mice even although their learning curve stayed positive during successive training sessions. ($p=0.036$, Figure 4-2)

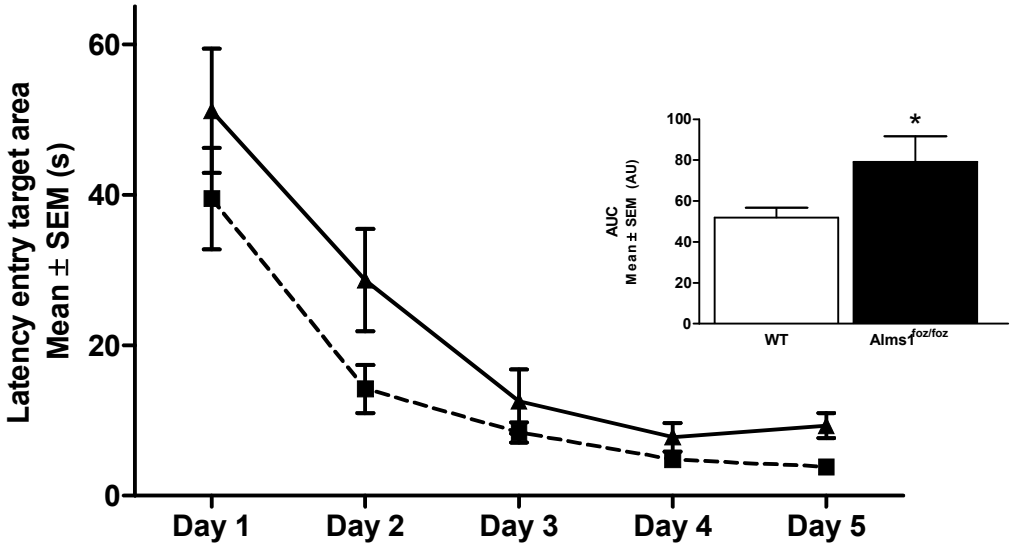

Figure 4-2: Young Alms1$^{foz/foz}$ mice latency during the training sessions

40-60 days old Alms1$^{foz/foz}$ mice (plain line, black bar, n=8) and control wildtype mice (dotted line, open bar, n=7) latency to reach the escape platform during the Morris watermaze task training sessions. Abbreviations: AUC: area under curve; SEM: standard error of the mean; WT: wildtype. * $p<0.05$

After the last training, mice memory was assessed during the probe test. The platform was removed from the pool and mice were tested on their ability to remember the position of the hidden platform in a limited time frame of 60 seconds.

The latency of first entry to the island zone was significantly longer in Alms1$^{foz/foz}$ mice compared to wildtype mice (p=0.011, Figure 4-3A). The number of island zone crossings was also significantly reduced in Alms1$^{foz/foz}$ mice compared to wildtype mice, showing that wildtype mice came back more often to the zone where the platform was placed during the training sessions (p=0.039, Figure 4-3B). Wildtype mice also spent significantly more time in the target zone compared to Alms1$^{foz/foz}$ mice. (p=0.047, Figure 4-3C)

These data suggest that although young Alms1$^{foz/foz}$ mice were able to learn the position of the escape platform over time, they were slower to learn and had difficulties to memorize the fastest path to reach the escape platform when compared to wildtype mice. This indicates that young Alms1$^{foz/foz}$ mice have a mild cognitive impairment.

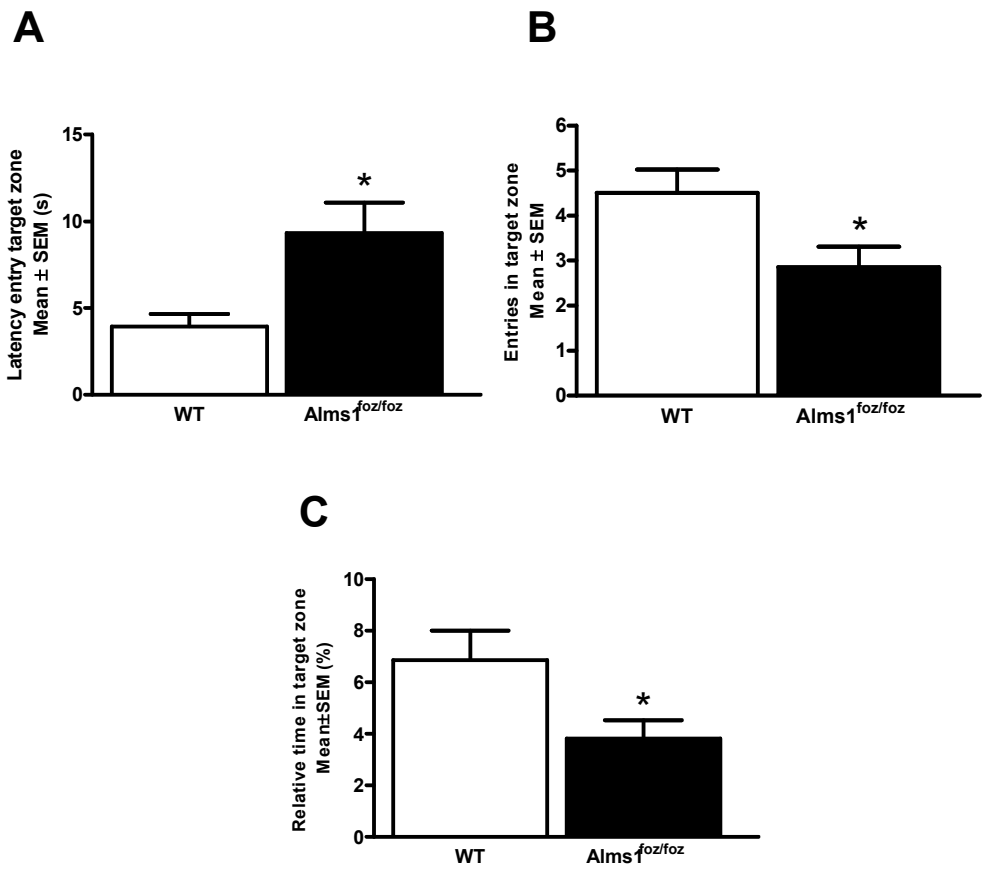

Figure 4-3: Young Alms1$^{foz/foz}$ mice memory assessment during the probe test

40-60 days old Alms1$^{foz/foz}$ mice (black bar, n=8) and control wildtype mice (open bar, n=7) memory was assessed during the Morris watermaze task probe test. The platform was removed and mice were allowed to swim for 60 seconds. A: Average latency to reach the island zone; B: Number of entries in the island zone; C: Relative time spend in the target quadrant. Abbreviations: FA: Fat Aussie; SEM: standard error of the mean. * $p<0.05$

Alms1$^{foz/foz}$ mice cognitive impairment worsens with age.

In order to investigate if the mild cognitive impairment seen in young Alms1$^{foz/foz}$ mice evolved with age, the same Morris task protocol was performed on 6 month old Alms1$^{foz/foz}$ and wildtype littermates. Alms1$^{foz/foz}$ mice at this age had the expected obese phenotype with significantly higher body weight than wildtype controls ($p<0.001$; Figure 4-4A) associated with a non significant slightly reduced swim speed in Alms1$^{foz/foz}$ mice (NS; Figure 4-4B).

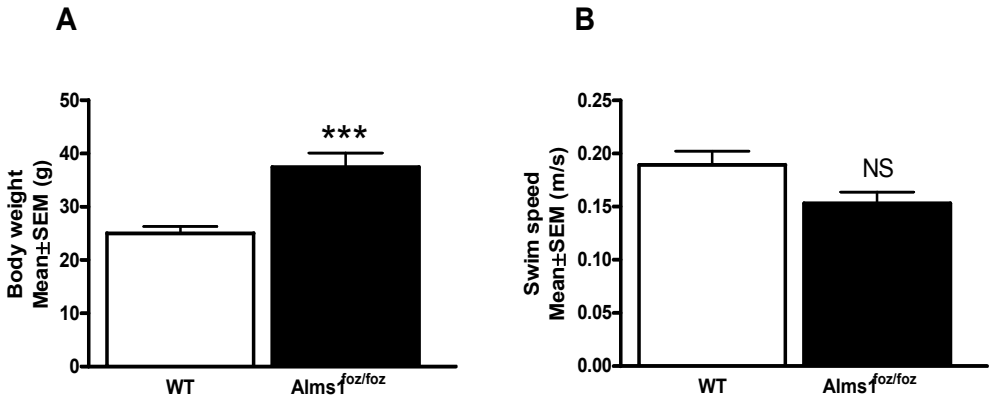

Figure 4-4: 6 month old FA mice body weight and swim speed

6 month old Alms1$^{foz/foz}$ mice (black bar, n=15) and control wildtype mice (open bar, n=11).A: Body weight; B: Average swim speed during the M Morris watermaze task. Abbreviation: FA: "Fat Aussie"; NS: not significant; SEM: standard error of the mean. *** $p<0.001$

During the five days training phase, 6 month old Alms1$^{foz/foz}$ displayed a significantly reduced learning curve compared to wildtype littermates. ($p<0.001$; Figure 4-5) Alms1$^{foz/foz}$ mice progressively memorized the best path to the platform from day 1 to day 3 but then failed to maintain a positive learning curve during the last two days of training.

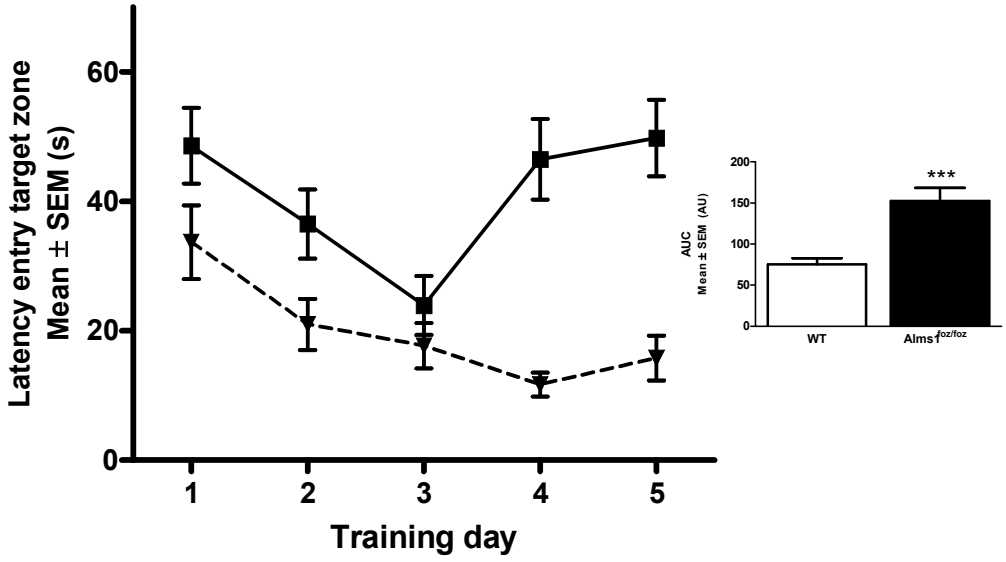

Figure 4-5: 6 month old Alms1$^{foz/foz}$ latency during the training sessions

6 month old Alms1$^{foz/foz}$ mice (plain line, black bar, n=15) and control wildtype mice (dotted line, open bar, n=11) latency to reach the escape platform during the Morris watermaze task training sessions. Abbreviations: AUC: area under curve; FA: "Fat Aussie"; SEM: standard error of the mean. *** $p<0.001$

During the probe test, Alms1$^{foz/foz}$ mice clearly displayed difficulties to efficiently memorize and reach the location of the escape platform. They showed a significant higher latency ($p=0.005$; Figure 4-6A) associated with a lower number of island zone crossings ($p<0.001$; Figure 4-6B). Alms1$^{foz/foz}$ mice also spent significantly less time in the target area compared to wildtype controls ($p=0.004$; Figure 4-6C). These data indicate that Alms1$^{foz/foz}$ mice develop greater cognitive impairment as they become older.

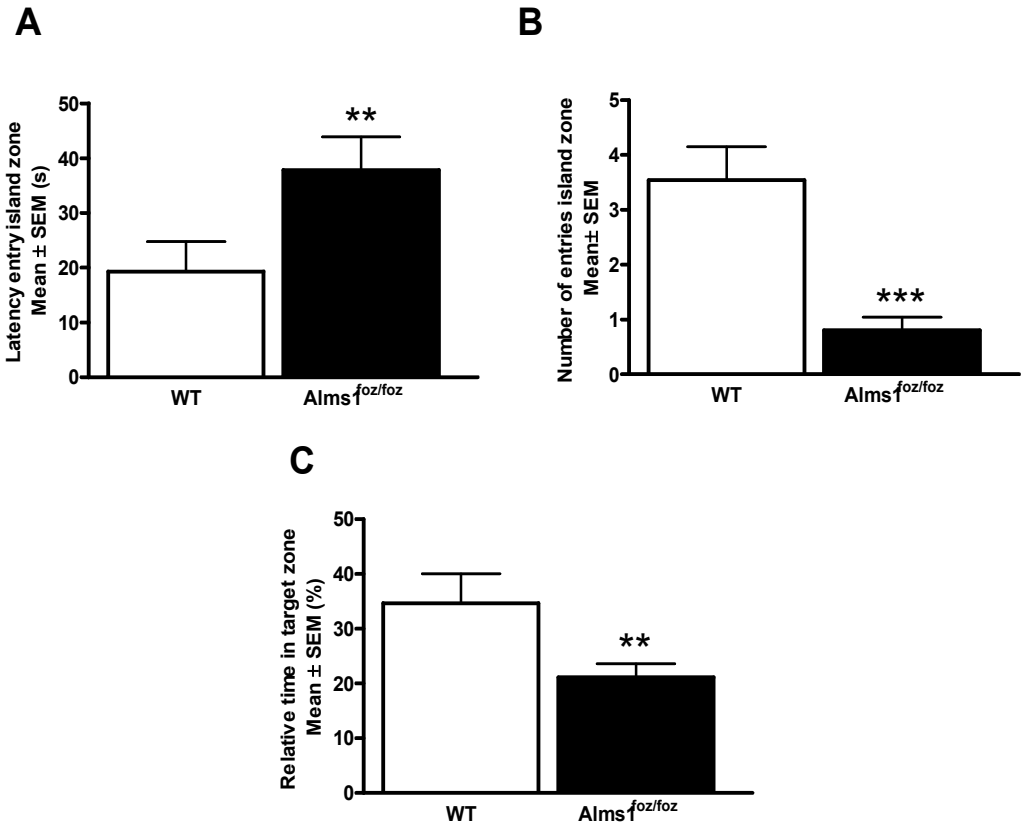

Figure 4-6: 6 month old Alms1$^{foz/foz}$ mice memory assessment during the probe test

6 month old Alms1$^{foz/foz}$ mice (black bar, n=15) and control wildtype mice (open bar, n=11) memory was assessed during the Morris watermaze task probe test. The platform was removed and mice were allowed to swim for 60 seconds. A: Average latency to reach the island zone; B: Number of entries in the island zone; C: Relative time spend in the target quadrant. Abbreviations: FA: Fat Aussie; SEM: standard error of the mean. ** $p<0.01$; *** $p<0.001$

Alms1$^{foz/foz}$ mice display reduced brain mass

In order to investigate what could be causing the cognitive impairment seen in Alms1$^{foz/foz}$ mice, whole brains were collected and weighed. Young Alms1$^{foz/foz}$ mice showed a significant lower brain mass compared to wildtype littermates ($p=0.013$, Figure 4-7). With age, the brain weight reduction compared to wildtype mice is even more pronounced in Alms1$^{foz/foz}$ mice ($p<0.001$, Figure 4-7). This indicates that Alms1$^{foz/foz}$ mice have an early onset brain development defect leading to a 10-20% reduced brain mass that could be responsible for the cognitive defect observed.

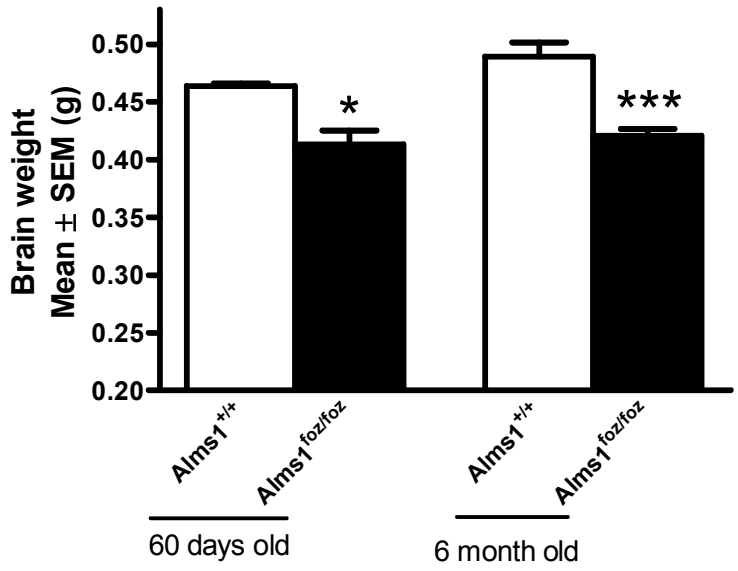

Figure 4-7: Alms1$^{foz/foz}$ mice brain weight comparison at 60 days and 6 months of age.

60 days old and 6 month old Alms1$^{foz/foz}$ (black bar, n=4-15) and Alms1$^{+/+}$ (open bar, n=4-11) mice whole brain were harvested and weighed. Abbreviations: FA: "Fat Aussie"; SEM: standard error of the mean. * $p<0.05$; *** $p< 0.001$

FA mice brains were then sectioned for histology analysis and staining with Congo Red in order to evaluate if Alms1$^{foz/foz}$ mice have evidence of neurodegeneration such as β-amyloid accumulation as the cause of the memory impairment.(Jucker and Ingram 1997) Brain sections showed macroscopically normal brain structures and did not show any positive Congo Red staining in either wildtype or Alms1$^{foz/foz}$ mice (Figure 4-8A and B) compared to positive β-amyloid accumulation in APPSwe/PS1dE9 Alzheimer mice control (Figure 4-8C). It therefore excludes brain plaques as a cause of the cognitive impairment in Alms1$^{foz/foz}$ mice.

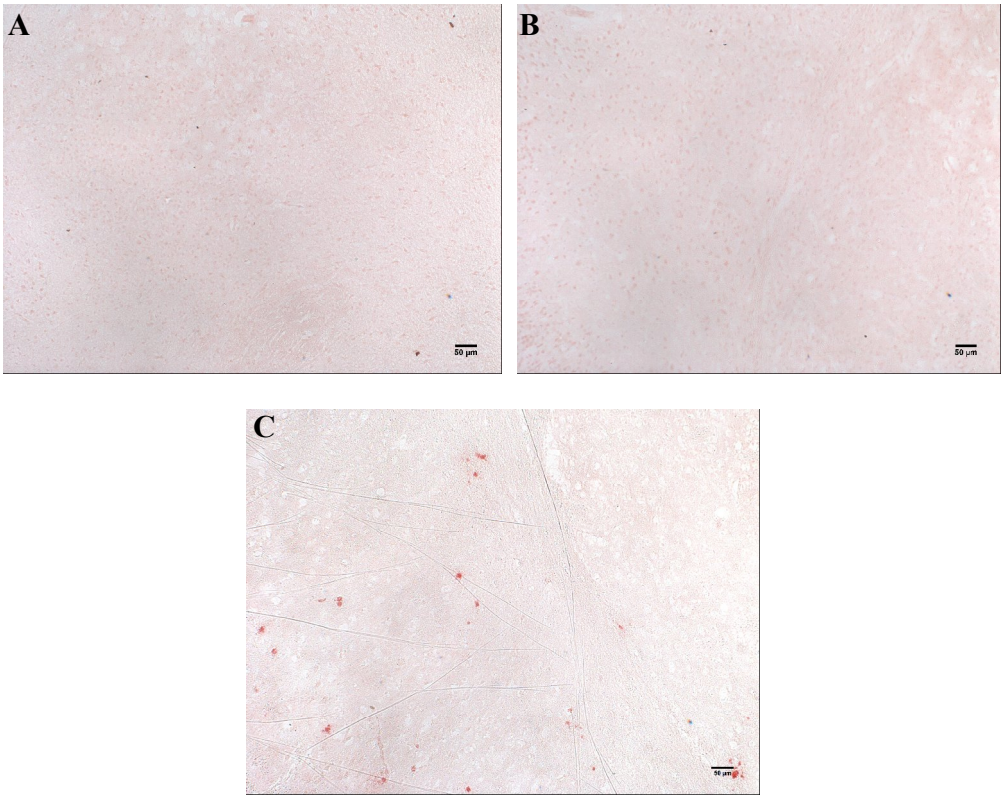

Figure 4-8: Congo red staining of brain sections.

Representative photo of 35µm brain sections stained with Congo red. A: WT; B: Alms1$^{foz/foz}$ and C: APPSwe/PS1dE9 transgenic Alzheimer model control. Abbreviations: FA: Fat Aussie; WT: wildtype.

Alms1 protein is axonally transported.

The sciatic nerve ligation model was used to investigate if Alms1 protein plays a role in neuronal transport. Results showed that Alms1 was transported in anterograde and retrograde direction up and down the sciatic nerve of wildtype mice (Figure 4-9). This is reflected in the fact that Alms1 protein accumulated at both the proximal and distal portion of the ligation site.

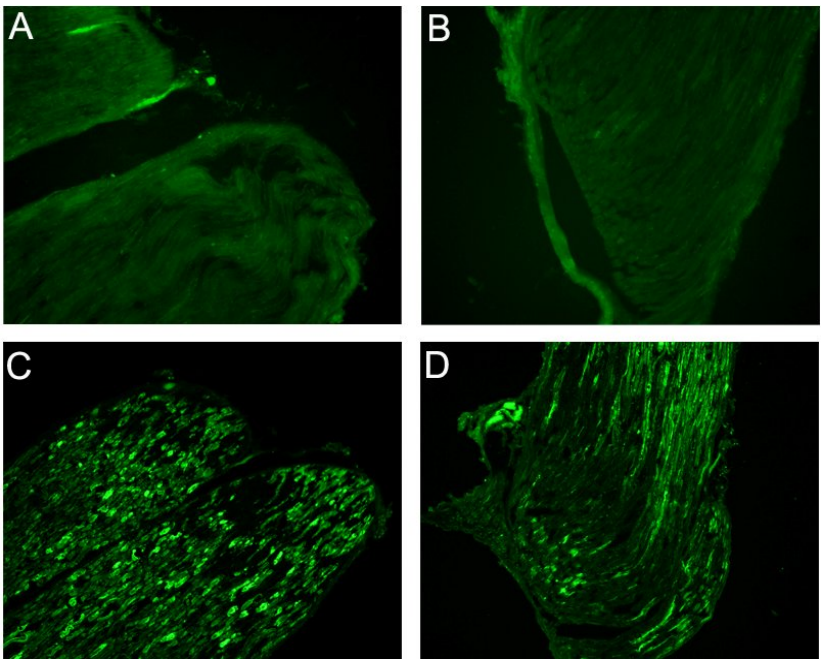

Figure 4-9: Bi-directional axonal transport of Alms1 protein.

Wildtype mouse sciatic nerve was ligated during 24 hours in order to allow the accumulation of vesicles and transporters to the ligation site. Proximal site (A, C) and distal site (B, D) were visualised under fluorescent microscope at objective 10X. A, B: Negative control; C, D: $Alms1_{Nter}$ staining.

Interestingly, the accumulation of Alms1 protein at the ligation site was also observed in Alms1$^{foz/foz}$ mice (Figure 4-10A, 4-10B) along with other neuro-transporters (Figure 4-10C to 4-10H). These data suggest that the truncated form of Alms1 is expressed in the mutant and the loss of the C_{ter} part doesn't inhibit its transport in the nerve. It also indicates that the transport of the markers tested was not impaired in Alms1$^{foz/foz}$ condition.

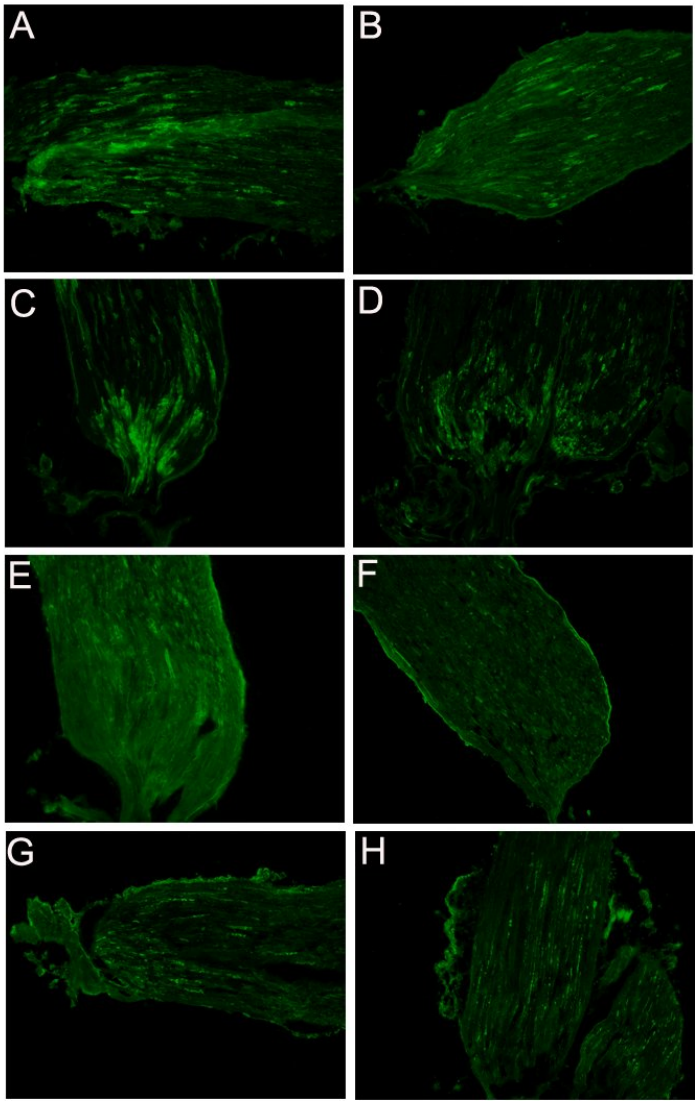

Figure 4-10: The axonal trafficking is not disrupted in Alms1$^{foz/foz}$ condition.

(A, C, E, G): Alms1$^{foz/foz}$; (B, D, F, H) WT sciatic nerve was ligated 24 hours in order to allow the accumulation of vesicles and transporters to the ligation site and stained with A, B: Alms1$_{Nter}$, C, D: p75NTR, E, F: SNAP25, G, H: synaptogamin. Staining was visualised under fluorescent microscope at objective 10X.

5. Discussion

AS is a pleiotropic genetic disorder with cardinal features ranging from metabolic disturbances to cardiac disease and neurosensory deficit. (Marshall, Bronson et al. 2005; Girard and Petrovsky 2011) Reports on neuronal disabilities remain limited considering that neuronal testing is not a routine procedure during clinical diagnosis of AS. Moreover, cognitive evaluation of patients with AS remains difficult due to the confounding effects of hearing and visual impairments.(Welsh 2007)

FA mice learning and memory ability were evaluated at <60 days and 6 months of age. The Morris behavioural task is a well described protocol used to study rodent models of neurodegenerative diseases.(Van der Staay 2006) FA mice had to navigate in a pool and use visual cues to remember the path to a hidden escape platform. Blindness is a main feature of AS.(Welsh 2007) Moreover, retinal and cochlear defects have been observed in another Alms1 disrupted mouse model.(Collin, Cyr et al. 2005) Although, there is no evidence of actual blindness in the Alms1 disrupted mouse model, reduced visual acuity cannot be excluded especially in 6 month old Alms1$^{foz/foz}$ mice. Young Alms1$^{foz/foz}$ mice showed positive learning curve during the five days training session even if delayed compared to wildtype littermates. Older Alms1$^{foz/foz}$ mice also showed

positive learning during the three first days of training. No obvious vision defect was noticed in Alms1$^{foz/foz}$ mice during the Morris watermaze task.

Alms1$^{foz/foz}$ mice displayed early mild cognitive impairment compared to wildtype controls during the test. The cognitive deficiency appeared to worsen with age. Spatial memory and visual recognition take place mainly in the hippocampus.(Broadbent, Squire et al. 2004; Sharma, Rakoczy et al. 2010) Hippocampal neurons have been specifically shown to have primary cilia (Berbari, Bishop et al. 2007; Amador-Arjona, Elliott et al. 2011). The neuronal primary cilium plays a role in neurogenesis, axonal growth and neuronal signalling (Breunig, Sarkisian et al. 2008; Lee and Gleeson 2010). Thus defective function of the primary cilium in hippocampal neurons could have a direct impact on cognitive function as seen in patients with BBS.(Bennouna-Greene, Kremer et al. 2011)

Alms1$^{foz/foz}$ mice had a significantly reduced brain weight at both <60 days and 6 month old. Whereas the brain weight of wildtype mice increases with age, the brain weight of Alms1$^{foz/foz}$ mice remains at the same average from 60 days of age to adulthood. This suggests either a developmental deficiency due to disrupted neurogenesis or could be due to a higher rate of neuronal death. Brain sections did not show positive staining with Congo red which rules out possible spontaneous amyloid accumulation as the cause of neurodegeneration and is

more in favour of disrupted neurogenesis as a cause for the observed reduced brain weight.

Protein trafficking is essential for primary cilium maintenance and signalling function. The axonal transport of Alms1 protein suggests a role of Alms1 in protein trafficking and potentially in neuronal signalling. Alms1 is transported in both an anterograde and retrograde direction in the sciatic nerve which can indicate that Alms1 could either be transported by another protein, or may itself be a part of the IFT transport machinery. The axonal transport of Alms1 and other tested transporters is not disrupted in Alms1$^{foz/foz}$ mice suggesting that a truncated form of Alms1 protein is still transported without interfering with general axonal protein trafficking.

In conclusion, this study sheds light to a potential role of Alms1 protein in neuronal function.

Chapter 5 : Alms1$^{foz/foz}$ chromaffin cells display reduced secretory activity but unaltered exocytosis

1. Summary

The exocytosis mechanism is essential in primary cilia maintenance and signalling. With previous data showing the axonal transport of the Alms1 protein, whether Alms1 was involved in protein trafficking via exocytosis was investigated. Chromaffin cells were harvested from the adrenal gland of young non obese Alms1$^{foz/foz}$ mice and wildtype littermates in order to compare catecholamine secretory activity by amperometry and investigate if the exocytosis mechanism is impaired in the mutant condition. Results showed that Alms1$^{foz/foz}$ chromaffin cells display significantly lower number of exocytotic events associated with decreased spike amplitude. This indicates that a lower number of vesicles undergo exocytosis and these vesicles might display reduced catecholamine loading. No difference was observed in the fusion pore kinetic parameters comparing Alms1$^{foz/foz}$ and wildtype mouse exocytosis events which indicate that the exocytosis mechanism itself is unaltered in Alms1$^{foz/foz}$ mice. These data suggest an involvement of the native Alms1 protein in vesicle transport and loading but not a direct role in the exocytosis mechanism itself.

Keys words: chromaffin cell, exocytosis, catecholamine oxidation, amperometry, fusion pore kinetics

2. Introduction

Vesicular trafficking is important in primary cilium maintenance and signalling as newly synthetised proteins are transported from the Golgi apparatus to the cilium.(Leroux 2007) Previous data suggests a role of Alms1 protein in neuronal function and as shown in Chapter 4 Alms1 protein is axonally transported via the sciatic nerve. The Alms1 protein may thereby be transported itself and be part of a bigger protein complex involved in vesicular trafficking. The axonal transport of Alms1 is not disrupted in Alms1$^{foz/foz}$ and could suggest that the role of Alms1 is at the end point of the synaptic transport and might concern synaptic exocytosis. Moreover, the FA and another Alms1 disrupted mouse model of AS have been shown to display hypertrophied pancreatic β islets and abnormal accumulation of vesicles in the inner segments of photoreceptors that could suggest defective vesicular trafficking or a failure of the vesicles to perform exocytosis.(Collin, Cyr et al. 2005; Arsov, Silva et al. 2006).

This study aimed to investigate if the exocytosis mechanism was impaired in Alms1$^{foz/foz}$ mice using primary culture of chromaffin cells as a well described cell model in exocytosis studies.(Garcia, Garcia-De-Diego et al. 2006; Keating, Dubach et al. 2008) Alms1$^{foz/foz}$ mice and wildtype chromaffin cells isolation was followed by amperometry recording of oxidised catecholamine released

from every single exocytotic event upon stimulation. The overall catecholamine secretion activity was investigated and the fusion pore kinetics parameters were characterised in order to assess the integrity of the exocytosis mechanism in Alms1$^{foz/foz}$ condition.

3. Material and Methods

Animal maintenance

This study was performed in accordance with the recommendations in the "Australian code of practice for the care and use of animals for scientific purposes" of the National Health and Medical Research Council. This project was approved by the Animal Ethics Committee of Flinders University under the approval number #671/08.

Young (<60 days old) Alms1$^{foz/foz}$ mice and Alms1$^{+/+}$ (WT) littermates were maintained in a C57BL/6J background in the animal facility at Flinders Medical Centre in a 12 hourly light/dark cycle. Mice had free access *ad libitum* to water and normal chow (Gordon's rat and mouse maintenance pellets, Gordon's specialty stockfeeds, Australia). Primers flanking the *foz* mutation were used

for PCR genotyping: forward ACA ACT TTT CAT GGC TCC AGT; reverse TTG GCT CAG AGA CAG TTG AAA.

Chromaffin cell culture

Chromaffin cell culture was performed using a protocol previously described.(Keating, Dubach et al. 2008) Adrenal glands were harvested from 2-3 months old non-obese Alms1$^{foz/foz}$ or Alms1$^{+/+}$ mice. The adrenal medulla was dissected out in cold Locke's buffer (154 mM NaCl, 5.6 mM KCl, 3.6 mM NaHCO3, 5.6 mM glucose, 5.0 mM HEPES, pH 7.4) using a dissection microscope. Adrenal medullas were then incubated with 3 mg/ml collagenase type A (Roche, Switzerland) in Locke's buffer for successively 15min, 10min and 5min in a shaking water-bath at 37°C. Medullas were resuspended 10 times using a P1000 pipette between each incubation time. The collagenase activity was neutralised in cold Locke's buffer and chromaffin cells were then centrifuged 10 minutes at 1000rpm, 4°C. Cells were resuspended in DMEM-glutaMAX culture medium (Life Technologies, USA) supplemented with 1% penicillin/streptomycin (Sigma-Aldrich, USA) and 10% heat inactivated fetal bovine serum (Thermo Fisher Scientific, USA) and passed through a 50µm nylon mesh filter. Cells were then plated in 35 mm culture dishes (Iwaki, Barloworld Scientific Ltd, UK) and incubated in a 37°C humidified incubator with 5% CO_2. The culture medium was changed the following day and

chromaffin cells were maintained in primary culture for 3 to 4 days prior to recording of exocytosis.

Recording of exocytotic events by amperometry

Recording of exocytotic events recording was performed on isolated chromaffin cells using amperometry. It involved the detection of oxidised catecholamine released from individual vesicles using a carbon probe.(Mosharov and Sulzer 2005) The amperometry recording was performed using a protocol previously described with minor changes.(Keating, Dubach et al. 2008) All solutions were applied to cells using a gravity perfusion system, the outlet of which was placed within 500 μm from the recorded cell. All experiments were carried out at 37°C. Cells were maintained in standard KREBS bath solution (140 mM NaCl, 5 mM KCl, 2 mM CaCl2, 1mM MgCl2, 5mM D-glucose, 10 mM HEPES, pH 7.4). A carbon fibre electrode (ProCFE, Dagan Corporation, USA) was placed on a chromaffin cell and þ800 mV applied to the electrode under voltage clamp conditions. Current due to catecholamine oxidation was recorded using an EPC-9 amplifier and Pulse software (HEKA Electronic, Germany), sampled at 10 kHz and low-pass filtered at 1 kHz.

Amperometry data analysis

For quantitative analysis files were converted to Axon Binary Files (ABF Utility, version 2.1, Synaptosoft, USA) and secretory spikes analysed (Mini Analysis, version 6.0.1, Synaptosoft, USA) for a period of 120 s from the start of stimulation with high K^+ KREBS solution. High K^+ KREBS solution was the same as control bath solution except that 70 mM K^+ replaced an equimolar amount of NaCl. Amperometric spikes were selected for analysis of event frequency if spike amplitude exceeded 10 pA and overlapping peaks were included. Cells with fewer than 10 events within the 60 s stimulation period were excluded from analysis. For kinetic analysis of spikes and spike feet, only those events which exceeded 20 pA or were not overlapping with other spikes were included.

Statistics

Statistical analyses were performed using GraphPad Prism 5 software (GraphPad Software, Inc., USA). Results are presented as mean ± SEM (standard error of the mean). Unpaired student t test was used for statistical comparison. A p value <0.05 was considered statistically significant.

4. Results

Alms1$^{foz/foz}$ chromaffin cells display reduced secretory rate of catecholamine

Chromaffin cells were isolated from young (<60 days old) non-obese Alms1$^{foz/foz}$ mice and wildtype littermates. Cells were kept in primary culture for three days and exocytosis activity was measured by amperometry by stimulating cells with High K+ KREBS solution and measuring oxidised catecholamine released from individual vesicles also called exocytotic event.

Upon stimulation with High K+ KREBS solution, Alms1$^{foz/foz}$ chromaffin cell displayed markedly different amperometry recording traces compared to wildtype cells, with Alms1$^{foz/foz}$ cells showing an overall reduced secretory rate (Figure 5-1A and B). This was confirmed by a significantly lower number of exocytotic events recorded in Alms1$^{foz/foz}$ chromaffin cells ($p=0.003$; Figure 5-1C). These data suggest a lower number of vesicles undergoing exocytosis or an impairment of the exocytosis mechanism itself in Alms1$^{foz/foz}$.

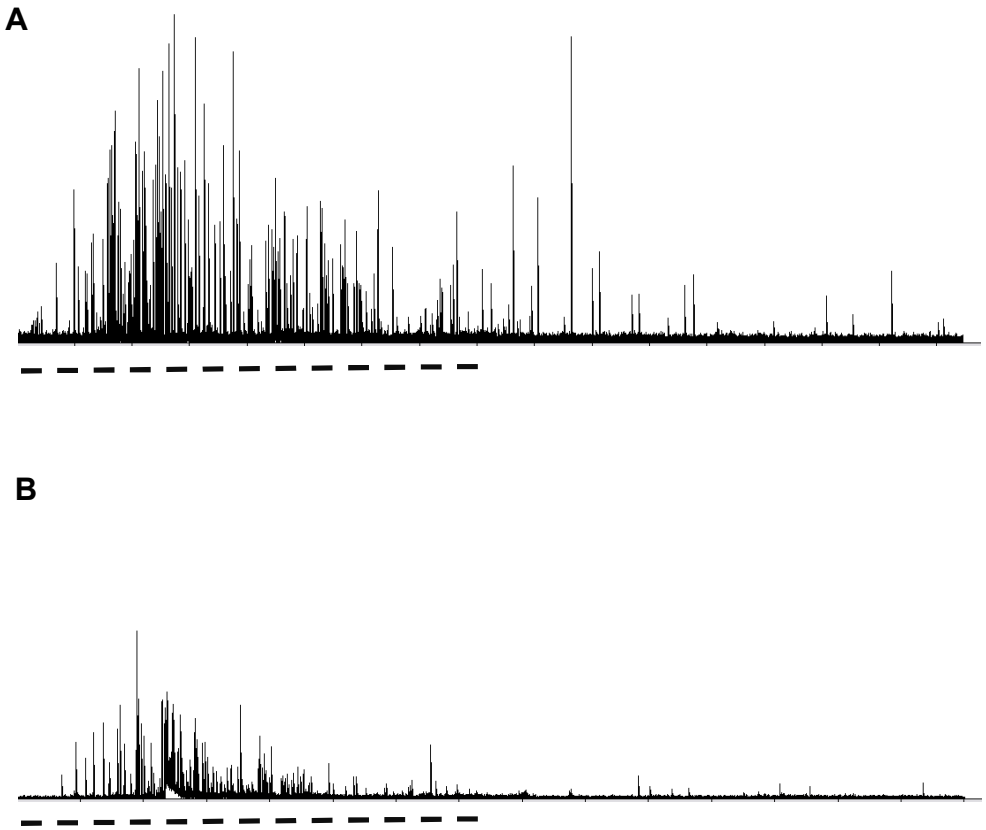
A
B
C
250
200
150
100
50
0
No. of Events
Mean ± SEM
**
WT
Alms1foz/foz

Figure 5-1: Amperometry recording traces and number of exocytotic events

Chromaffin cells were stimulated during 1 minute with High K+ KREBS solution (indicated by dashed line). A: Representative amperometry recording traces of A: WT and B: Alms1$^{foz/foz}$ chromaffin cells. C: Number of events recorded during 2 minutes upon High K+ stimulation using WT (open bars n=17) and Alms1$^{foz/foz}$ (black bars n=16) chromaffin cells. Abbreviations: SEM: standard error of the mean; WT: wildtype. ** $p<0,01$

Alms1$^{foz/foz}$ chromaffin cells display reduced spike amplitude but normal fusion pore kinetics

Fusion pore kinetics analysis on chromaffin cell amperometry recordings showed that Alms1$^{foz/foz}$ spike amplitude was significantly reduced compared to WT mice (p=0.03; Figure 5-2 A). The charge or amount of catecholamine released per exocytotic event was also slightly reduced in Alms1$^{foz/foz}$ condition without reaching significance (NS; Figure 5-2 B).

Other parameters such as rise time, half-width (width of a spike at half its maximal height) and decay time were similar between Alms1$^{foz/foz}$ and WT exocytotic events therefore indicating that there is no defect in fusion pore kinetics in mutant condition (NS, Figure 5-2 C, D and E).

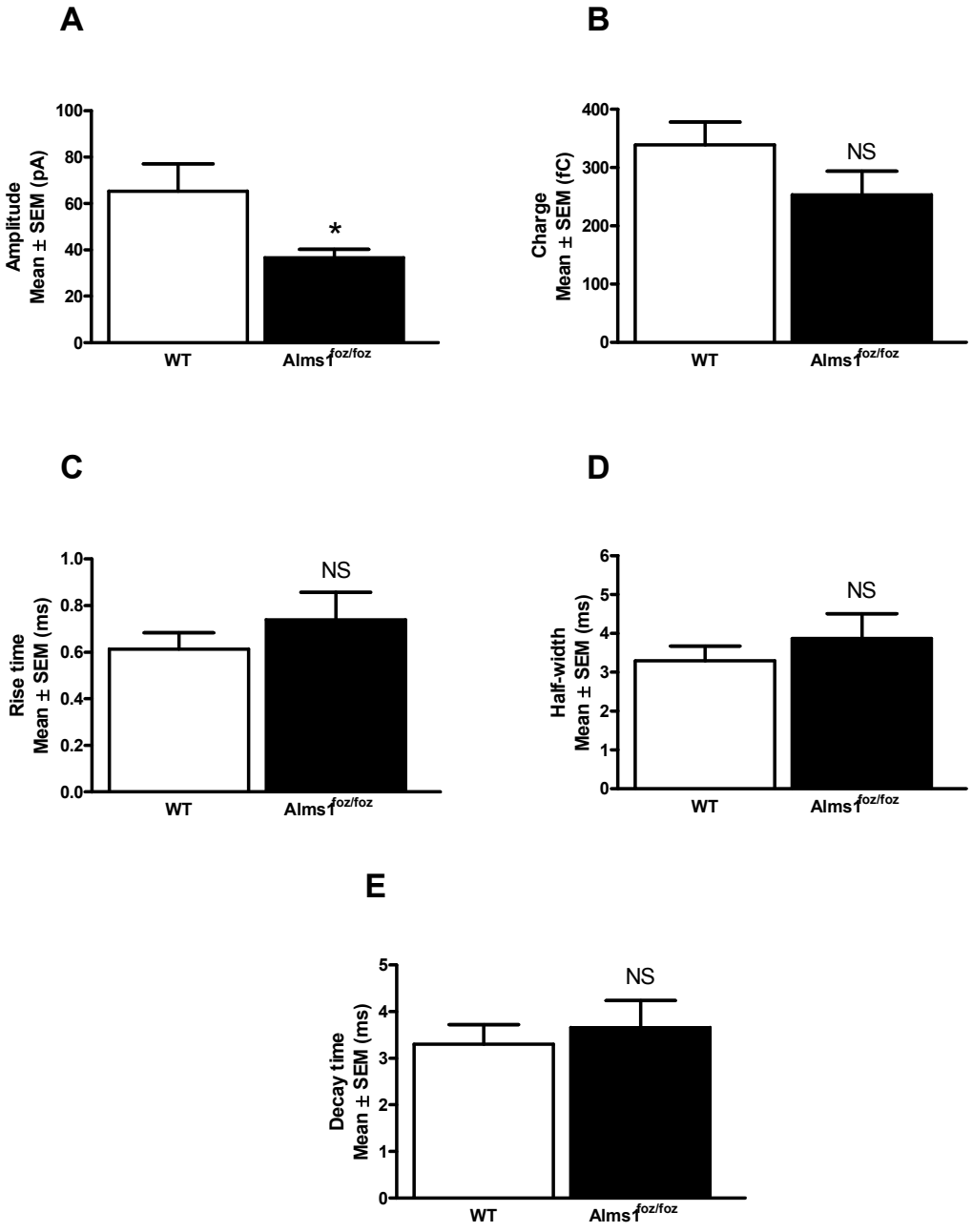
A
Amplitude
Mean ± SEM (pA)
100
80
60
40
20
0
*
WT
Alms1foz/foz
B
Charge
Mean ± SEM (fC)
400
300
200
100
0
NS
WT
Alms1foz/foz
C
Rise time
Mean ± SEM (ms)
1.0
0.8
0.6
0.4
0.2
0.0
NS
WT
Alms1foz/foz
D
Half-width
Mean ± SEM (ms)
6
5
4
3
2
1
0
NS
WT
Alms1foz/foz
E
Decay time
Mean ± SEM (ms)
5
4
3
2
1
0
NS
WT
Alms1foz/foz

Figure 5-2: Fusion pore kinetics parameters of exocytotic events

Analysis of the fusion pore kinetics parameters of exocytotic events recorded from Alms1$^{foz/foz}$ (black bar, n=16) and WT (open bar, n=17) stimulated chromaffin cells. A: Amplitude, B: Quantal size (or charge), C: Rise time, D: Half-width, E: Decay time. Abbreviations: NS: not significant; SEM: standard error of the mean; WT: wildtype. * $p<0.05$

5. Discussion

Little is known about exocytosis in AS. Only a single previous study has reported a large number of exocytotic vesicles in dermal fibroblasts cultured from AS patients using electron microscopy with the authors suggesting that ALMS1 fibroblast display active secretion of collagen (Sun, Kusminski et al. 2011). However, the high number of vesicles could also suggest impairment in the induction of exocytosis leading to an abnormal accumulation of vesicles at the cell membrane.

In this study, young Alms1$^{foz/foz}$ mice chromaffin cells were isolated in order to investigate the exocytosis mechanism. Since Alms1$^{foz/foz}$ mice were less than 60 days of age, their body weight matched wildtype controls and allowed obesity to be excluded as a confounder factor.

The data highlights an underlying catecholamine secretion defect in Alms1$^{foz/foz}$ chromaffin cells. While the exocytosis rate of catecholamine and spike amplitude was reduced in Alms1$^{foz/foz}$ chromaffin cell, the fusion pore kinetics and more precisely vesicle docking and release mechanism was not impaired. These data showed that the exocytosis mechanism is unaltered in Alms1$^{foz/foz}$ chromaffin cell and suggest that Alms1$^{foz/foz}$ chromaffin cell exocytotic vesicles are either smaller or release less catecholamine due to reduced loading. These data could also indicate that the migration of exocytotic vesicles to the

membrane might be impaired in Alms1$^{foz/foz}$ condition therefore explaining the significant reduced secretory rate observed.

In conclusion these data suggest a significant reduction of chromaffin cell secretory activity in Alms1$^{foz/foz}$ mice suggesting a potential role of Alms1 protein in intracellular vesicle trafficking.

Chapter 6 : Perspectives

AS belongs to a new class of disorders that involve the functional impairment of an often dismissed vestigial organelle called a primary cilium. AS features severe multi-organ pathology due to mutations in the ALMS1 gene.

Metabolic disorders including obesity and insulin resistance remain the cardinal features in young patients with AS suggesting a critical role of Alms1 protein in homeostasis and insulin signalling. The "Fat Aussie" (FA) mouse or Alms1$^{foz/foz}$ is a model for AS that carries a spontaneous deletion (*foz*) in exon 8 of the ALMS1 gene. The Alms1$^{foz/foz}$ mouse recapitulates the metabolic disorders occurring in AS patients and represents a unique opportunity to better characterise the pathogenic mechanisms underlying AS-associated disorders such as obesity, insulin resistance and T2DM.

When compared to wildtype littermates, young Alms1$^{foz/foz}$ mice had a significantly reduced glucose lowering response to insulin during the ITT while after the IPGTT no differences were observed in the glucose profile and endogenous insulin secretion. Young male Alms1$^{foz/foz}$ mice had significantly higher fasting hyperinsulinemia and HOMA-IR scores compared to wildtype littermates. The metabolic phenotypic study undertaken in this project has revealed that early peripheral insulin resistance is an inherent primary consequence of the ALMS1 gene disruption in Alms1$^{foz/foz}$ mice at a time that β-cell function isn't affected. Insulin resistance may thereby drive the subsequent

severe metabolic complications, making the Alms1$^{foz/foz}$ mouse model a unique monogenic model to study pathogenic pathways leading to obesity and T2DM.

This study has also shown that adipocytes are already enlarged in young lean Alms1$^{foz/foz}$ mice suggesting that white adipose tissue might be insulin sensitive at this stage and the underlying insulin resistance might come from either liver or muscle. Since more insights into the underlying metabolic disturbances driving the Alms1$^{foz/foz}$ mouse towards obesity and T2DM are unravelled, the next step would be to determine the insulin sensitivity status of each Alms1$^{foz/foz}$ insulin responsive tissue (liver, adipose tissue or muscle) at an early age in order to determine where the primary source of insulin resistance lies and characterise its progression with age.

More importantly, these data also suggest that the defect leading to insulin resistance in Alms1$^{foz/foz}$ mice must be downstream of AS160 (TBC1D4) phosphorylation in the insulin pathway and might concern either the translocation of GLUT4 or its recycling (Kramer, Witczak et al. 2006; Ramm, Larance et al. 2006). Thus, future research should focus on the possible role of Alms1 on the Glut4 translocation mechanism in order to shed lights into the role of the native Alms1 protein in the insulin pathway signalling and define the defective intracellular signalling consequences due to Alms1 protein truncation in mutant condition (Figure 6-1).

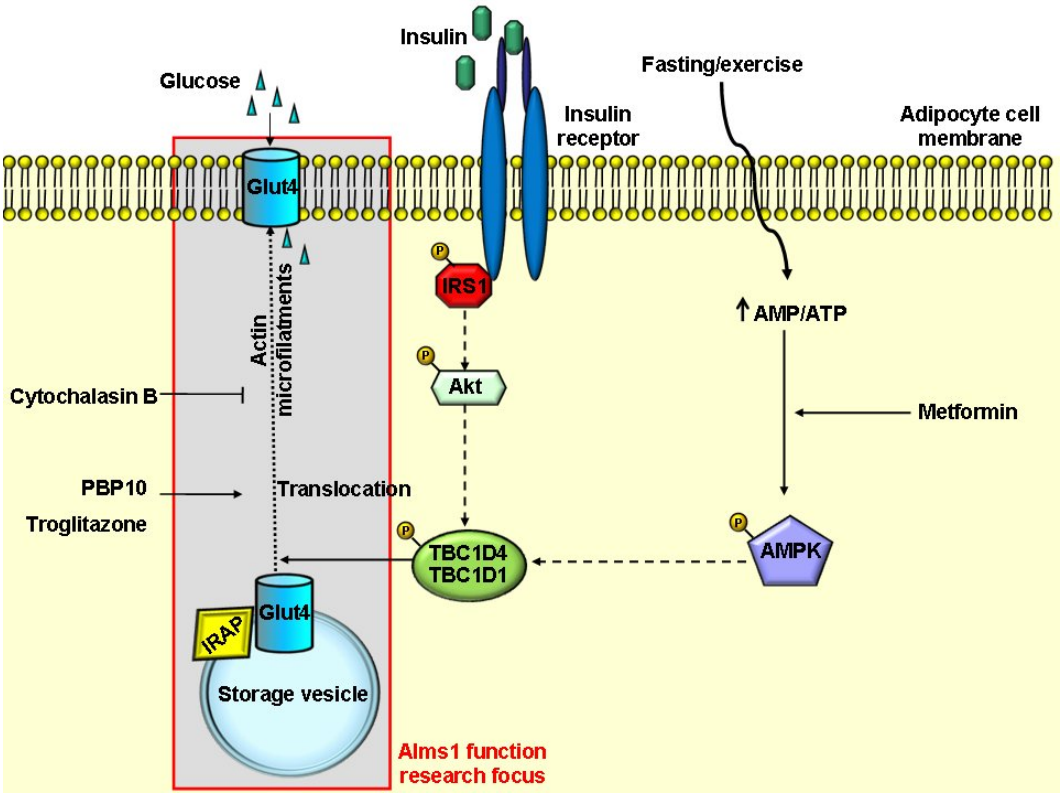

Figure 6-1: Alms1 function research focus in the insulin signalling pathway

The research focus on the function of Alms1 protein in the insulin pathway signalling is highlighted in grey and concern the intracellular signalling cascade downstream TBC1D4/TBC1D1 (or AS160) phosphorylation that ultimately leads to glucose uptake via the translocation of Glut4 from the cytoplasmic storage vesicle to the cell membrane. Abbreviations: AMPK: AMP-activated protein kinase; Glut4: Glucose transporter 4; IRAP: Insulin-regulated aminopeptidase; IRS1: Insulin receptor substrate 1.

Female NOD/Alms1$^{foz/foz}$ mice were then used as a new model to investigate the intricate relationship between metabolic disturbances such as obesity and T2DM and the onset of auto-immune type 1 diabetes mellitus (T1DM). Obese and insulin resistant NOD/Alms1$^{foz/foz}$ mice were protected against T1DM.

Data showed that β cell destruction was significantly suppressed with NOD/Alms1$^{foz/foz}$ mice displaying mainly intact hyperplastic islets, limited immune cell infiltration and unaltered insulin secretory capacity. Neither a significant body weight loss nor injection of cyclophosphamide induced the onset of T1DM in NOD/Alms1$^{foz/foz}$ mice. This suggests that obesity itself is not the cause of NOD/Alms1$^{foz/foz}$ mice T1DM protection and could indicate an immune dysregulation in NOD/Alms1$^{foz/foz}$ mice. Another explanation could be that lean NOD/Alms1$^{foz/foz}$ mice remain hyperinsulinemic after body weight loss and therefore remain insulin resistant which may be a factor behind ongoing protection against T1DM, given the known ability of insulin to induce immune tolerance and prevent T1DM.

However, since NOD/Alms1$^{foz/foz}$ mice become insulin resistant before they reach the age range of T1DM onset, the protection they acquire at an early age might not be reversible. NOD/Alms1$^{foz/foz}$ mice metabolic disturbances might be the cause of T1DM remission and future research should focus on characterising where the early protection against T1DM lies. NOD/Alms1$^{foz/foz}$

mice could be placed on a restricted diet after weaning in order to repress the onset of insulin resistance and obesity and see if they are still protected against T1DM. Then, the challenge will be to determine if the protection come from an immune system tolerance and/or a protection from the β islets themselves using techniques such as adoptive transfer of splenocytes or islet transplants to investigate the underlying protection mechanism against T1DM.

This project has also shed light on new features not previously reported before in any published AS studies. Alms1$^{foz/foz}$ mice were found to display early mild cognitive impairment that worsened with age and was associated with reduced brain mass. Altogether these data suggest a development defect and a possible role of Alms1 in neuronal function.

The Alms1 protein was found to be transported bi-directionally via the sciatic nerve which indicates that Alms1 protein could be transported by cargo proteins or involved in intracellular trafficking involved in neuronal signalling. A recent study has shown that Alms1 localises to the nucleus and interacts with the RNA polymerase II (RNAPII) (Moeller, Xie et al. 2011). Similarly, the axonal transport of Alms1 further suggests that Alms1 protein does not exclusively localise to the centrosome therefore extending the range of potential functions of Alms1 protein.

Studying the integrity of the exocytosis mechanism using Alms1$^{foz/foz}$ mice chromaffin cells showed a significantly reduced exocytosis rate of catecholamine in mutant condition but unaltered pore fusion kinetics (membrane docking and fusion) compared to wildtype controls. This indicates that a reduced number of vesicles are undergoing exocytosis in Alms1$^{foz/foz}$ condition and suggests a possible involvement of the Alms1 protein in vesicular trafficking such as intracellular vesicle transport but no involvement in the exocytosis mechanism itself. These data further indicate that the Alms1 protein might play a key role in intracellular trafficking.

To conclude, this project has helped better characterise the underlying defects that drive the Alms1$^{foz/foz}$ mouse model of AS toward multi-organs pathology by finding potential clues to Alms1 protein function. It provides evidence towards involvement of Alms1 protein in intracellular trafficking and identifies a role in pathways not associated to primary cilia function (e.g. insulin pathway signalling). Research into unravelling Alms1 protein function will not only lead to improved treatments for patients with AS, but could also provide a better understanding of cellular pathways involved in more common disorders such as obesity and type 2 diabetes.

References

Adams, M., U. M. Smith, et al. (2008). "Recent advances in the molecular pathology, cell biology and genetics of ciliopathies." Journal of Medical Genetics **45**: 257-267.

Adams, N. A., A. Awadein, et al. (2007). "The Retinal Ciliopathies." Ophthalmic Genetics **28**(3): 113 - 125.

Alstrom, C. H., B. Hallgren, et al. (1959). "Retinal degeneration combined with obesity, diabetes mellitus and neurogenous deafness: a specific syndrome (not hitherto described) distinct from the Laurence-Moon-Bardet-Biedl syndrome: a clinical, endocrinological and genetic examination based on a large pedigree." Acta Psychiatr Neurol Scand Suppl **129**: 1-35.

Amador-Arjona, A., J. Elliott, et al. (2011). "Primary Cilia Regulate Proliferation of Amplifying Progenitors in Adult Hippocampus: Implications for Learning and Memory." The Journal of Neuroscience **31**(27): 9933-9944.

Andersen, J. S., C. J. Wilkinson, et al. (2003). "Proteomic characterization of the human centrosome by protein correlation profiling." Nature **426**(6966): 570-574.

Anderson, M. S. and J. A. Bluestone (2005). "The NOD mouse: a model of immune dysregulation." Annual review of immunology **23**: 447-485.

Arnaiz, O., A. Malinowska, et al. (2009). "Cildb: a knowledgebase for centrosomes and cilia." Database **2009**(0): bap022-.

Arsov, T., C. Z. Larter, et al. (2006). "Adaptive failure to high-fat diet characterizes steatohepatitis in Alms1 mutant mice." Biochemical and Biophysical Research Communications **342**: 1152–1159.

Arsov, T., D. G. Silva, et al. (2006). "Fat aussie: a new Alström syndrome mouse showing a critical role for ALMS1 in obesity, diabetes, and spermatogenesis." Molecular Endocrinology **20**(7): 1610-1622.

Arteel, G. E. (2012). "Beyond reasonable doubt: Who is the culprit in lipotoxicity in NAFLD/NASH?" Hepatology: n/a-n/a.

Association, A. D. (2006). "Diagnosis and classification of diabetes mellitus." Diabetes care **29**(suppl 1): S43-S48.

Awazu, M., T. Tanaka, et al. (1997). "Hepatic dysfunction in two sibs with Alström syndrome: Case report and review of the literature." American Journal of Medical Genetics **69**(1): 13-16.

Bach, J.-F. (1994). "Insulin-dependent diabetes mellitus as an autoimmune disease." Endocrine reviews **15**(4): 516-542.

Badano, J. L., N. Mitsuma, et al. (2006). "The Ciliopathies: An Emerging Class of Human Genetic Disorders." Annual Review of Genomics and Human Genetics **7**(1): 125-148.

Badano, J. L., T. M. Teslovich, et al. (2005). "The centrosome in human genetic disease." Nature Reviews genetics **6**(3): 194-205.

Baker, K. and P. L. Beales (2009). "Making Sense of Cilia in Disease:The Human Ciliopathies." American Journal of Medical Genetics Part C (Seminars in Medical Genetics) **151C**: 281-295.

Baldari, C. T. and J. Rosenbaum (2009). "Intraflagellar transport: it's not just for cilia anymore." Current opinion in cell biology **22**: 1-6.

Beales, P. L., N. Elcioglu, et al. (1999). "New criteria for improved diagnosis of Bardet-Biedl syndrome: results of a population survey." Journal of Medical Genetics **36**(6): 437-446.

Bennouna-Greene, V., S. Kremer, et al. (2011). "Hippocampal dysgenesis and variable neuropsychiatric phenotypes in patients with Bardet–Biedl syndrome underline complex CNS impact of primary cilia." Clinical Genetics **80**(6): 523-531.

Benso, C., E. Hadjadj, et al. (2002). "Three new cases of Alström syndrome." Graefe's Archive for Clinical and Experimental Ophthalmology **240**(8): 622-627.

Berbari, N. F., G. A. Bishop, et al. (2007). "Hippocampal neurons possess primary cilia in culture." Journal of Neuroscience Research **85**(5): 1095-1100.

Berbari, N. F., J. S. Lewis, et al. (2008). "Bardet–Biedl syndrome proteins are required for the localization of G protein-coupled receptors to primary cilia." PNAS **105**(11): 4242-4246.

Bettini, V., P. Maffei, et al. (2012). "The progression from obesity to type 2 diabetes in Alström syndrome." Pediatric Diabetes **13**(1): 59-67.

Betts, P., J. Mulligan, et al. (2005). "Increasing body weight predicts the earlier onset of insulin-dependant diabetes in childhood: testing the 'accelerator hypothesis' (2)." Diabetic Medicine **22**(2): 144-151.

Bielas, S. L., J. L. Silhavy, et al. (2009). "Mutations in INPP5E, encoding inositol polyphosphate-5-phosphatase E, link phosphatidyl inositol signaling to the ciliopathies." Nat Genet **41**(9): 1032-1036.

Bond, J., K. Flintoff, et al. (2005). "The importance of seeking ALMS1 mutations in infants with dilated cardiomyopathy." Journal of Medical Genetics **42**(2): e10-e10.

Bonnafe, E., M. Touka, et al. (2004). "The Transcription Factor RFX3 Directs Nodal Cilium Development and Left-Right Asymmetry Specification." Mol. Cell. Biol. **24**(10): 4417-4427.

Brailov, I., M. Bancila, et al. (2000). "Localization of 5-HT6 receptors at the plasma membrane of neuronal cilia in the rat brain." Brain research **872**(1-2): 271-275.

Bratanova-Tochkova, T. K., H. Cheng, et al. (2002). "Triggering and Augmentation Mechanisms, Granule Pools, and Biphasic Insulin Secretion." Diabetes **51**(90001): S83-90.

Breunig, J. J., M. R. Sarkisian, et al. (2008). "Primary cilia regulate hippocampal neurogenesis by mediating sonic hedgehog signaling." Proceedings of the National Academy of Sciences **105**(35): 13127-13132.

Broadbent, N. J., L. R. Squire, et al. (2004). "Spatial memory, recognition memory,and the hippocampus." PNAS **101** (40): 14515-14520.

Brode, S., T. Raine, et al. (2006). "Cyclophosphamide-induced type-1 diabetes in the NOD mouse is associated with a reduction of $CD4^+$ $CD25^+$ $Foxp3^+$ regulatory T cells." The journal of immunology **177**: 6603-6612.

Cardenas-Rodriguez, M. and J. L. Badano (2009). "Ciliary Biology: Understanding the Cellular and Genetic Basis of Human Ciliopathies." American Journal of Medical Genetics Part C (Seminars in Medical Genetics) **151C**(263-280).

Chen, Y., C. Hu, et al. (2002). "Targeted Disruption of the Melanin-Concentrating Hormone Receptor-1 Results in Hyperphagia and Resistance to Diet-Induced Obesity." Endocrinology **143**(7): 2469-2477.

Coll, A. P., I. S. Farooqi, et al. (2007). "The Hormonal Control of Food Intake." Cell **129**(2): 251–262.

Collin, G., J. Marshall, et al. (1997). "Homozygosity mapping at Alstrom syndrome to chromosome 2p." Hum. Mol. Genet. **6**(2): 213-219.

Collin, G. B., E. Cyr, et al. (2005). "Alms1-disrupted mice recapitulate human Alström syndrome." Human Molecular Genetics **14**(16): 2323-2333.

Collin, G. B., E. Cyr, et al. (2005). "Alms1-disrupted mice recapitulate human Alström syndrome." Human Molecular Genetics **14**(16): 2323–2333.

Collin, G. B., J. D. Marshall, et al. (1999). "Alström syndrome: further evidence for linkage to human chromosome 2p13." Human Genetics **105**(5): 474-479.

Collin, G. B., J. D. Marshall, et al. (2002). "Mutations in ALMS1 cause obesity, type 2 diabetes and neurosensory degeneration in Alström syndrome." Nature Genetics **31**: 74-78.

Connolly, M. B., J. E. Jan, et al. (1991). "Hepatic dysfunction in Alström disease." American Journal of Medical Genetics **40**(4): 421-424.

Corbetti, F., R. Razzolini, et al. (2012). "Alström Syndrome: Cardiac Magnetic Resonance findings." International Journal of Cardiology **AOP**.

Davenport, J. R., A. J. Watts, et al. (2007). "Disruption of Intraflagellar Transport in Adult Mice Leads to Obesity and Slow-Onset Cystic Kidney Disease." Current Biology **17**: 1586–1594.

Davenport, J. R. and B. K. Yoder (2005). "An incredible decade for the primary cilium: a look at a once-forgotten organelle." Am J Physiol Renal Physiol **289**(6): F1159-1169.

Davis, E. E., M. Brueckner, et al. (2006). "The Emerging Complexity of the Vertebrate Cilium: New Functional Roles for an Ancient Organelle." Developmental Cell **11**(1): 9-19.

Davis, R. E., R. E. Swiderski, et al. (2007). "A knockin mouse model of the Bardet–Biedl syndrome 1 M390R mutation has cilia defects, ventriculomegaly, retinopathy, and obesity." PNAS **104**(49): 19422-19427.

Dawe, H. R., H. Farr, et al. (2006). "Centriole/basal body morphogenesis and migration during ciliogenesis in animal cells." Journal of cell science **120**(1).

Deane, J. A. and S. D. Ricardo (2007). "Polycystic kidney disease and the renal cilium " Nephrology **12**(6): 559-564.

Domire, J. S., J. A. Green, et al. (2011). "Dopamine receptor 1 localizes to neuronal cilia in a dynamic process that requires the Bardet-Biedl syndrome proteins." Cellular and molecular life sciences **68**(17): 2951-2960.

Donath, M. Y. and J. A. Ehses (2006). "Type 1, type 1.5, and type 2 diabetes: *NOD* the diabetes we thought it was." PNAS **103**(33): 12217-12218.

Dunaif, A. (1997). "Insulin Resistance and the Polycystic Ovary Syndrome: Mechanism and Implications for Pathogenesis." Endocr Rev **18**(6): 774-800.

Ellacott, K. L. J. and R. D. Cone (2004). "The Central Melanocortin System and the Integration of Short- and Long-term Regulators of Energy Homeostasis." Recent Progress in Hormone Research **59**: 395-408.

Emmer, B. T., D. Maric, et al. "Molecular mechanisms of protein and lipid targeting to ciliary membranes." J Cell Sci **123**(4): 529-536.

Essner, J. J., K. J. Vogan, et al. (2002). "Left-right development: Conserved function for embryonic nodal cilia. ." Nature **418**(6893): 37-38.

Finetti, F., S. R. Paccani, et al. (2009). "Intraflagellar transport is required for polarized recycling of the TCR/CD3 complex to the immune synapse. ." Nature cell biology **11**(11): 1332-1339.

Fliegauf, M., T. Benzing, et al. (2007). "When cilia go bad: cilia defects and ciliopathies. ." Nature Reviews. Molecular Cell Biology **8**(11): 880-893.

Forlenza, G. P. and M. Rewers (2011). "The epidemic of type 1 diabetes: what is it telling us?" Current Opinion in Endocrinology, Diabetes and Obesity **18**(4): 248-251 210.1097/MED.1090b1013e32834872ce.

Fuchs, J. L. and H. D. Schwark (2004). "Neuronal primary cilia: a review." Cell Biology International **28**: 111-118.

Garcia, A. G., A. M. Garcia-De-Diego, et al. (2006). "Calcium Signaling and Exocytosis in Adrenal Chromaffin Cells." Physiol. Rev. **86**(4): 1093-1131.

Genter, M. B., P. P. Van Veldhoven, et al. (2003). "Microarray-based discovery of highly expressed olfactory mucosal genes: potential roles in the various functions of the olfactory system." Physiol. Genomics **16**(1): 67-81.

Gerdes, J. M., E. E. Davis, et al. (2009). "The Vertebrate Primary Cilium in Development, Homeostasis, and Disease." Cell **137**(1): 32-45.

Gherman, A., E. E. Davis, et al. (2006). "The ciliary proteome database: an integrated community resource for the genetic and functional dissection of cilia." Nature Genetics **38**(9): 961-962.

Girard, D. and N. Petrovsky (2011). "Alstrom syndrome: insights into the pathogenesis of metabolic disorders." Nat Rev Endocrinol **7**(2): 77-88.

Goerler, H., G. Warnecke, et al. (2007). "Heart-Lung Transplantation in a 14-year-old Boy With Alström Syndrome." The Journal of heart and lung transplantation : the official publication of the International Society for Heart Transplantation **26**(11): 1217-1218.

Goldstein, J. and P. Fialkow (1973). "The Alström syndrome: report of three cases with further delineation of the clinical, pathophysiological, and genetic aspects of the disorder. ." Medicine (Baltimore) **52**(1): 53-71.

Gottlieb, P. A. and G. S. Eisenbarth (2002). "Insulin-Specific Tolerance in Diabetes." Clinical Immunology **102**(1): 2-11.

Graser, S., Y.-D. Stierhof, et al. (2007). "Cep164, a novel centriole appendage protein required for primary cilium formation." The Journal of Cell Biology **179**(2): 321-330.

Gupta PS, Prodromou NV, et al. (2009). "Can faulty antennae increase adiposity? The link between cilia proteins and obesity." J Endocrinol. **203**(3): 327-336.

Hamamy, H., M. Barham, et al. (2006). "Alström syndrome in four sibs from northern Jordan." Ann Saudi Med. **26**(6): 480-483.

Hampshire, D. J., M. Ayub, et al. (2006). "MORM syndrome (mental retardation, truncal obesity, retinal dystrophy and micropenis), a new autosomal recessive disorder, links to 9q34." Eur J Hum Genet **14**(5): 543-548.

Han, J. C., D. A. Lawlor, et al. (2010). "Childhood obesity." The Lancet **375**(9727): 1737-1748.

Händel, M., S. Schulz, et al. (1999). "Selective targeting of somatostatin receptor 3 to neuronal cilia." Neuroscience **89**(3): 909-926.

Harada, M. and S. Makino (1984). "Promotion of spontaneous diabetes in non-obese diabetes-prone mice by cyclophosphamide." Diabetologia **27**: 604-606.

Hart, L. M., J. A. Maassen, et al. (2003). "Lack of association between gene variants in the ALMS1 gene and Type 2 diabetes mellitus." Diabetologia **46**(7): 1023-1024.

Hearn, T., G. L. Renforth, et al. (2002). "Mutation of ALMS1, a large gene with a tandem repeat encoding 47 amino acids, causes Alström syndrome." Nature Genetics **31**: 79-83.

Hearn, T., C. Spalluto, et al. (2005). "Subcellular Localization of ALMS1 Supports Involvement of Centrosome and Basal Body Dysfunction in the Pathogenesis of Obesity, Insulin Resistance, and Type 2 Diabetes." Diabetes **54**: 1581-1587.

Hildebrandt, F. and E. Otto (2005). "Cilia and centrosomes: a unifying pathogenic concept for cystic kidney disease?" Nat Rev Genet **6**(12): 928-940.

Hitz, M.-P., H. Bertram, et al. (2008). "Levosimendan for bridging in a pediatric patient with Alström syndrome awaiting heart-lung transplantation." Clinical Research in Cardiology **97**(11): 846-848.

Hoffman, J. D., Z. Jacobson, et al. (2005). "Familial variable expression of dilated cardiomyopathy in Alström syndrome: A report of four sibs." American Journal of Medical Genetics Part A **135A**(1): 96-98.

Holder, M., W. Hecker, et al. (1995). "Impaired Glucose Tolerance Leads to Delayed Diagnosis of Alstrom Syndrome." Diabetes Care **18**(5): 698-700.

Huang-Doran, I. and R. K. Semple (2010). "Knockdown of the Alstrom syndrome-associated gene Alms1 in 3T3-L1 preadipocytes impairs adipogenesis but has no effect on cell-autonomous insulin action." Int J Obes.

Hui Wang, L. L.-y. W., Xing-Yun Song, Xue-Gang Luo, Jin-Hua Zhong, Robert A. Rush, Xin-Fu Zhou, (2006). "Axonal transport of BDNF precursor in primary sensory neurons." European Journal of Neuroscience **24**(9): 2444-2452.

Inglis, P. N., K. A. Boroevich, et al. (2006). "Piercing together a ciliome." TRENDS in Genetics **22**(9): 491-500.

Ishikawa, H., J. Thompson, et al. (2012). "Proteomic Analysis of Mammalian Primary Cilia." Current Biology **22**(5): 414-419.

Jacoby, M., J. J. Cox, et al. (2009). "*INPP5E* mutations cause primary cilium signaling defects, ciliary instability and ciliopathies in human and mouse." Nature Genetics **41**(9): 1027-1033.

Jagger, D., G. Collin, et al. (2011). "Alström Syndrome protein ALMS1 localizes to basal bodies of cochlear hair cells and regulates cilium-dependent planar cell polarity." Human Molecular Genetics **20**(3): 466-481.

James, D. E. and R. C. Piper (1994). "Insulin resistance, diabetes, and the insulin-regulated trafficking of GLUT-4." The Journal of Cell Biology **126**(5): 1123-1126.

Joy, T., H. Cao, et al. (2007). "Alstrom syndrome (OMIM 203800): a case report and literature review." Orphanet Journal of Rare Diseases **2**(49).

Jucker, M. and D. K. Ingram (1997). "Murine models of brain aging and age-related neurodegenerative diseases." Behavioural Brain Research **85**(1): 1-25.

Juric-Sekhar, G., J. Adkins, et al. (2012). "Joubert syndrome: brain and spinal cord malformations in genotyped cases and implications for

neurodevelopmental functions of primary cilia." Acta Neuropathologica **123**(5): 695-709.

Keating, D. J., D. Dubach, et al. (2008). "DSCR1/RCAN1 regulates vesicle exocytosis and fusion pore kinetics: implications for Down syndrome and Alzheimer's disease." Hum. Mol. Genet. **17**(7): 1020-1030.

Kibirige, M., B. Metcalf, et al. (2003). "Testing the Accelerator Hypothesis: the relationship between body mass and age at diagnosis of type 1 diabetes." Diabetes care **26**(10): 2865-2870.

Koç, E., G. Bayrak, et al. (2006). "Rare case of Alstrom syndrome without obesity and with short stature, diagnosed in adulthood." Nephrology **11**: 81-84.

Kordonouri, O. and R. Hartmann (2005). "Higher body weight is associated with earlier onset of Type 1 diabetes in children: confirming the 'Accelerator Hypothesis'." Diabetic Medicine **22**(12): 1783-1784.

Kramer, H. F., C. A. Witczak, et al. (2006). "AS160 Regulates Insulin- and Contraction-stimulated Glucose Uptake in Mouse Skeletal Muscle." Journal of Biological Chemistry **281**(42): 31478-31485.

Kumamoto, N., Y. Gu, et al. (2012). "A role for primary cilia in glutamatergic synaptic integration of adult-born neurons." Nat Neurosci **15**(3): 399-405.

Larter, C. Z., M. M. Yeh, et al. (2009). "Roles of adipose restriction and metabolic factors in progression of steatosis to steatohepatitis in obese, diabetic mice." Journal of Gastroenterology and Hepatology **24**(10): 1658-1668.

Lee, C.-H., Y.-G. Chen, et al. (2006). "Novel Leptin Receptor Mutation in NOD/LtJ Mice Suppresses Type 1 Diabetes Progression." Diabetes **55**(1): 171-178.

Lee, C.-H., P. C. Reifsnyder, et al. (2005). "Novel Leptin Receptor Mutation in NOD/LtJ Mice Suppresses Type 1 Diabetes Progression." Diabetes **54**(9): 2525-2532.

Lee, J. H. and J. G. Gleeson (2010). "The role of primary cilia in neuronal function." Neurobiology of Disease **38**(2): 167-172.

Lee, N.-C., J. D. Marshall, et al. (2009). "Caloric restriction in Alström syndrome prevents hyperinsulinemia." American Journal of Medical Genetics Part A **149A**(4): 666-668.

Leroux, M. R. (2007). "Taking vesicular transport to the cilium." Cell **129**: 1041-1043.

Li, G., R. Vega, et al. (2007). "A Role for Alström Syndrome Protein, Alms1, in Kidney Ciliogenesis and Cellular Quiescence." PLoS Genetics **3**(1): 9-20.

Liu, Q., G. Tan, et al. (2007). "The Proteome of the Mouse Photoreceptor Sensory Cilium Complex." Molecular & Cellular Proteomics **6**(8): 1299-1317.

Loudon, M., N. Bellenger, et al. (2009). "Cardiac magnetic resonance imaging in Alstrom syndrome." Orphanet Journal of Rare Diseases **4**(1): 14.

Louvi, A. and Elizabeth A. Grove (2011). "Cilia in the CNS: The Quiet Organelle Claims Center Stage." Neuron **69**(6): 1046-1060.

Lucker, B. F., R. H. Behal, et al. (2005). "Characterization of the Intraflagellar Transport Complex B Core." Journal of Biological Chemistry **280**(30): 27688-27696.

Macari, F., C. Lautier, et al. (1998). "Refinement of genetic localization of the Alström syndrome on chromosome 2p12-13 by linkage analysis in a North African family." Human Genetics **103**: 658-661.

Maffei, P., M. Boschetti, et al. (2007). "Characterization of the IGF system in 15 patients with Alström syndrome." Clinical Endocrinology **66**(2): 269-275.

Mahamid, J., A. Lorber, et al. (2012). "Extreme Clinical Variability of Dilated Cardiomyopathy in Two Siblings With Alström Syndrome." Pediatric Cardiology: 1-4.

Makaryus, A., M. Zubrow, et al. (2007). "Cardiac manifestations of Alström syndrome: echocardiographie findings." J Am Soc Echocardiogr. **20**(12): 1359-1363.

Malm, E., V. Ponjavic, et al. (2008). "Full-Field Electroretinography and Marked Variability in Clinical Phenotype of Alstrom Syndrome." Arch Ophthalmol **126**(1): 51-57.

Marion, V., C. Stoetzel, et al. (2009). "Transient ciliogenesis involving Bardet-Biedl syndrome proteins is a fundamental characteristic of adipogenic differentiation." PNAS **106**(6): 1820-1825.

Marley, A. and M. von Zastrow (2010). "DISC1 Regulates Primary Cilia That Display Specific Dopamine Receptors." PLoS ONE **5**(5): e10902.

Marshall, J. D., S. Beck, et al. (2007). "Alström Syndrome." European Journal of Human Genetics **15**: 1193-1202.

Marshall, J. D., R. T. Bronson, et al. (2005). "New Alstrom Syndrome Phenotypes Based on the Evaluation of 182 Cases." Arch Intern Med **165**(6): 675-683.

Marshall, J. D., E. G. Hinman, et al. (2007). "Spectrum of ALMS1 variants and evaluation of genotype-phenotype correlations in Alstrom syndrome." Hum Mutat **28**(11): 1114-1123.

Marshall, J. D., P. Maffei, et al. (2011). "Alström Syndrome: Genetics and Clinical Overview." Current Genomics **12** (3): 225–235.

McEwen, D. P., R. K. Koenekoop, et al. (2007). "Hypomorphic CEP290/NPHP6 mutations result in anosmia caused by the selective loss of G proteins in cilia of olfactory sensory neurons." Proceedings of the National Academy of Sciences **104**(40): 15917-15922.

Michaud, E. J. and B. K. Yoder (2006). "The Primary Cilium in Cell Signaling and Cancer." Cancer Res **66**(13): 6463-6467.

Michaud, J. L., E. Héon, et al. (1996). "Natural history of Alström syndrome in early childhood: Onset with dilated cardiomyopathy." The Journal of Pediatrics **128**(2): 225-229.

Mihai, C., D. Catrinoiu, et al. (2008). "Cilia, Alström syndrome--molecular mechanisms and therapeutic perspectives." Journal of Medicine and Life **1**(3): 254-261.

Mihai, C. M., D. Catrinoiu, et al. (2009). "Impaired IGF1-GH axis and new therapeutic options in Alström Syndrome patients: a case series." Cases journal **2**(19): 1-9.

Minton, J. A., K. R. Owen, et al. (2006). "Syndromic obesity and diabetes: changes in body composition with age and mutation analysis of ALMS1 in 12 United Kingdom kindreds with Alstrom syndrome." J Clin Endocrinol Metab **91**(8): 3110-3116.

Moeller, A., S. Q. Xie, et al. (2011). "Proteomic analysis of mitotic RNA polymerase II reveals novel interactors and association with proteins dysfunctional in disease." Molecular & Cellular Proteomics.

Mok, C., E. Héon, et al. (2009). "Ciliary dysfunction and obesity." Clinical Genetics **77**(1): 18-27.

Mokashi, A. and E. A. Cummings (2011). "Presentation and course of diabetes in children and adolescents with Alstrom syndrome." Pediatric Diabetes **12**(3pt2): 270-275.

Moritz, O. L., B. M. Tam, et al. (2001). "Mutant rab8 Impairs Docking and Fusion of Rhodopsin-bearing Post-Golgi Membranes and Causes Cell Death of Transgenic Xenopus Rods." Mol. Biol. Cell **12**(8): 2341-2351.

Morris, R. (1984). "Developments of a water-maze procedure for studying spatial learning in the rat." Journal of Neuroscience Methods **11**(1): 47-60.

Mosharov, E. V. and D. Sulzer (2005). "Analysis of exocytotic events recorded by amperometry." Nature Methods **2**(9): 651-658.

Muller, J., C. Stoetzel, et al. (2010). "Identification of 28 novel mutations in the Bardet–Biedl syndrome genes: the burden of private mutations in an extensively heterogeneous disease." Human Genetics **127**(5): 583-593.

Nachury, M. V., A. V. Loktev, et al. (2007). "A core complex of BBS proteins cooperated with the GTPase Rab8 to promote ciliary membrane biogenesis." Cell **129**(1201-1213).

Naik, R. G., B. M. Brooks-Worrell, et al. (2009). "Latent Autoimmune Diabetes in Adults." J Clin Endocrinol Metab **94**(12): 4635-4644.

Nogales-Cadenas, R., F. Abascal, et al. (2009). "CentrosomeDB: a human centrosomal proteins database." Nucl. Acids Res. **37**(suppl_1): D175-180.

Nonaka, S., H. Shiratori, et al. (2002). "Determination of left-right patterning of the mouse embryo by artificial nodal flow. ." Nature **418**(6893): 96-99.

Nonaka, S., Y. Tanaka, et al. (1998). "Randomization of Left-Right Asymmetry due to Loss of Nodal Cilia Generating Leftward Flow of Extraembryonic Fluid in Mice Lacking KIF3B Motor Protein." Cell **95**(6): 829-837.

O'Connell, M. A., S. Donath, et al. (2007). "Major increase in Type 1 diabetes—no support for the Accelerator Hypothesis." Diabetic Medicine **24**(8): 920-923.

Orphanet. (2010). "Alstrom syndrome Orphanet."

Özgül, R., I. Satman, et al. (2007). "Molecular analysis and long-term clinical evaluation of three siblings with Alstrom syndrome." Clinical Genetics **72**(4): 351-356.

Paisey, R. B. (2009). "New insights and therapies for the metabolic consequences of Alstrom syndrome." Current Opinion in Lipidology **20**(4): 315-320 310.1097/MOL.1090b1013e32832dd32851a.

Paisey, R. B., C. M. Carey, et al. (2004). "Hypertriglyceridaemia in Alstrom's syndrome: causes and associations in 37 cases." Clinical Endocrinology **60**(2): 228-231.

Paisey, R. B., D. Hodge, et al. (2008). "Body fat distribution, serum glucose, lipid and insulin response to meals in Alstrom syndrome." Journal of Human Nutrition and Dietetics **21**(3): 268-274.

Paisey, R. B., R. M. Paisey, et al. (2009). "Protection From Clinical Peripheral Sensory Neuropathy in Alstrom Syndrome in Contrast to Early-Onset Type 2 Diabetes." Diabetes Care **32**(3): 462-464.

Patel, S., J. A. Minton, et al. (2006). "Common variations in the ALMS1 gene do not contribute to susceptibility to type 2 diabetes in a large white UK population." Diabetologia **49**(6): 1209-1213.

Pazour, G. J. and G. B. Witman (2003). "The vertebrate primary cilium is a sensory organelle." Current opinion in cell biology **15**: 105-110.

Poretsky, L., N. A. Cataldo, et al. (1999). "The Insulin-Related Ovarian Regulatory System in Health and Disease." Endocr Rev **20**(4): 535-582.

Porter, J. and T. Barrett (2004). "Braking the Accelerator Hypothesis?" Diabetologia **47**(2): 352-353.

Pozzilli, P. and R. Buzzetti (2006). "A new expression of diabetes: double diabetes." TRENDS in endocrinology and metabolism **18**(2): 52-57.

Praetorius, H. and K. Spring (2003). "The renal cell primary cilium functions as a flow sensor." Curr Opin Nephrol Hypertens. **12**(5): 517-520.

Praetorius, H. A., J. Praetorius, et al. (2004). "β1-Integrins in the primary cilium of MDCK cells potentiate fibronectin-induced Ca2+ signaling." Am J Physiol Renal Physiol **287**(5): F969-978.

Purvis, T. L., T. Hearn, et al. (2010). "Transcriptional regulation of the Alström syndrome gene ALMS1 by members of the RFX family and Sp1." Gene.

Rahmouni, K., M. A. Fath, et al. (2008). "Leptin resistance contributes to obesity and hypertension in mouse models of Bardet-Biedl syndrome." The Journal of Clinical Investigation **118**(4): 1458-1467.

Ramm, G., M. Larance, et al. (2006). "A Role for 14-3-3 in Insulin-stimulated GLUT4 Translocation through Its Interaction with the RabGAP AS160." Journal of Biological Chemistry **281**(39): 29174-29180.

Raychowdhury, M. K., A. J. Ramos, et al. (2009). "Vasopressin receptor-mediated functional signaling pathway in primary cilia of renal epithelial cells." Am J Physiol Renal Physiol **296**(1): F87-97.

Reinehr, T., E. Shober, et al. (2006). "β-cells autoantibodies in children with type 2 diabetes mellitus: subgroup or misclassification?" Arch. Dis. Child. **91**: 473-477.

Rewers, M. (2011). "The fallacy of reduction." Pediatric Diabetes: 1-4.

Romano, S., G. Milan, et al. (2008). "Regulation of Alström syndrome gene expression during adipogenesis and its relationship with fat cell insulin sensitivity." International journal of molecular medicine **21**: 731-736.

Rosenbaum, J. L. and G. B. Witman (2002). "Intraflagellar transport. ." Nature Reviews. Molecular Cell Biology **3**(11): 813-825.

Russell-Eggitt, I. M., P. T. Clayton, et al. (1998). "Alström syndrome : : Report of 22 cases and literature review." Ophthalmology **105**(7): 1274-1280.

Sakamoto, K. and G. D. Holman (2008). "Emerging role for AS160/TBC1D4 and TBC1D1 in the regulation of GLUT4 traffic." American Journal of Physiology - Endocrinology And Metabolism **295**(1): E29-E37.

Satir, P. (2007). "Cilia Biology: stop overeating now!" Current Biology **17**(22): R963-R965.

Satman, I., M. T. Yilmaz, et al. (2002). "Evaluation of insulin resistant diabetes mellitus in Alström syndrome: a long-term prospective follow-up of three siblings." Diabetes Research and Clinical Practice **56**(3): 189-196.

Schwartz, M. W., S. C. Woods, et al. (2000). "Central nervous system control of food intake." Nature **404**: 661-671.

Seo, S., D.-F. Guo, et al. (2009). "Requirement of Bardet-Biedl syndrome proteins for leptin receptor signaling." Hum. Mol. Genet. **18**(7): 1323-1331.

Sharma, S., S. Rakoczy, et al. (2010). "Assessment of spatial memory in mice." Life Sciences **87**(17–18): 521-536.

Simpson, F., M. C. Kerr, et al. (2009). "Trafficking, development and hedgehog." Mechanisms of development **126**: 279-288.

Singla, V. and J. F. Reiter (2006). "The Primary Cilium as the Cell's Antenna: Signaling at a Sensory Organelle." Science **313**(5787): 629-633.

Sinha, S., A. Bhangoo, et al. (2007). "Effect of metformin and rosiglitazone in a prepubertal boy with Alström syndrome." J Pediatr Endocrinol Metab. **20**(9): 1045-1052.

Smith, J. C., B. McDonnell, et al. (2007). "Is arterial stiffening in Alstrom syndrome linked to the development of cardiomyopathy?" European Journal of Clinical Investigation **37**(2): 99-105.

Stanic, D., H. Malmgren, et al. (2009). "Developmental changes in frequency of the ciliary somatostatin receptor 3 protein." Brain research **1249**: 101-112.

Stockli, J., J. R. Davey, et al. (2008). "Regulation of Glucose Transporter 4 Translocation by the Rab Guanosine Triphosphatase-Activating Protein AS160/TBC1D4: Role of Phosphorylation and Membrane Association." Molecular Endocrinology **22**(12): 2703-2715.

Sun, K., C. M. Kusminski, et al. (2011). "Adipose tissue remodeling and obesity." The Journal of Clinical Investigation **121**(6): 2094-2101.

Swinburn, B. A., G. Sacks, et al. (2011). "The global obesity pandemic: shaped by global drivers and local environments." The Lancet **378**(9793): 804-814.

Tai, T. S., S. Y. Lin, et al. (2003). "Metabolic Effects of Growth Hormone Therapy in an Alstrom Syndrome Patient." Hormone Research **60**(6): 297-301.

Teoh, N. C., J. Williams, et al. (2010). "Short-term therapy with peroxisome proliferation-activator receptor-alpha agonist Wy-14,643 protects murine fatty liver against ischemia-reperfusion injury." Hepatology **51**(3): 996-1006.

Titomanlio, L., D. De Brasi, et al. (2004). "Alstrom syndrome: intrafamilial phenotypic variability in sibs with a novel nonsense mutation of the ALMS1 gene." Clin Genet **65**(2): 156-157.

Toriello, H. V. and M. A. Parisi (2009). "Cilia and the Ciliopathies: An Introduction." American Journal of Medical Genetics Part C (Seminars in Medical Genetics) **151C**: 261-262.

Van den Abeele, K., M. Craen, et al. (2001). "Ophthalmologic and systemic features of the Alström syndrome: report of 9 cases." Bull Soc Belge Ophtalmol. **281**: 67-72.

Van der Staay, F. J. (2006). "Animal models of behavioral dysfunctions: Basic concepts and classifications, and an evaluation strategy." Brain Research Reviews **52**(1): 131-159.

Van Rooyen, D. M., C. Z. Larter, et al. (2011). "Hepatic Free Cholesterol Accumulates in Obese, Diabetic Mice and Causes Nonalcoholic Steatohepatitis." Gastroenterology **141**(4): 1393-1403.e1395.

Visser, J., F. Klatter, et al. (2003). "Long-term prophylactic insulin treatment can prevent spontaneous diabetes and thyroiditis development in the diabetes-prone bio-breeding rat, while short-term treatment is ineffective." European Journal of Endocrinology **149**(3): 223-229.

Wang, Y.-J., A. Pollard, et al. (2009). "Intramuscular delivery of a single chain antibody gene reduces brain AÎ² burden in a mouse model of Alzheimer's disease." Neurobiology of aging **30**(3): 364-376.

Wang, Y.-J., X. Wang, et al. (2011). "p75NTR Regulates Aβ Deposition by Increasing Aβ Production But Inhibiting Aβ Aggregation with Its Extracellular Domain." The Journal of Neuroscience **31**(6): 2292-2304.

Welsh, L. W. (2007). "Alström Syndrome: Progressive Deafness and Blindness." The Annals of Otology, Rhinology & Laryngology **116**(4): 281-285.

Whitfield, J. F. (2004). "The neuronal primary cilium—an extrasynaptic signaling device." Cellular Signalling **16**: 763-767.

Wilkin, T. J. (2001). "The accelerator hypothesis: weight gain as the missing link between type 1 and type 2 diabetes." Diabetologia **44**: 914-922.

Wilkin, T. J. (2009). "The accelerator hypothesis: a review of the evidence for insulin resistance as the basis for type I as well as type II diabetes." International Journal of Obesity **33**(7): 716-726.

Wilkin, T. J. (2011). "The convergence of type 1 and type 2 diabetes in childhood The accelerator hypothesis." Pediatric Diabetes: no-no.

Worthley, M. I. and C. J. Zeitz (2001). "Case of Alström syndrome with late presentation dilated cardiomyopathy." Internal Medicine Journal **31**(9): 569-570.

Wu, W.-C., S.-C. Chen, et al. (2003). "Alström Syndrome with Acute Pancreatitis: A Case Report." The Kaohsiung Journal of Medical Sciences **19**(7): 358-360.

Yen, H.-J., M. K. Tayeh, et al. (2006). "Bardet-Biedl syndrome genes are important in retrograde intracellular trafficking and Kupffer's vesicle cilia function." Human Molecular Genetics **15**(5): 667-677.

Yilmaz, C., H. Çaksen, et al. (2006). "Alstrom syndrome associated with cerebral involvment: an unusual presentation." European Journal of General Medicine **3**(1): 32-34.

Zaghloul, N. A. and N. Katsanis (2009). "Mechanistic insights into Bardet-Biedl syndrome, a model ciliopathy." The Journal of Clinical Investigation **119**(3): 428-437.

Zhu, D., S. Shi, et al. (2009). "Growth arrest induces primary-cilium formation and sensitizes IGF-1-receptor signaling during differentiation induction of 3T3-L1 preadipocytes." J Cell Sci **122**(15): 2760-2768.

Zumsteg, U., P. Muller, et al. (2000). "Alstrom syndrome: confirmation of linkage to chromosome 2p12-13 and phenotypic heterogeneity in three affected sibs." Journal of Medical Genetics **37**(7): E8.